Hundred-year advances in volcano seismology and acoustics

[1]Diana C. Roman, [2]Robin S. Matoza
[1]Carnegie Science; [2]University of California, Santa Barbara

image: R. Krimmel, USGS

Volcano Seismology in 1919

- Well-established that volcanic eruptions are preceded by earthquakes (e.g., Scrope [1825])
- Some recognition of different ‘classes’ of volcano-seismic events (e.g., Omori [1912], Jaggar [1920])
- Recognition of need to record volcano-seismic events on multiple instruments (e.g., Cross [1920])

Volcano Seismology in 1919

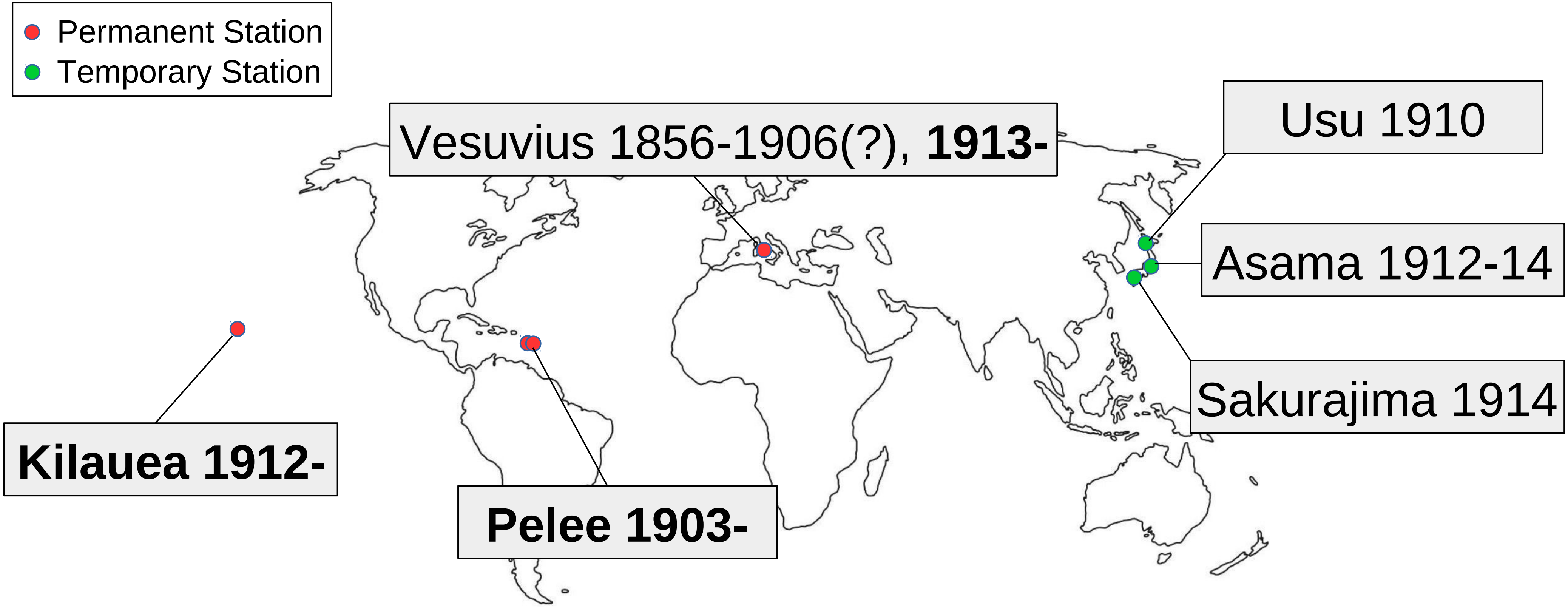

Volcano Seismology in 1919

Fig. 11: Origin of Explosion at the surface.   Fig. 12: Origin of Explosion some depth below the surface.

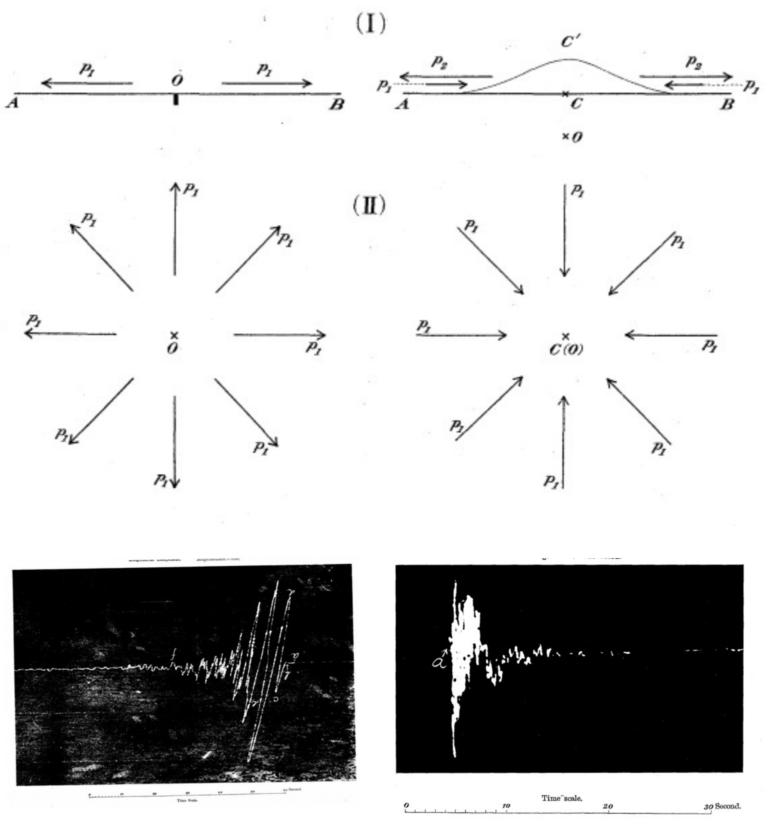

Mechanism of volcanic earthquakes:

“...a seismic disturbance...**due to the direct action of the volcanic force**, or one whose origin lies under, or in the immediate vicinity of a volcano, whether active, dormant, or extinct.”

Omori [1912]

Volcano Seismology in 1919

Fig. 2.—Cracks two feet wide, looking southwest toward Kapoho village. About April 24, 1924.
Photo by Tai Sing Loo.

Photo from Jaggar and Finch [1924]

Mechanism of volcanic earthquakes:

“Local earthquakes and tremors may be caused variously, but the centers are more or less **fixed rift surfaces at points of maximum friction**…. Where so-called tectonic control ends and magmatic thrust begins, are matters as yet rather of philoso-phy than of measurement.”

Jaggar [1920]

Expansion of Permanent Seismic Networks

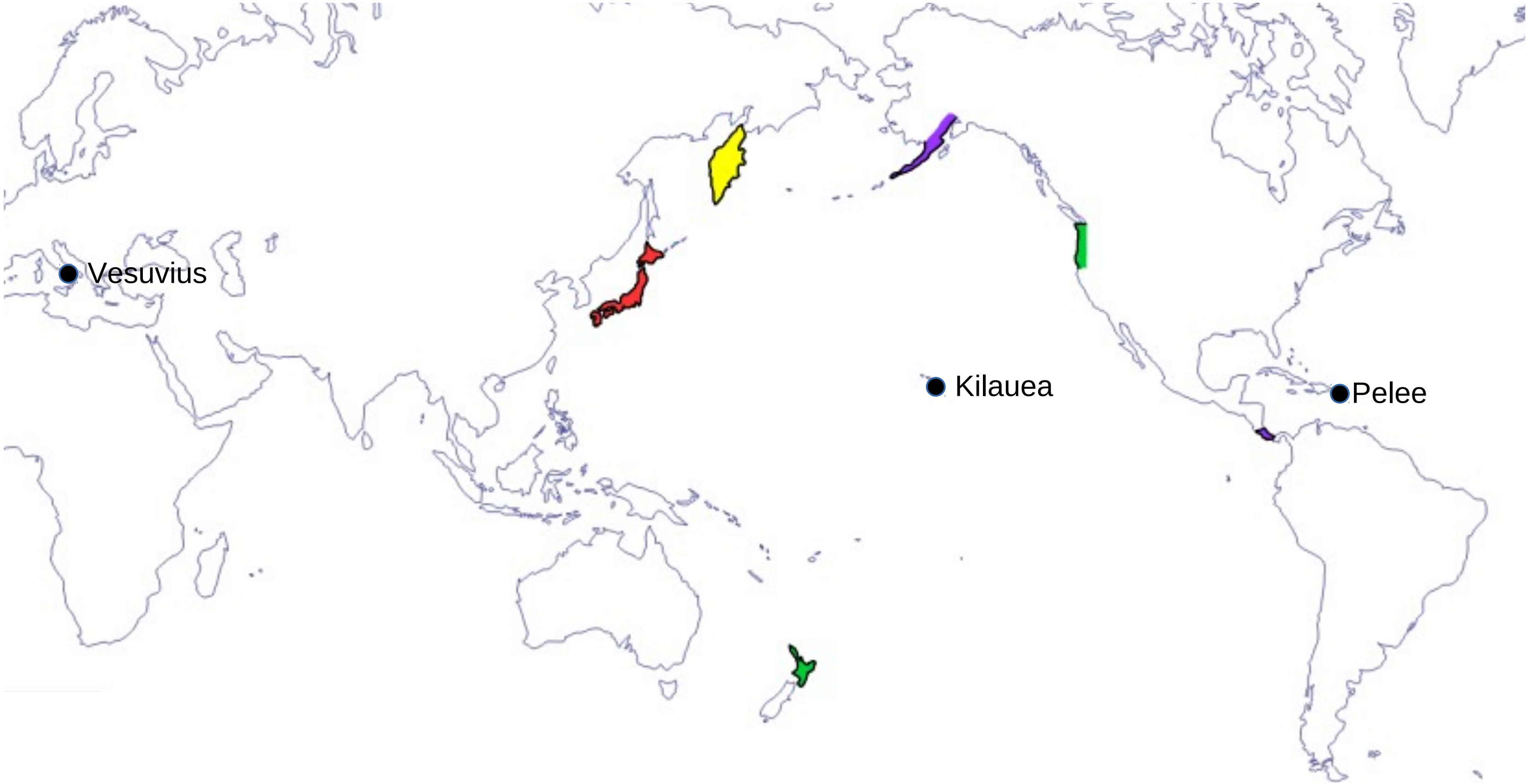

- In 1920 (3)
- 1920-29
- 1930-39
- 1940-49
- 1950-59
- 1960-69
- 1970-79

Krakatoa 1883; VEI 6

36 years earlier…

- 1883 August 27 VEI 6 eruption of Krakatoa a major focus of scientific investigation (Royal Society collection); e.g., earliest work in volcano acoustics
- Audible “canon-like” sounds documented by eyewitnesses at ~5,000 km

Symons [1888]

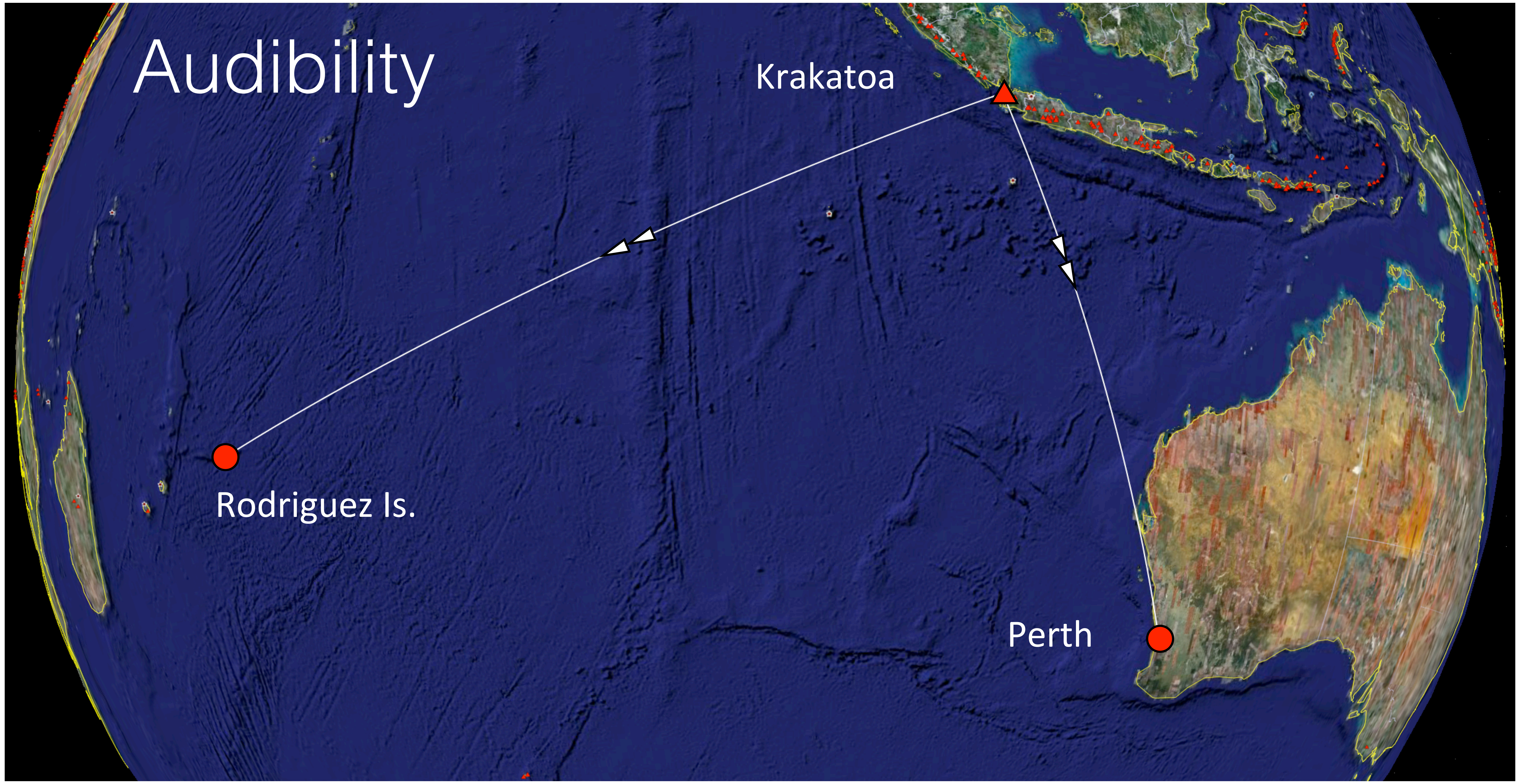

Scott [1883]

Krakatoa 1883; VEI 6

36 years earlier…

- Weather barographs (measuring atmospheric pressure) around the world record the blast wave from Krakatoa
- Pressure waves observed globally on >50 weather barometers; low-frequency acoustic wave periods 100–200 min; 7 laps of the globe

http://www.hemswell-antiques.com/antiques/other-scientific-items/victorian-barograph-36676.html

Recording barometers

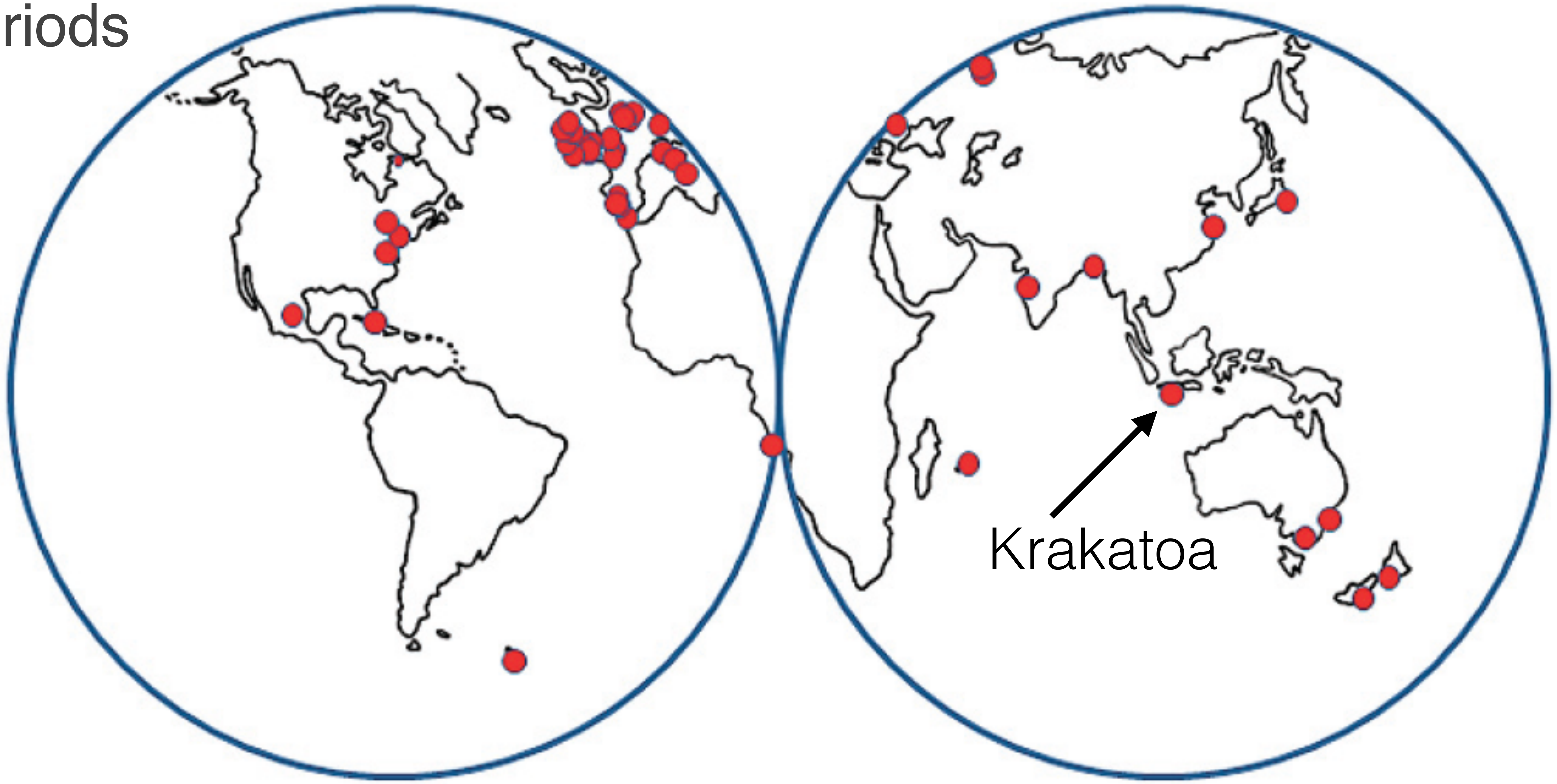

Scott [1883]

Krakatoa 1883; VEI 6

36 years earlier…

- Weather barographs (measuring atmospheric pressure) around the world record the blast wave from Krakatoa
- Pressure waves observed globally on >50 weather barometers; low-frequency acoustic wave periods 100–200 min; 7 laps of the globe

http://www.hemswell-antiques.com/antiques/other-scientific-items/victorian-barograph-36676.html

- Development of theory to explain these acoustic-gravity waves (e.g., *LeConte* 1884; *Lamb* 1911; *Taylor* 1929, 1936; *Pekeris* 1939; *Pierce* 1963; *Press and Harkrider* 1962, 1966; *Harkrider* 1964; *Harkrider and Press* 1967)

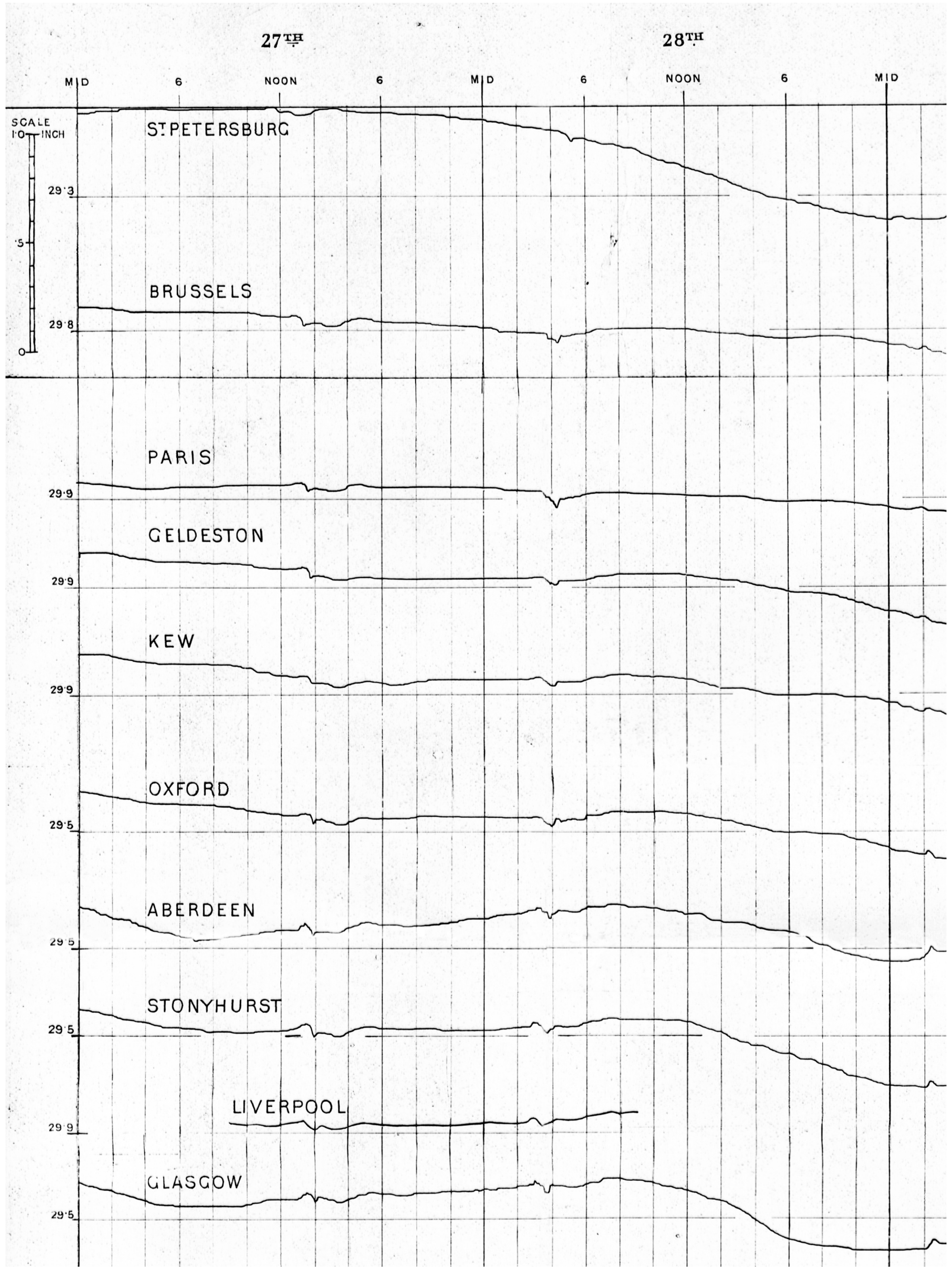

Scott [1883]

Early work in volcano seismology

- e.g., Luigi Palmieri 1856 “continuous tremor” at Vesuvius
- Omori [1912]: “The eruptions and earthquakes of the Asama-Yama”
- Omori’s two-component horizontal pendulum seismograph “tromometer” was the basis of the Bosch-Omori seismograph, later deployed worldwide

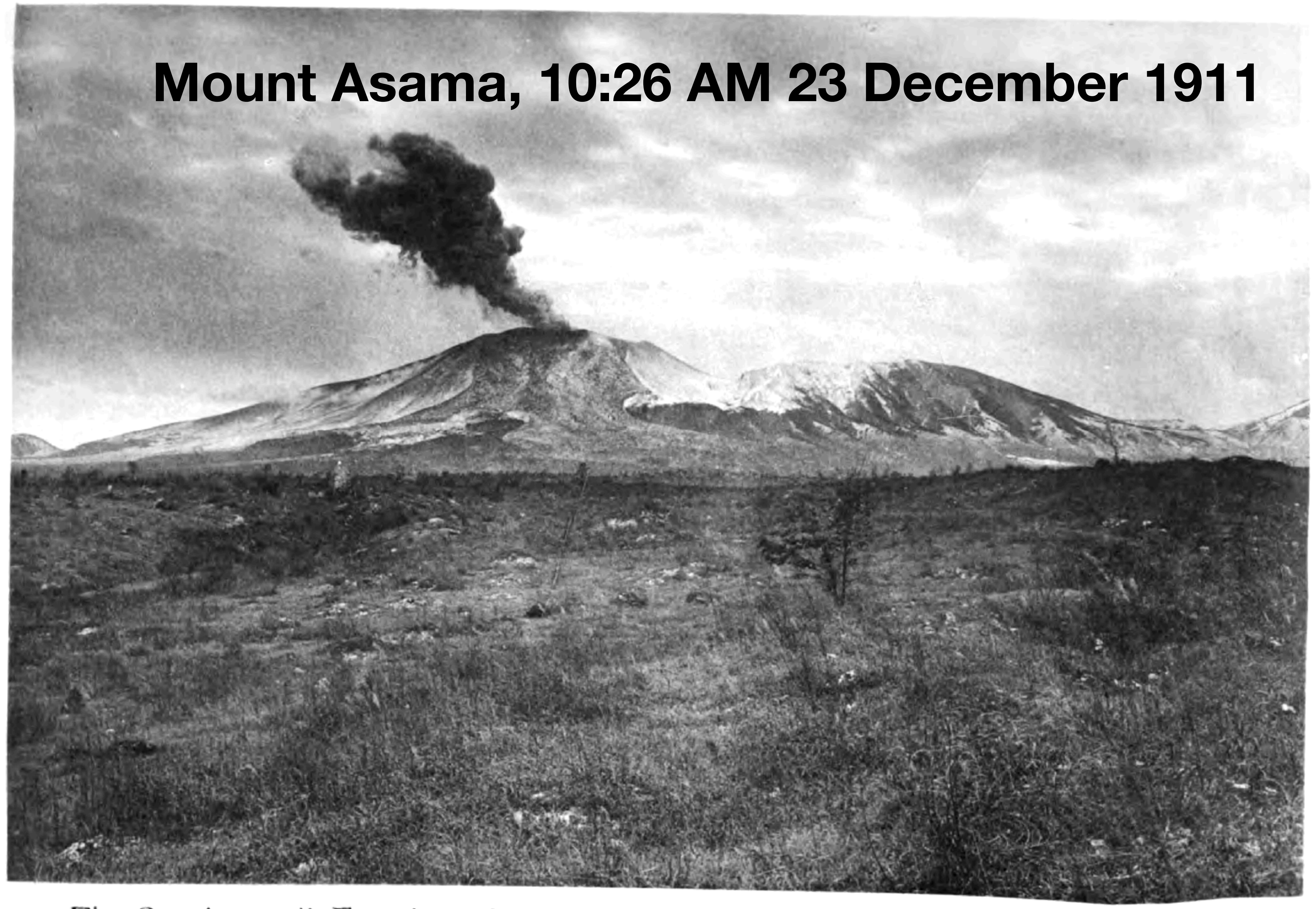

Fig. 2. A small Eruption of the Asama-yama, on Dec. 23rd, 1911, at 10.25 am, seen due southwards from the vicinity of the Kamahara-mura at the north base of the mountain. (F. Omori, photo.)

Pl. XX

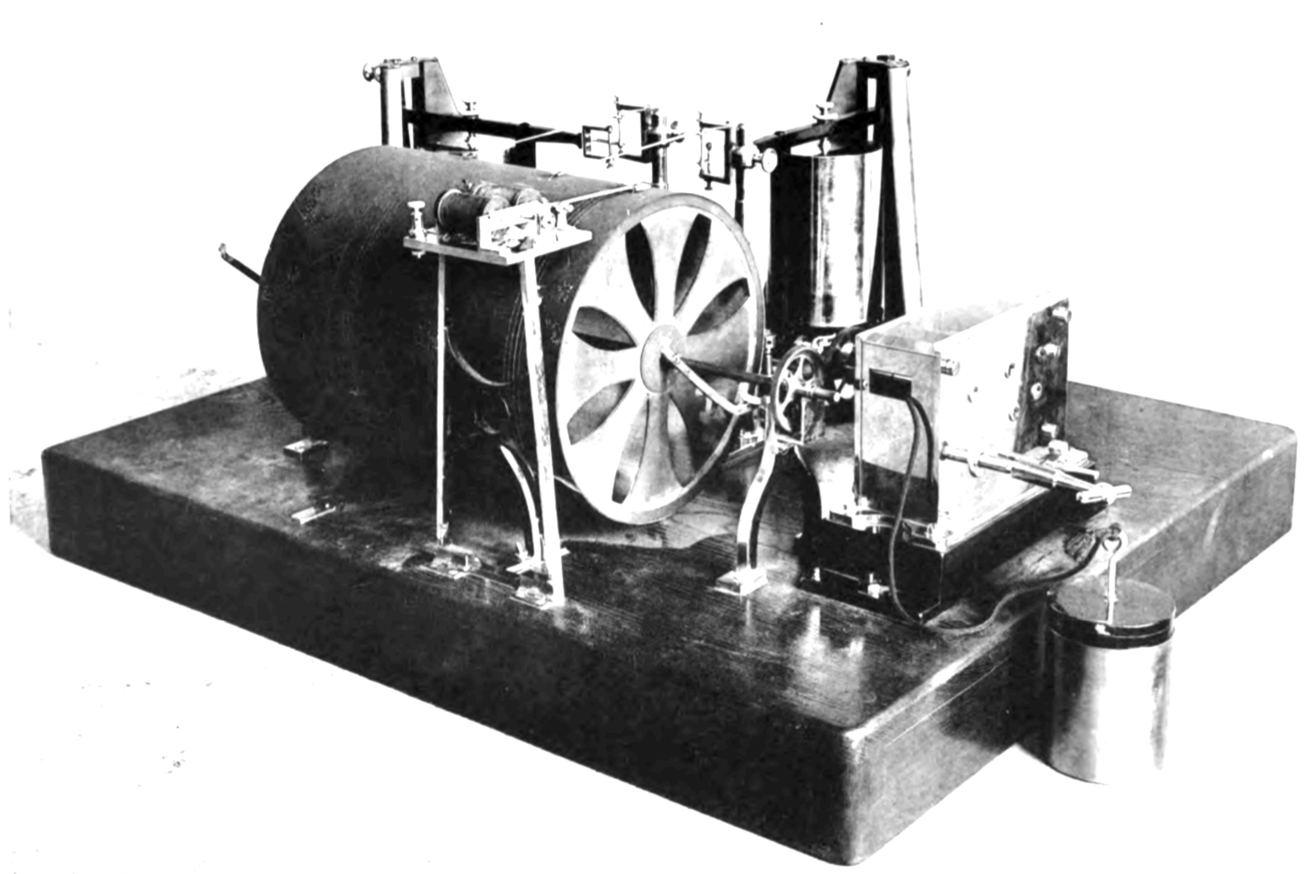

A Portable Two-component Horizontal Tremor Recorder.

THE ERUPTIONS AND EARTHQUAKES OF THE ASAMA-YAMA.(1)

By

F. OMORI, Sc. D.,

Member of the Imperial Earthquake Investigation Committee.

Fig. 49. Tromometer Observation at Ashino-taira, on the Asama-yama: Diagrams of a Volcanic Earthquake not accompanying an Eruption.

Asama-yama Earthquake of Feb. 22nd, 1911; 11.47.04 pm.

Longitudinal Vibration.

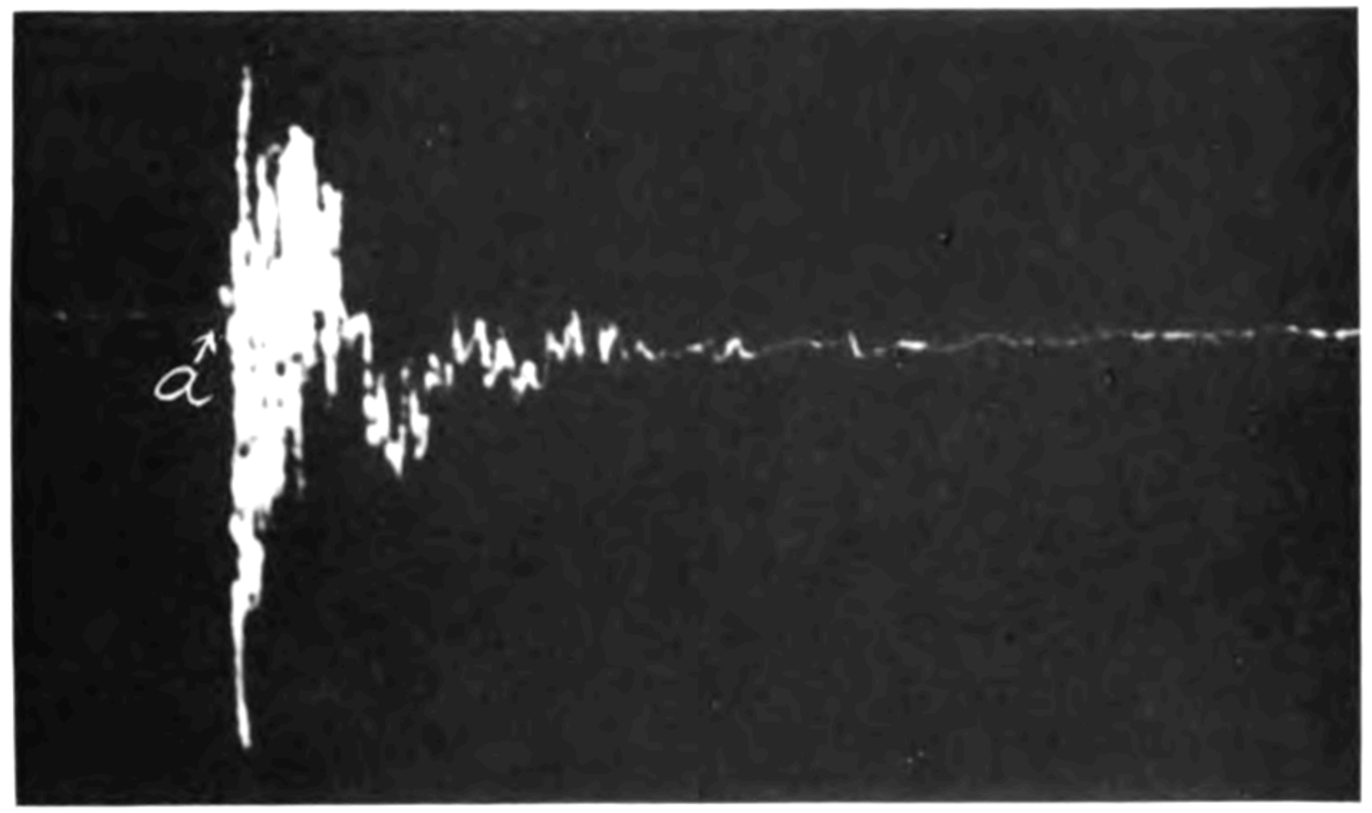

Time scale.
0 10 20 30 Second.

Transverse Vibration.

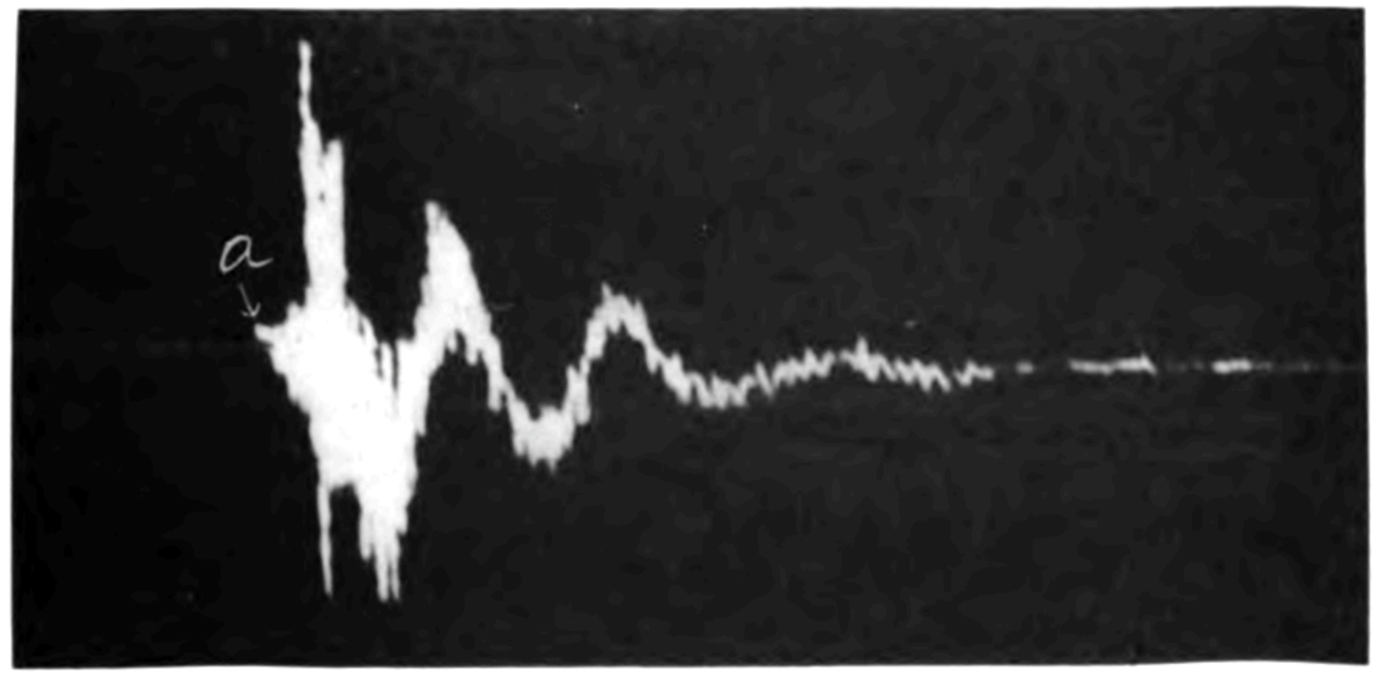

Magnification = 850.

Omori [1912]

Early work in volcano acoustics

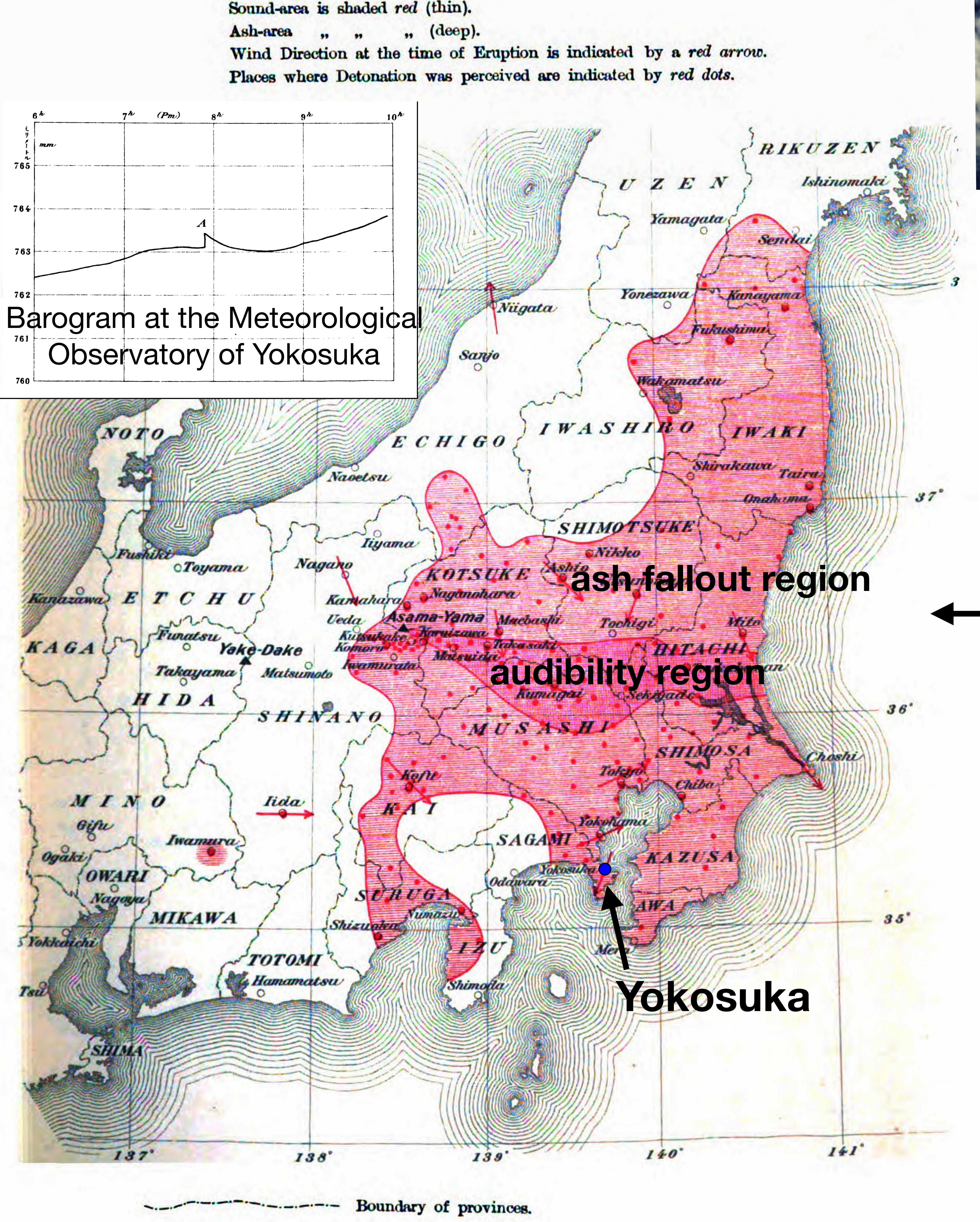

- **1912**
- Omori [1912] used seismometers and barometers to discriminate seismic signals from airborne explosions (“detonations”) and non-explosion earthquakes at Mount Asama, Japan

Early work in volcano acoustics

- **1906–1943**
- Pioneering seismic and acoustic work by Frank Perret at Vesuvius, Etna, Stromboli, Kilauea, Sakurajima, Pelee, Montserrat using moving-coil microphones (audible acoustic signals)

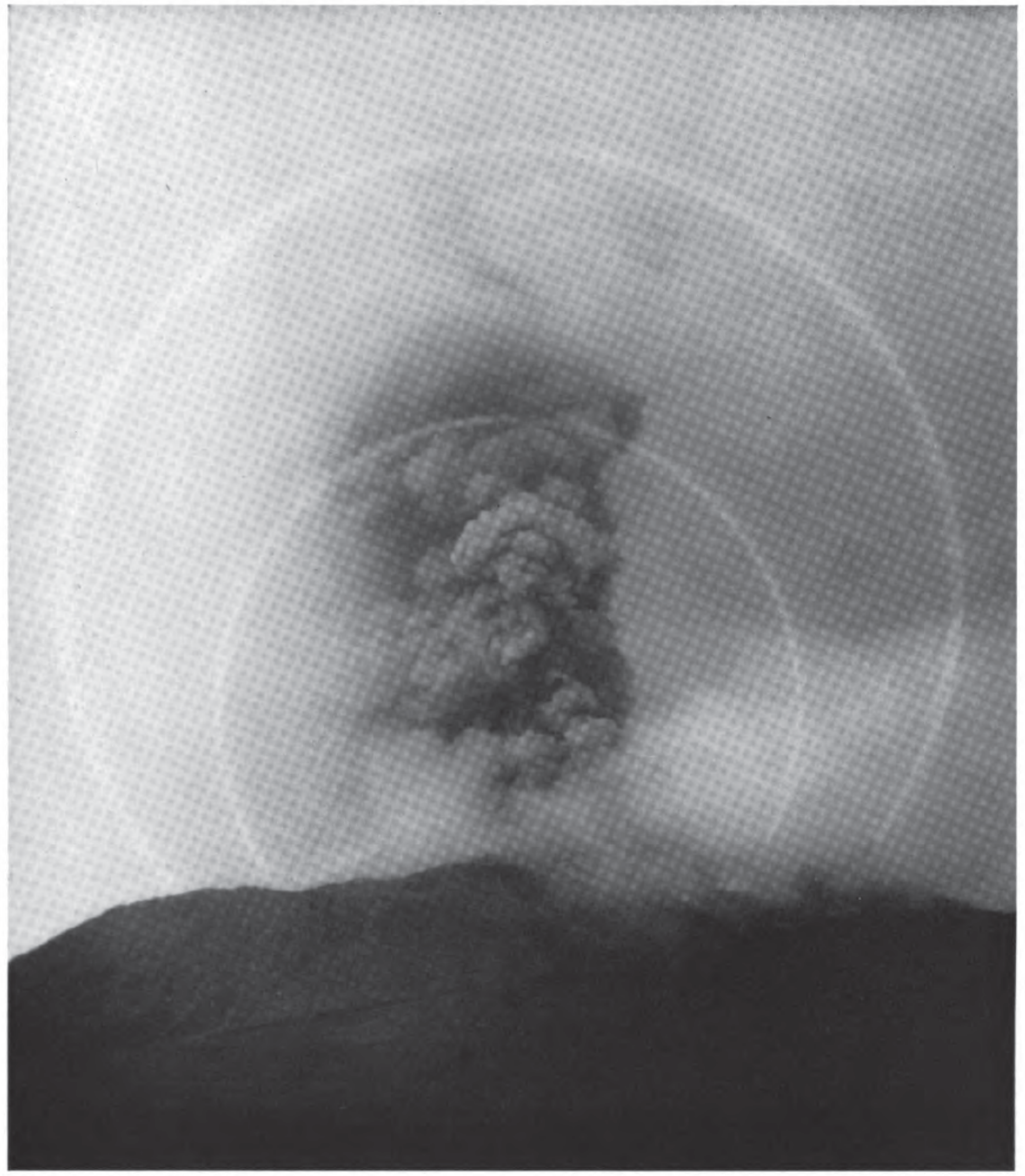

Fig. 71. Flashing arcs at Vesuvius as they would appear if caught by the camera. The edge of a spherical sound wave made visible by reflection and refraction (pages 81–82).

- **1912**
- Omori [1912] used seismometers and barometers to discriminate seismic signals from airborne explosions ("detonations") and non-explosion earthquakes at Mount Asama, Japan

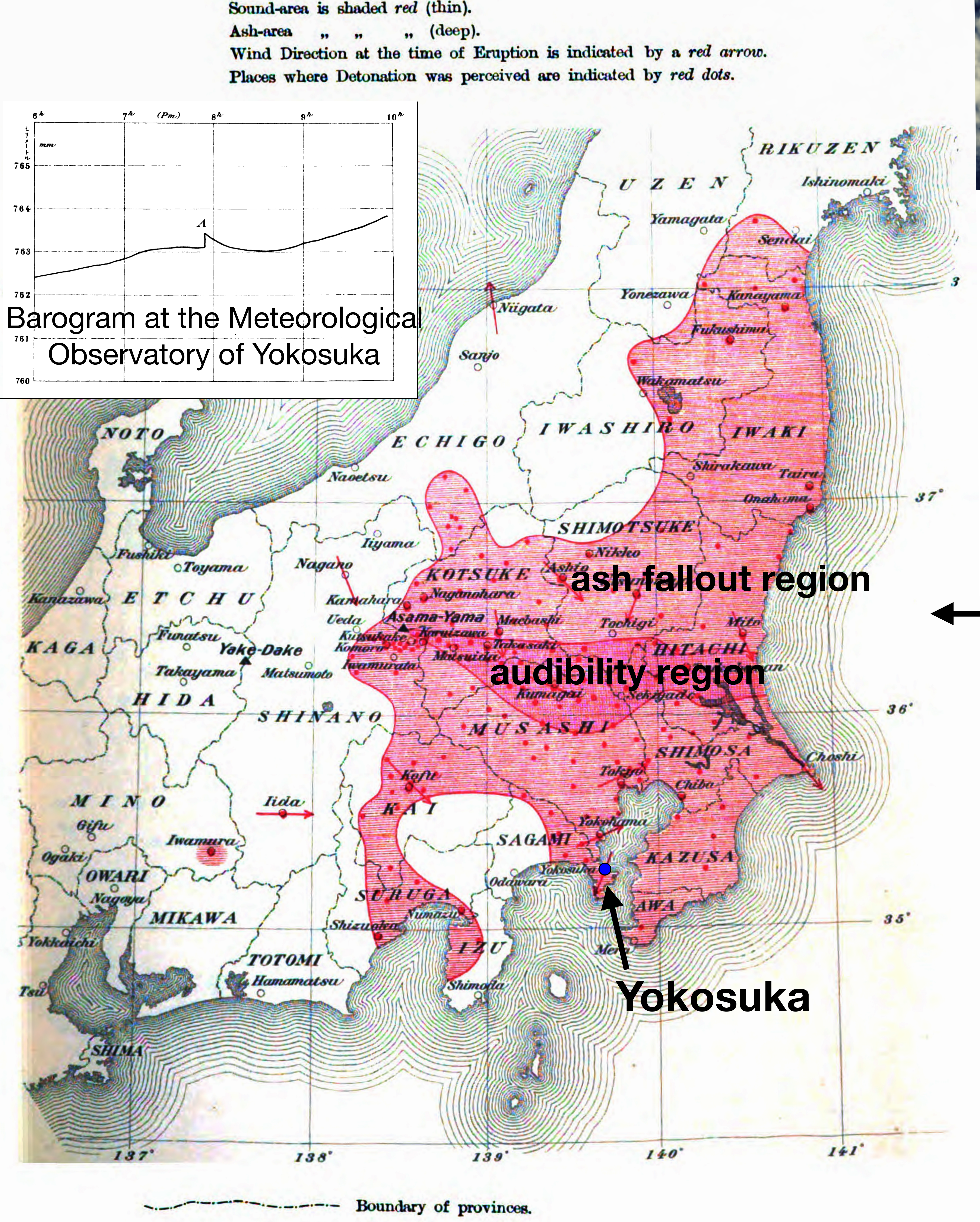

Instrumentation changes 1919–2019

- Volcano seismology and acoustics are highly observational fields
- What you see depends on instrumentation

- 1919–2019 major advances in:
  - Bandwidth (frequency range) of signals captured
  - Portability and ruggedness of instrumentation, telemetry
  - Computer revolution: Efficiency with which data can be processed and stored

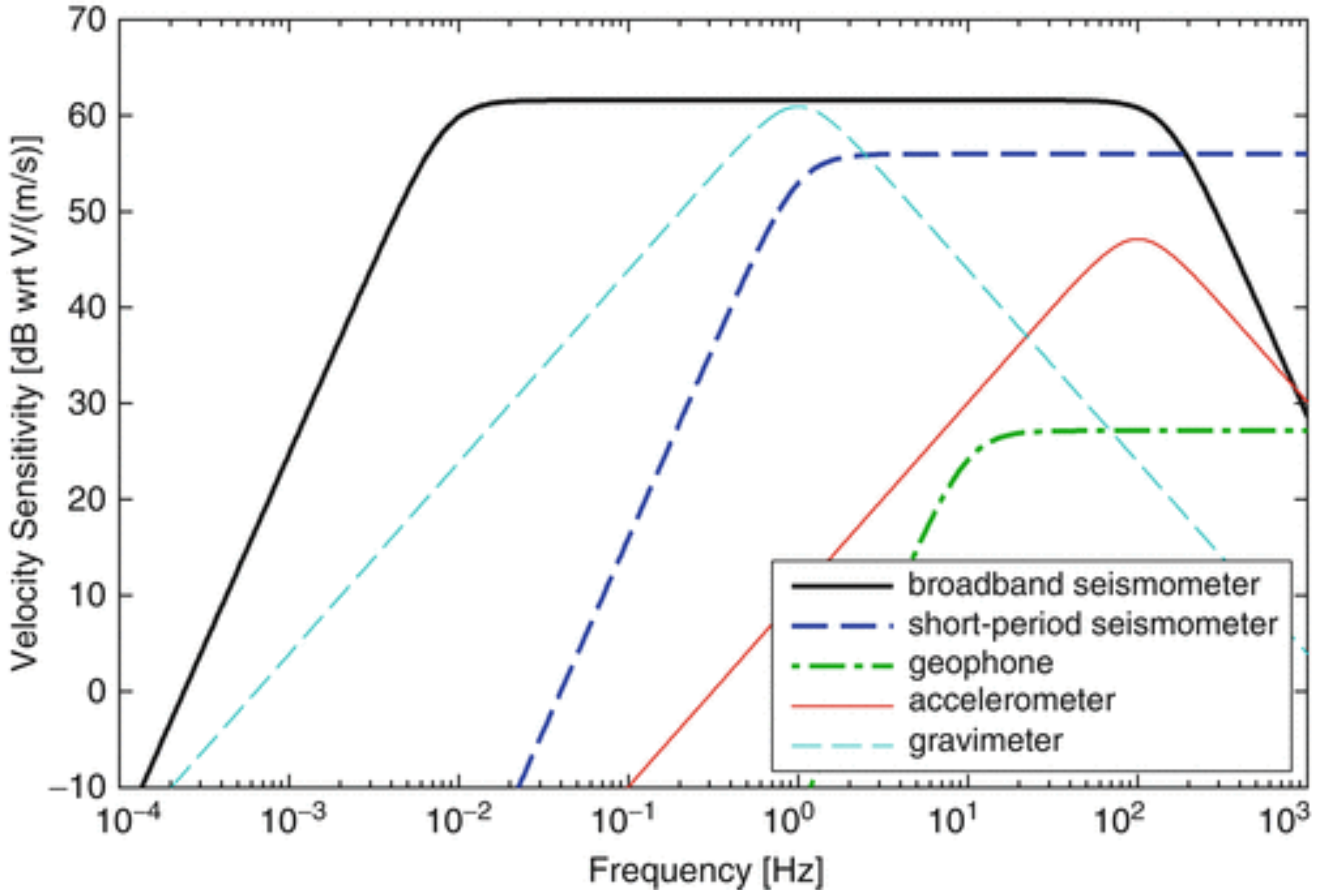

Ackerley [2015]
https://doi.org/10.1007/978-3-642-35344-4_172

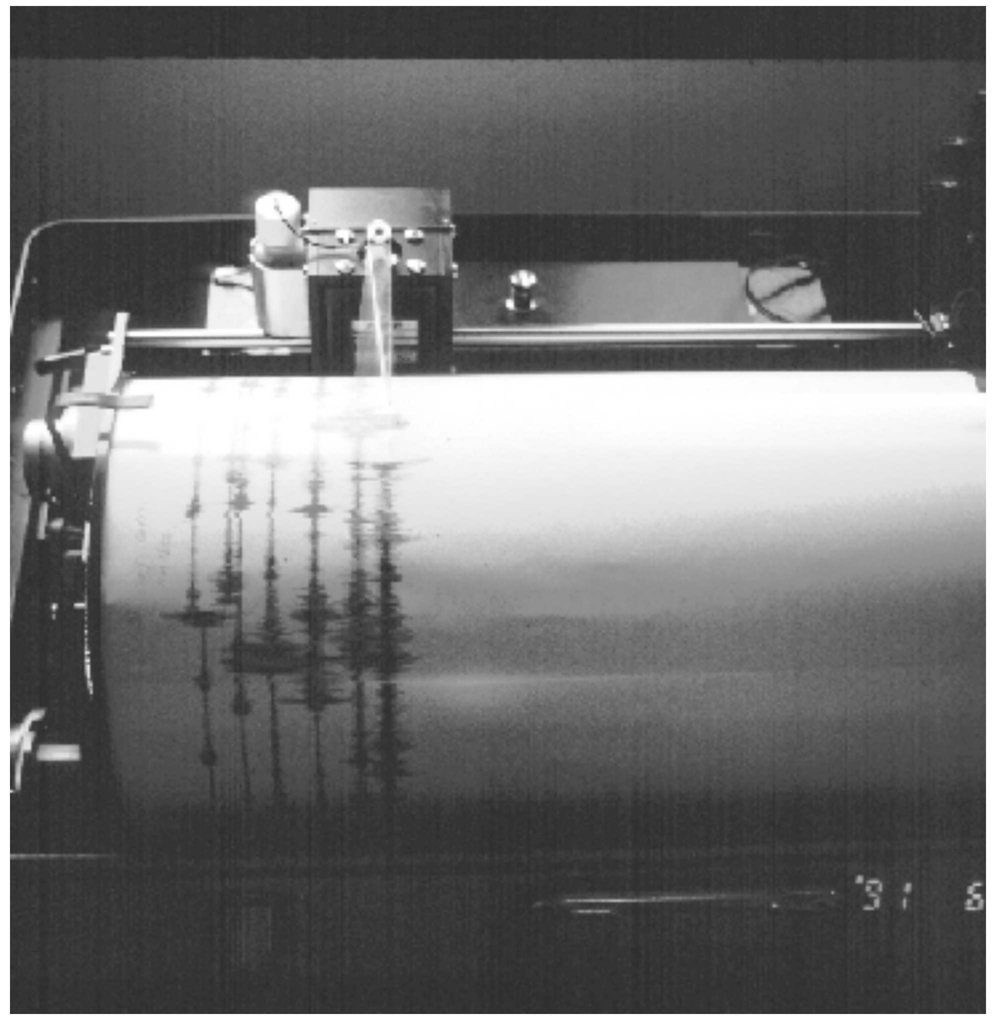

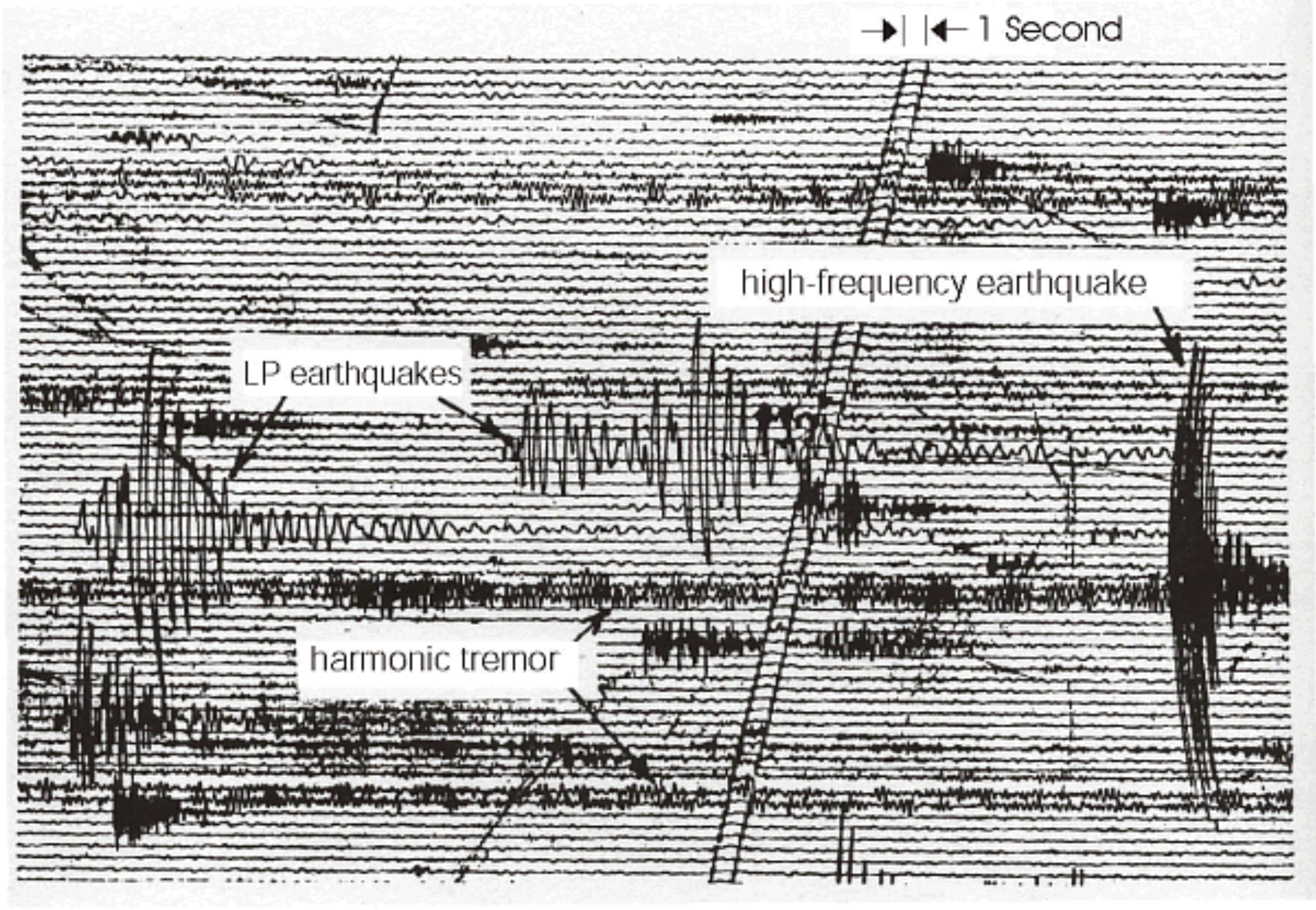

USGS

Instrumentation changes 1919–2019

e.g., Kilauea Iki, 1976

- **1970s:** limited portability
  - Installing and maintaining seismic equipment highly laborious
  - e.g., 4 miles of military grade Spiral-4 cable. Spiral-4 came in spools weighing 100 pound each; 40 were used.
  - Data stored on paper, digitized by hand to punch cards

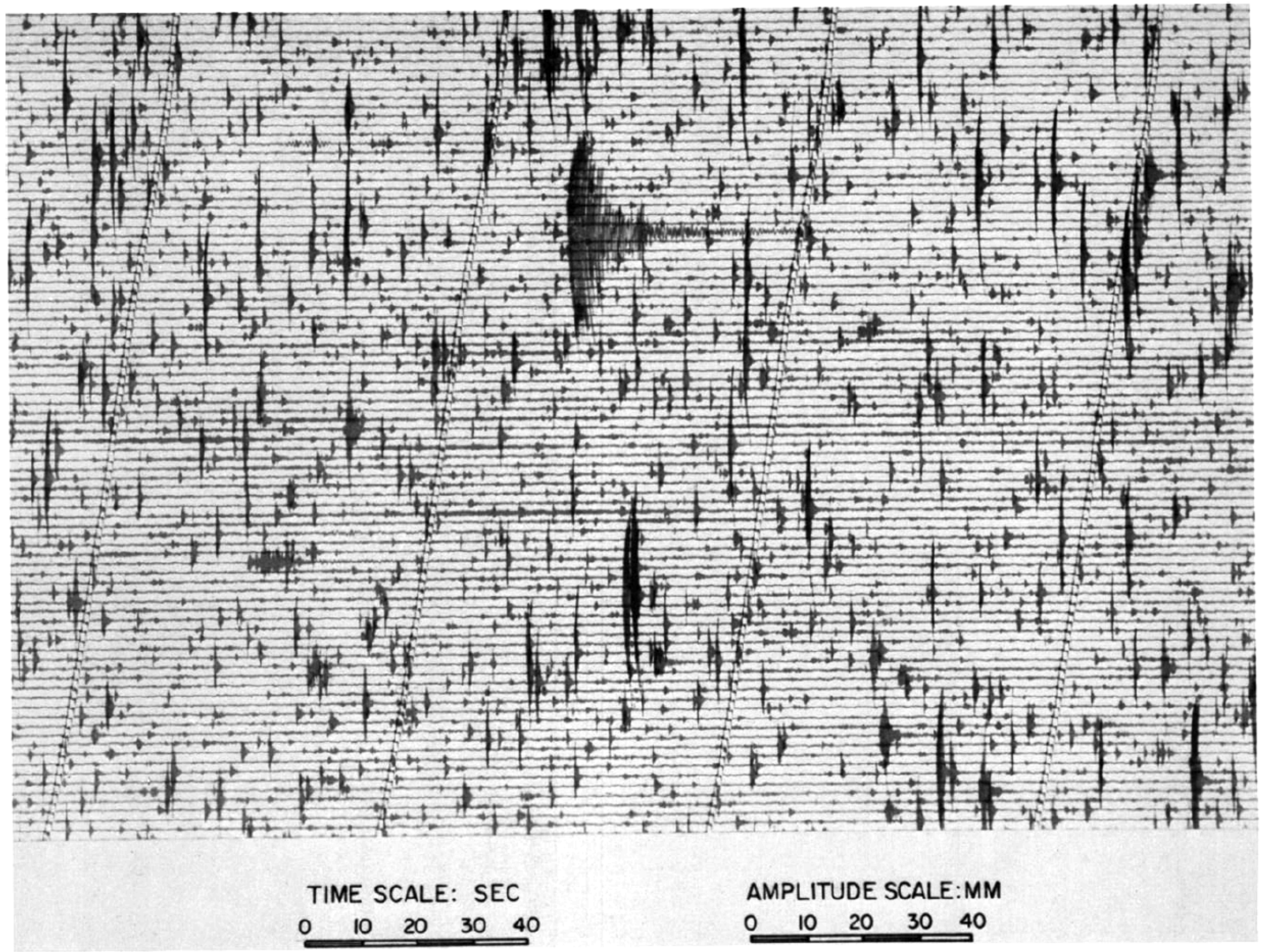

Fig. 3. Sample of record of the vertical component of motion obtained at nail 17 (see Figure 6*a*) with the portable seismograph. The tick marks shown are minute marks.

Sprengnether MEQ-800 smoke drum recorder with L-4C geophone

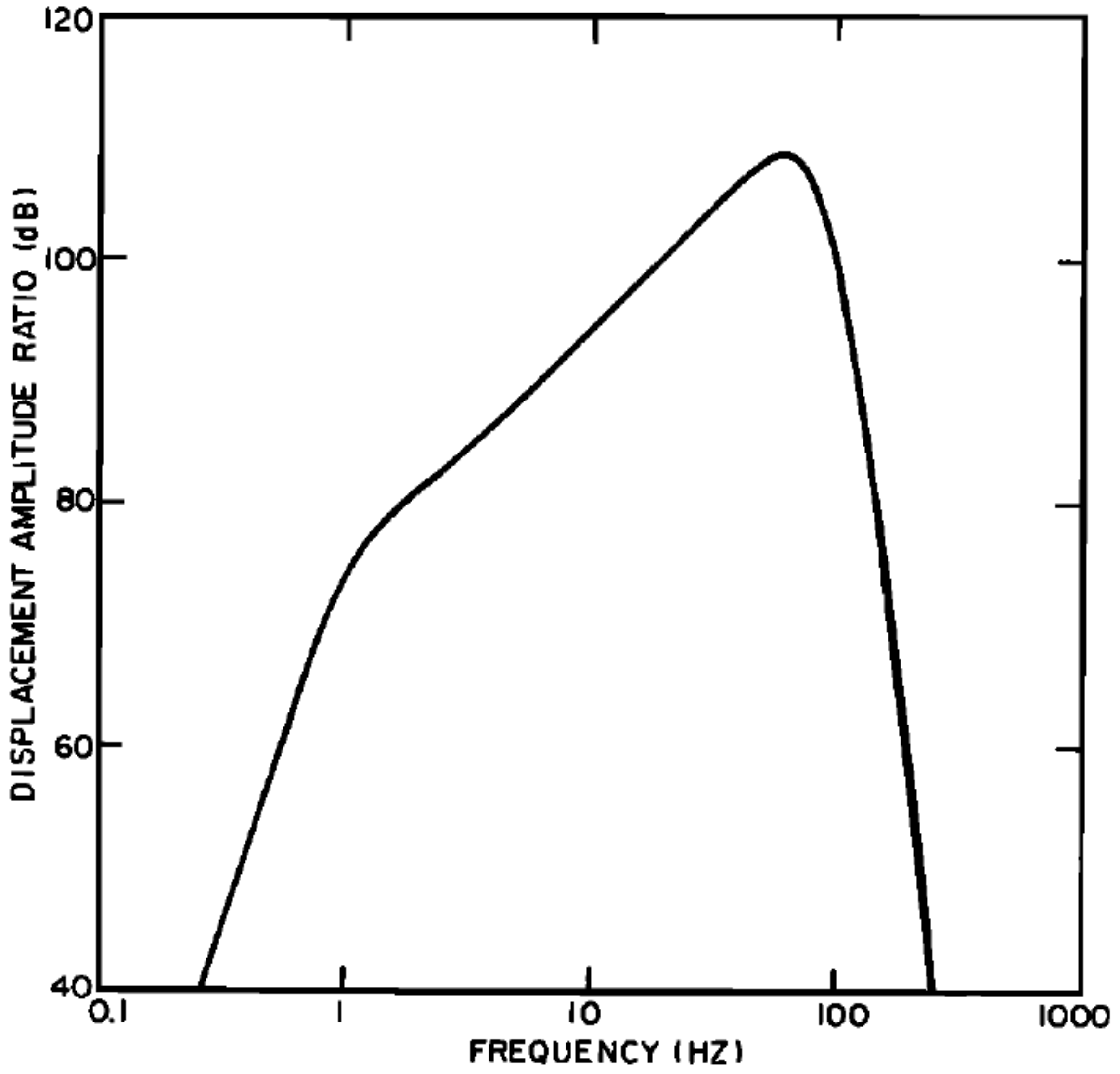

Fig. 2. Amplitude-frequency response (chart recorder trace to ground displacement amplitude ratio) of the portable seismograph used in the 1976 survey of seismic activity in Kilauea Iki. We used a drum-recording Sprengnether model MEQ-800 instrument with a vertical L-4C geophone as sensor.

Chouet, B. (1979), Sources of seismic events in the cooling lava lake of Kilauea Iki, Hawaii, *J. Geophys. Res.*, 84(B5), 2315– 2330, doi:10.1029/JB084iB05p02315.

Instrumentation changes 1919–2019

e.g., Mount St. Helens 1980–1986

- **1980s:** beginning of digital data capture and storage
  - e.g., Fehler (1983) — a prototype 12-bit recorder designed and built at MIT primarily for ocean bottom deployment.
  - Records long-period (LP) **0.5–5 Hz** seismicity and tremor at Mount St. Helens

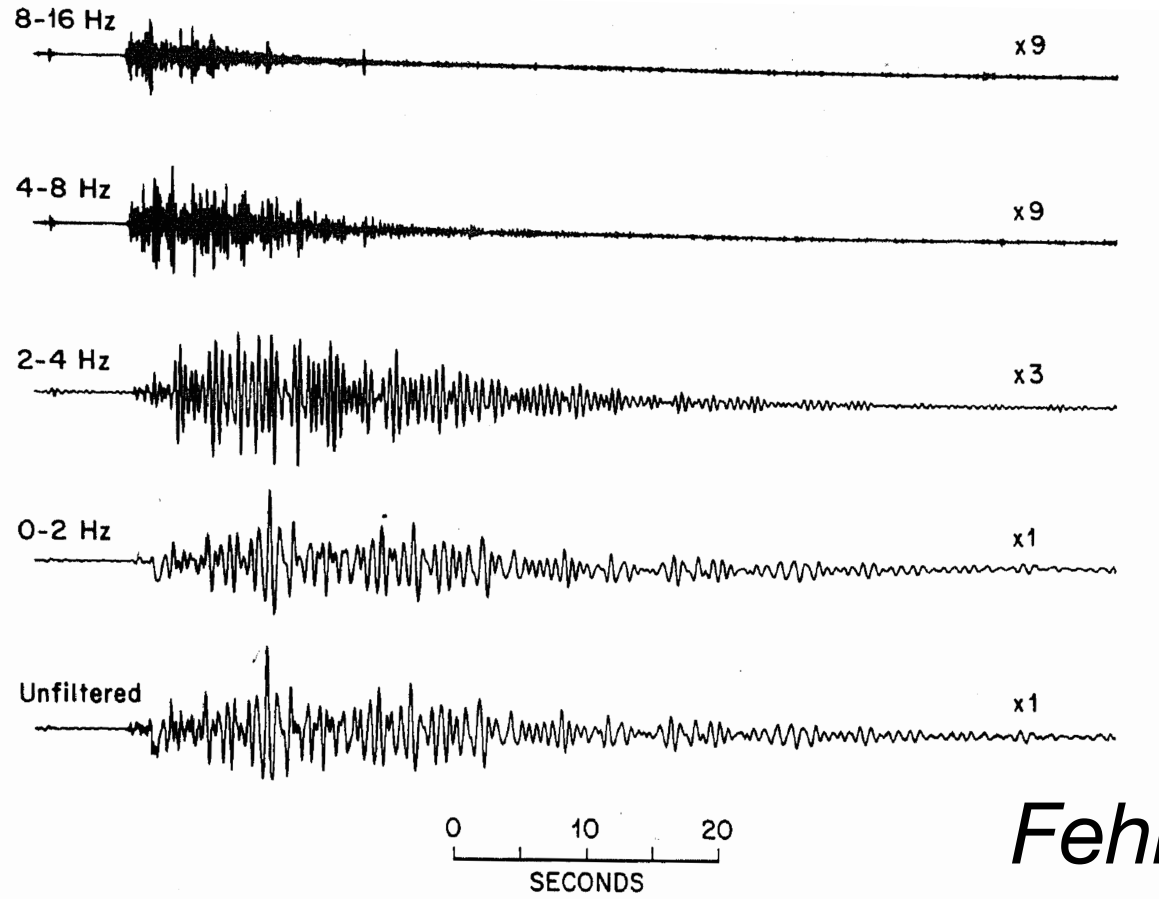

Fehler [1983]

Fig. 9. Waveform of a typical long-period earthquake recorded at Mount St. Helens in October 1980 (lower trace). Upper traces show the result when the waveform is filtered with a band pass filter. The passband of the filter is labeled next to each trace. Note that some of the filtered traces have been magnified compared to the original traces.

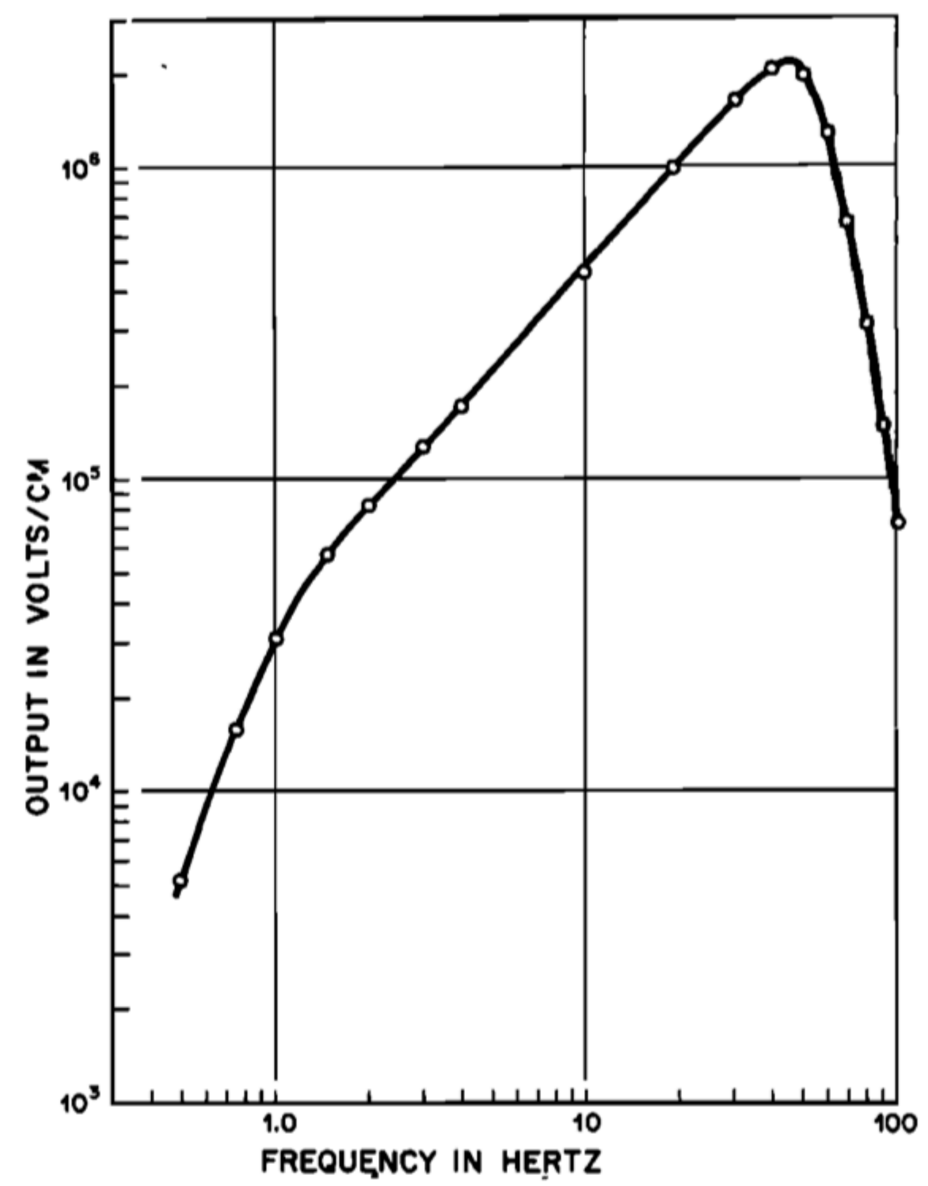

Fig. 1. Frequency response of digital event recorder system used to record volcanic tremor data at Mount St. Helens. Figure shows response of instrument to ground displacement when instrument is at maximum gain. Absolute response varies from event to event because of automatic gain control feature of the instrument.

Fehler, M. (1983), Observations of volcanic tremor at Mount St. Helens Volcano, J. Geophys. Res., 88(B4), 3476– 3484, doi: 10.1029/JB088iB04p03476.

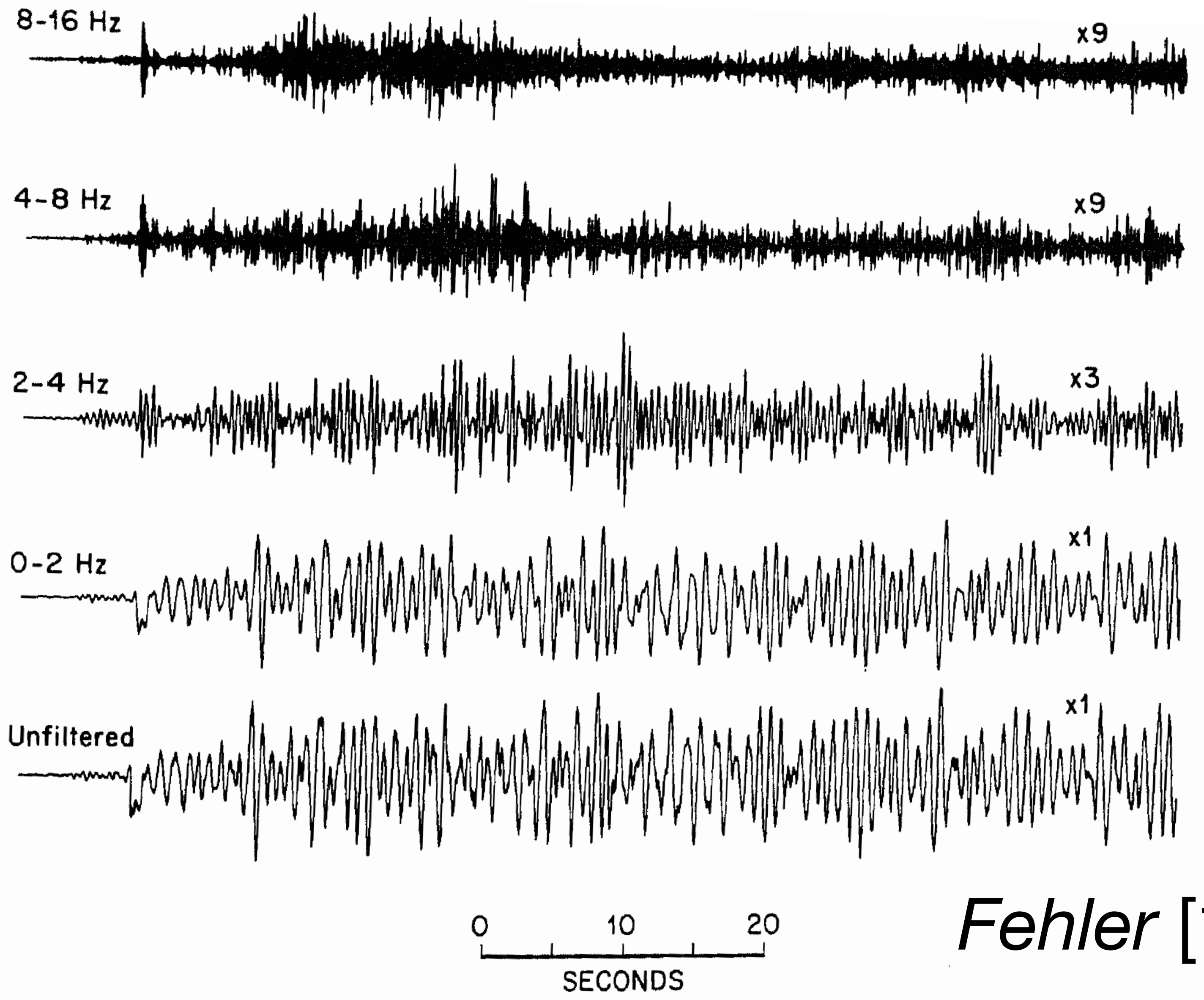

Fehler [1983]

Fig. 10. Waveform of a tremor event and filtered traces.

Instrumentation changes 1919–2019

Mount St. Helens 1980

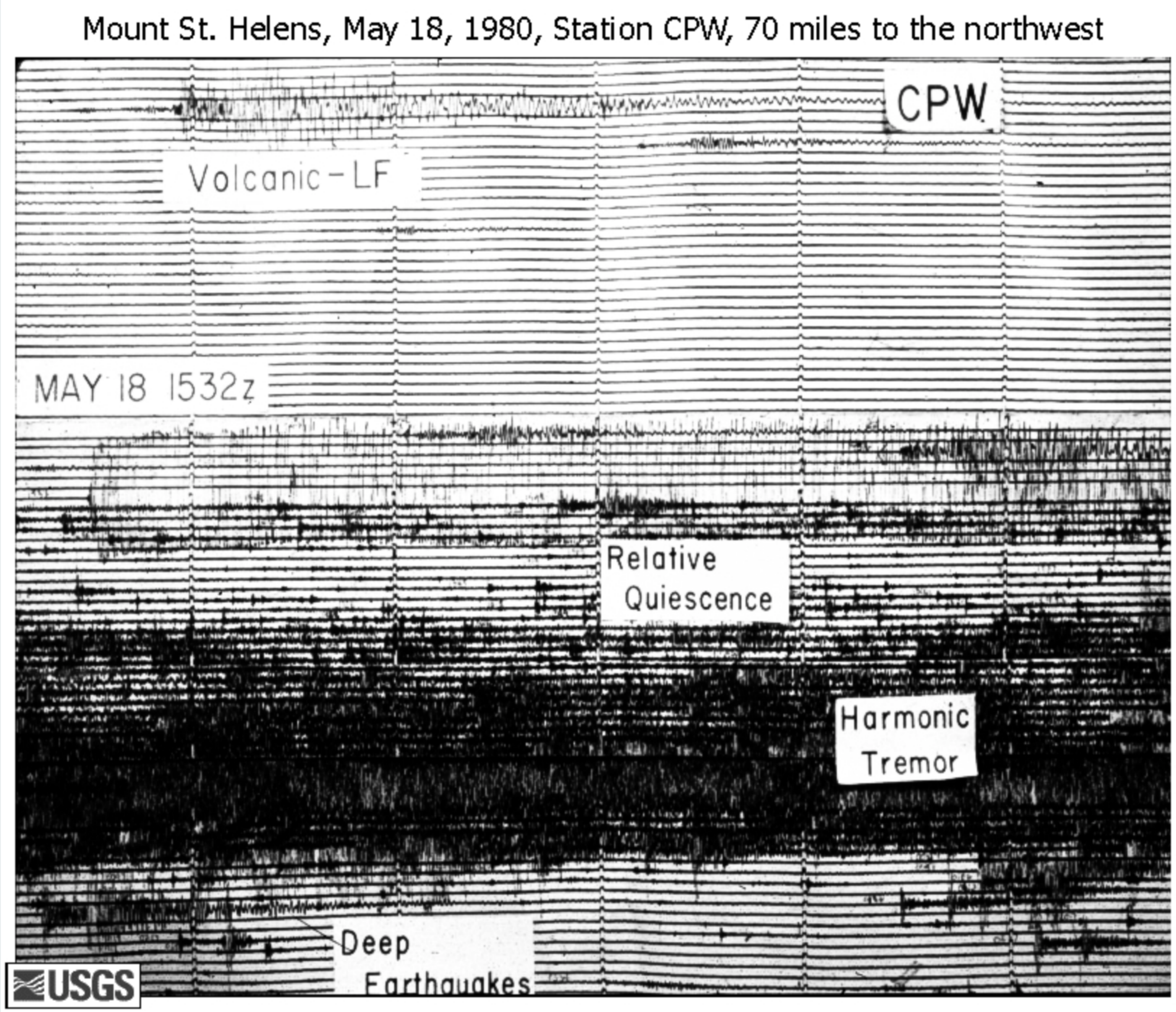

Pinatubo 1991

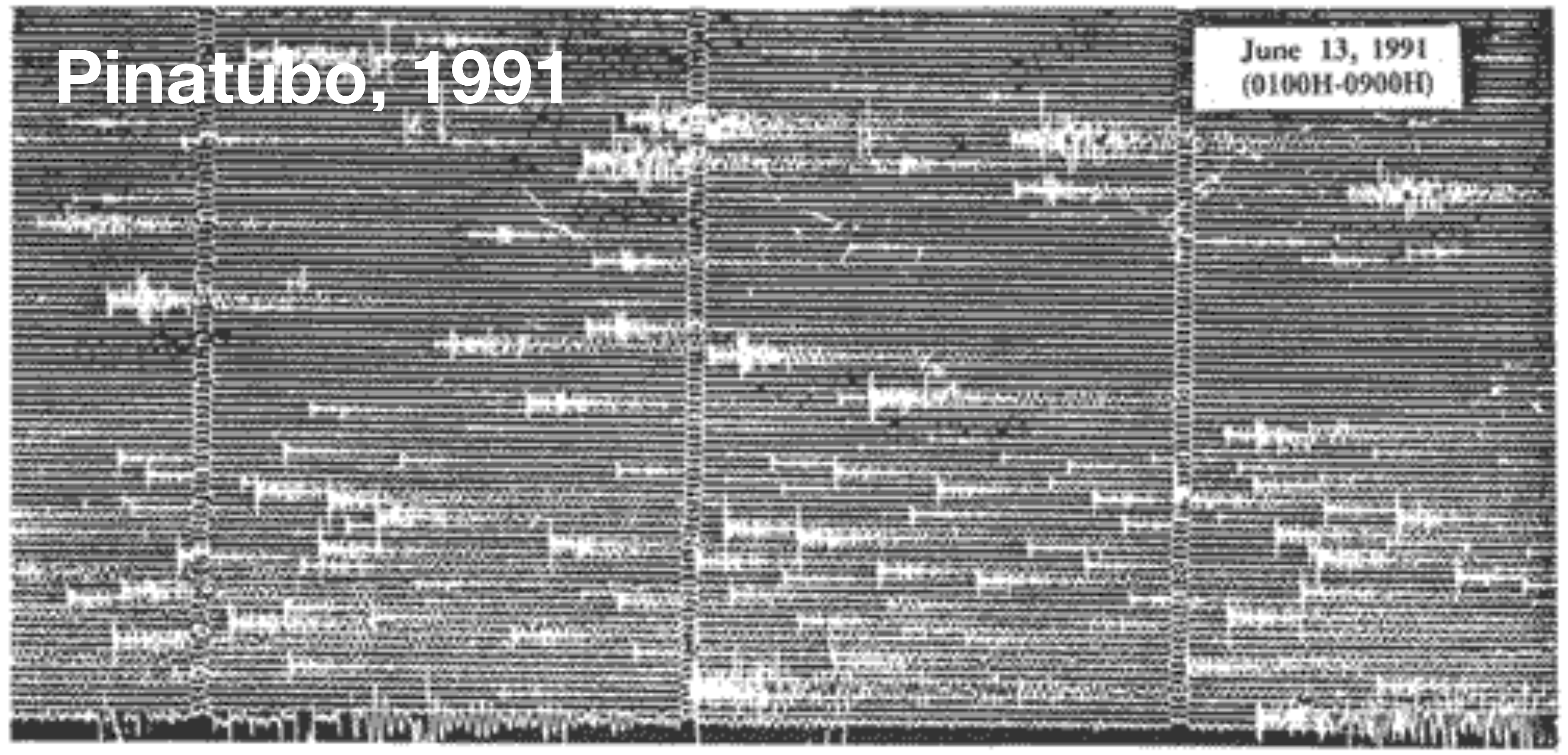

Sabit et al. [1996]

Ramos et al. [1996]

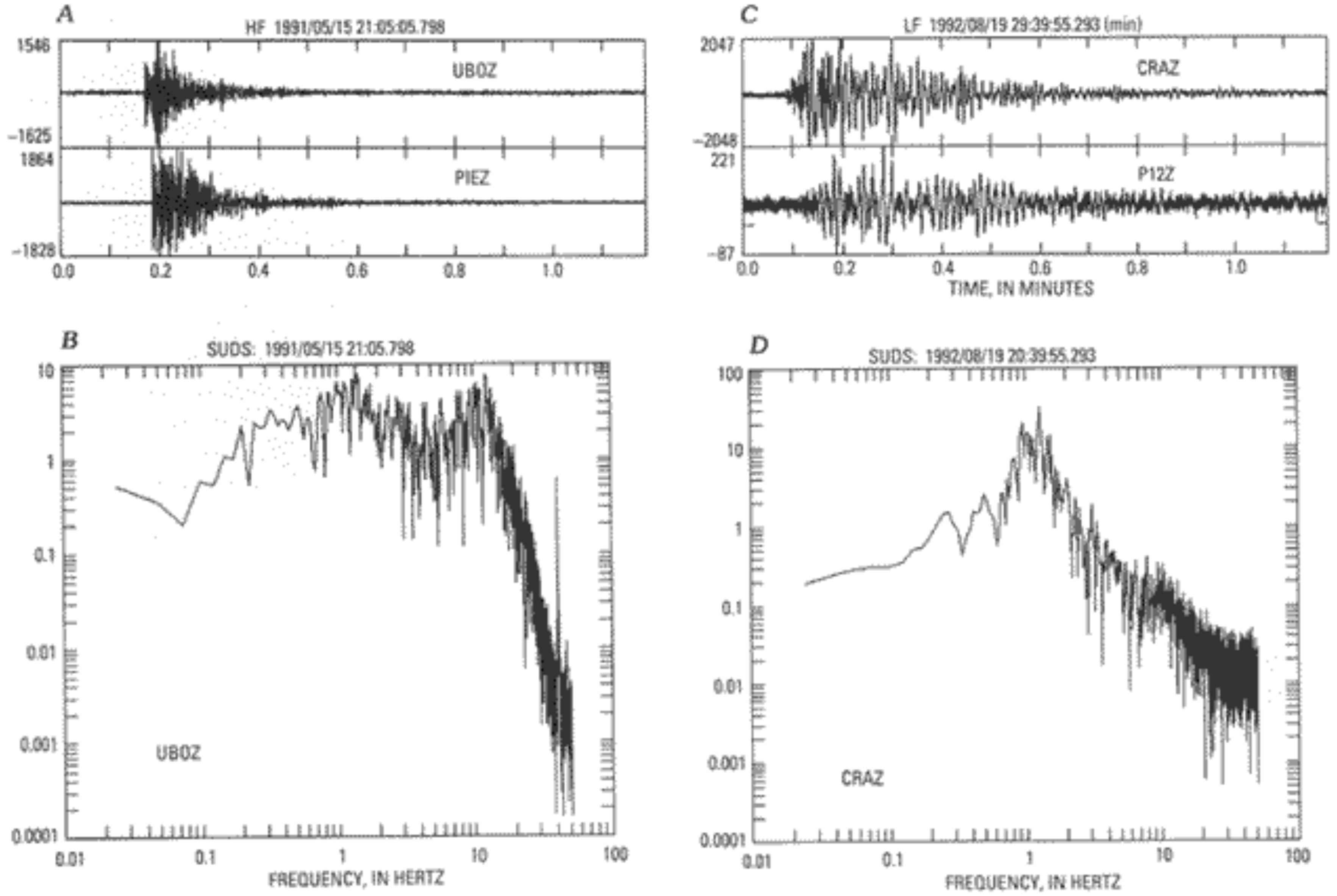

Instrumentation changes 1919–2019

Sakurajima

Kawakatsu et al. [1992]

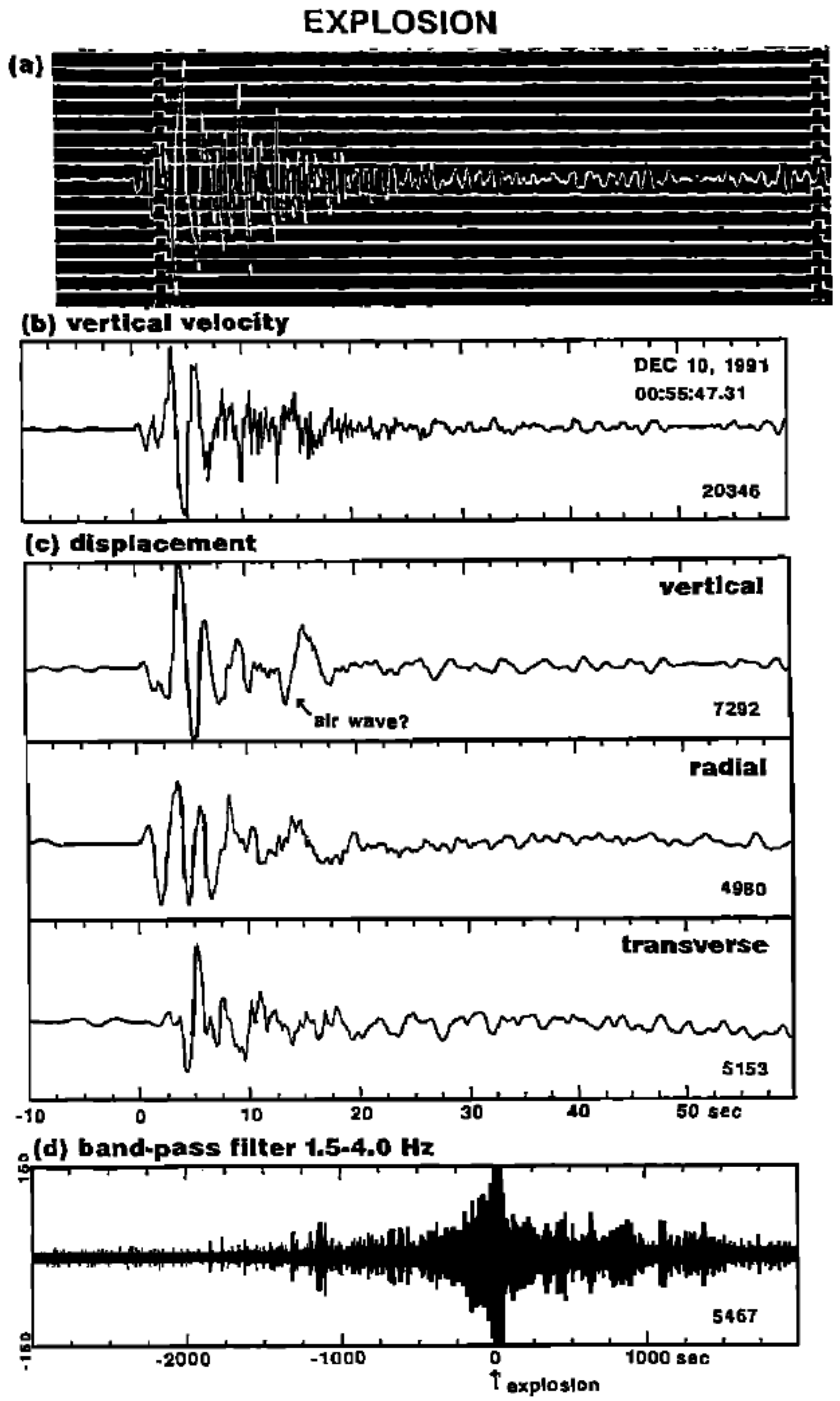

Stromboli

Neuberg et al. [1994]

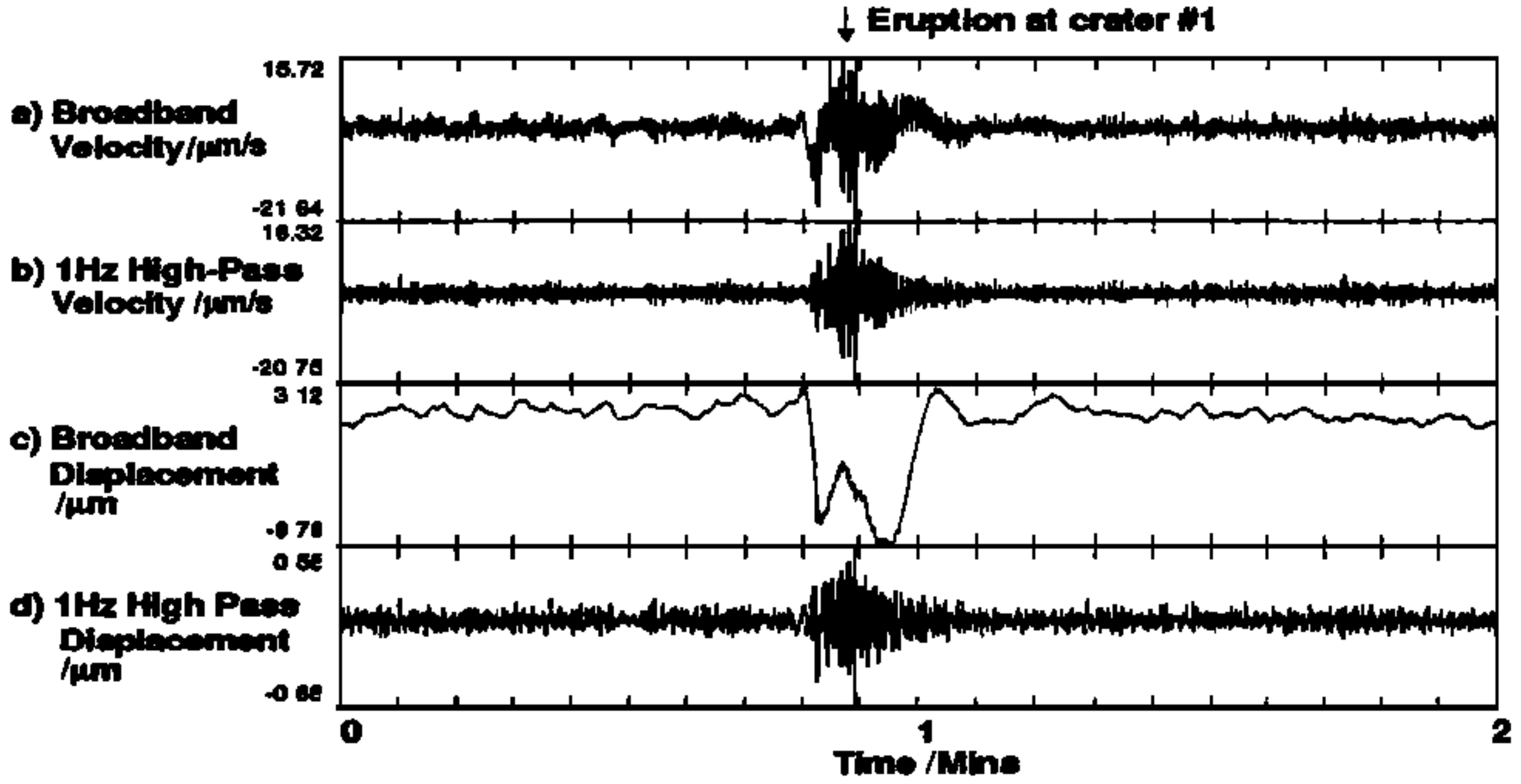

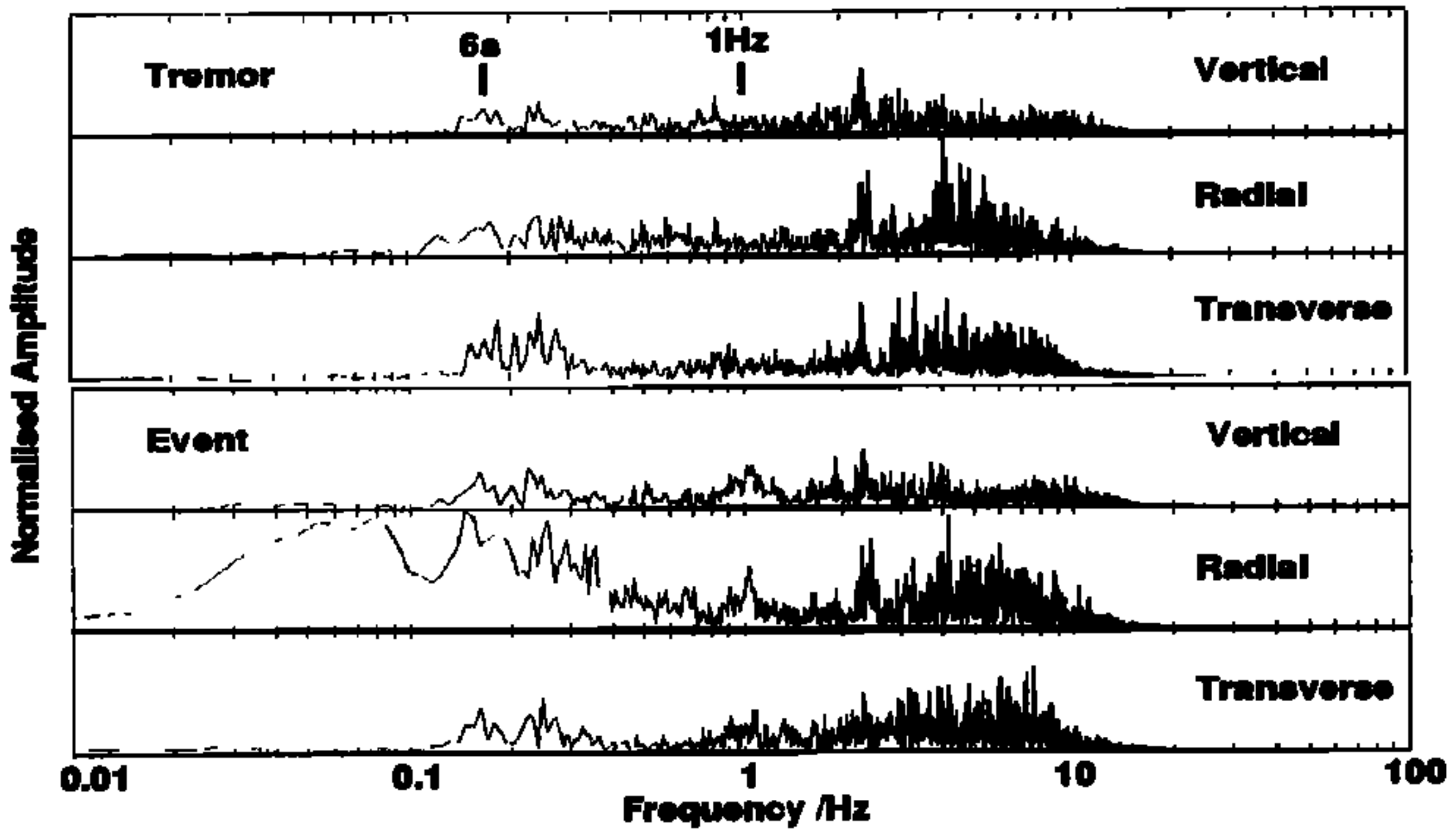

- **1990s:** the advent of (portable) broadband seismometry at volcanoes
- Led to discoveries of new signals: Very-Long-Period (VLP) **0.01–0.5 Hz** and Ultra-Long-Period (ULP) **<0.01 Hz**

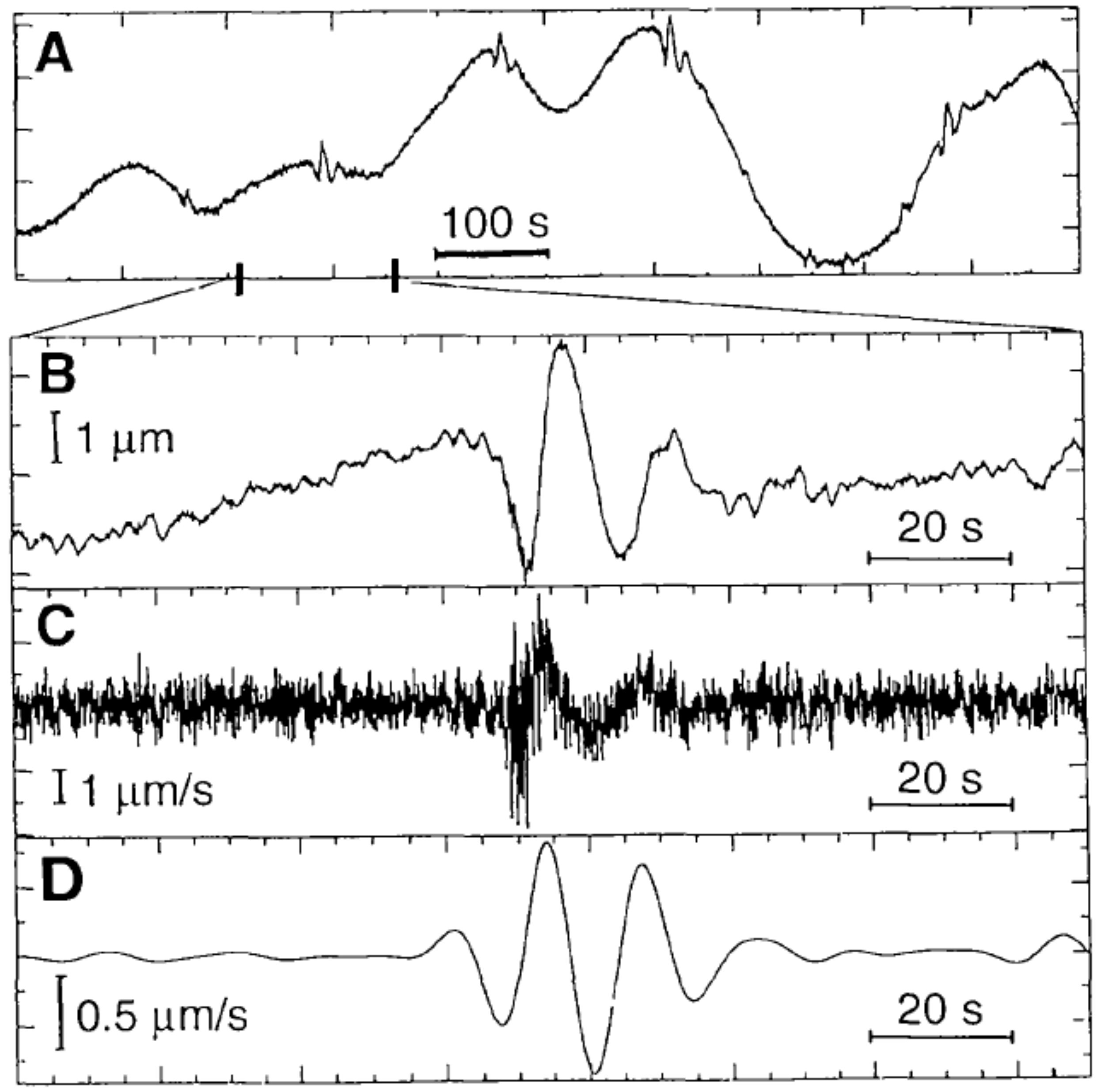

Aso

Kaneshima et al. [1996]

Instrumentation changes 1919–2019

Stromboli; Ripepe et al. [1996]

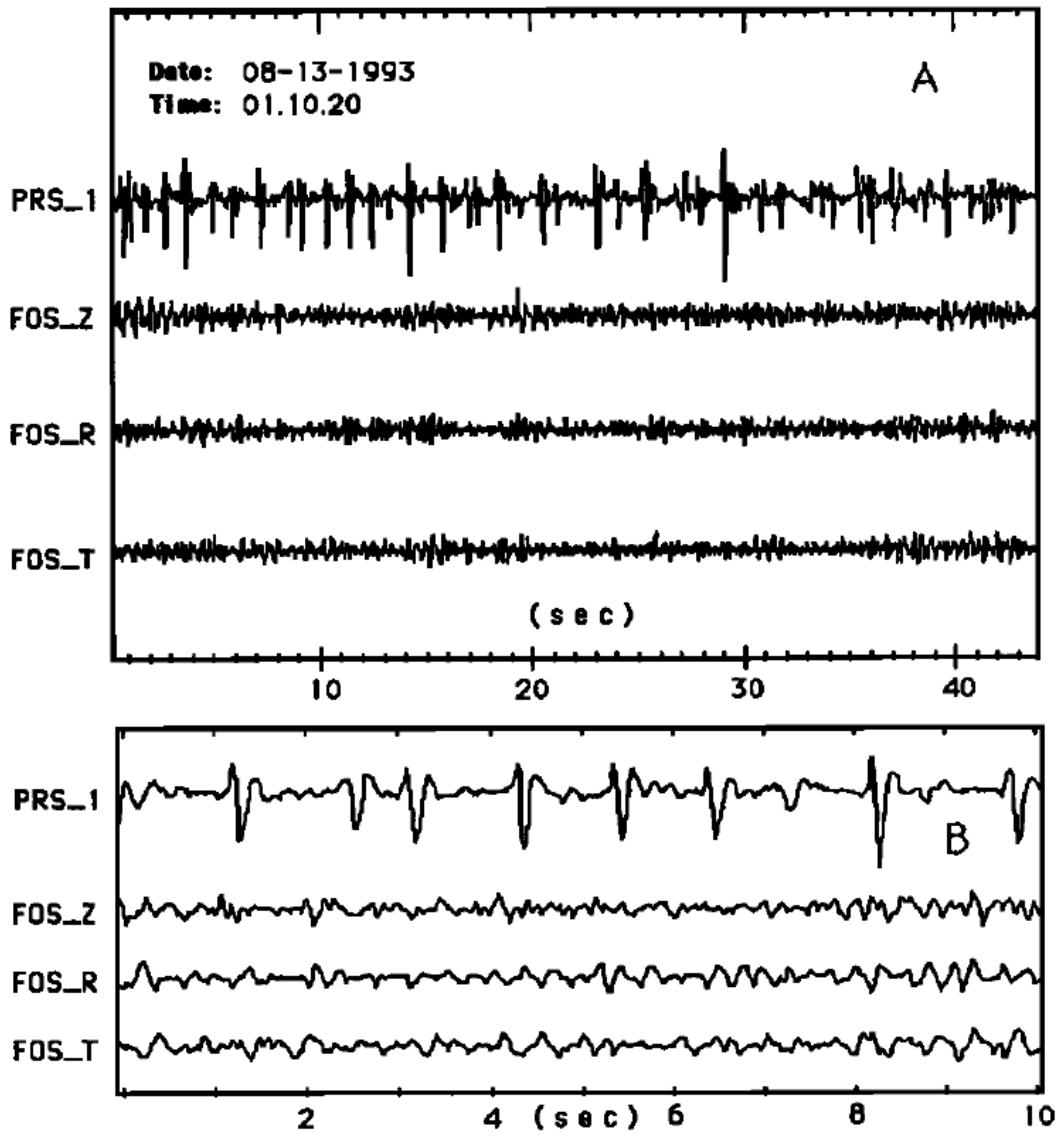

Stromboli; Vergniolle and Brandeis [1994]

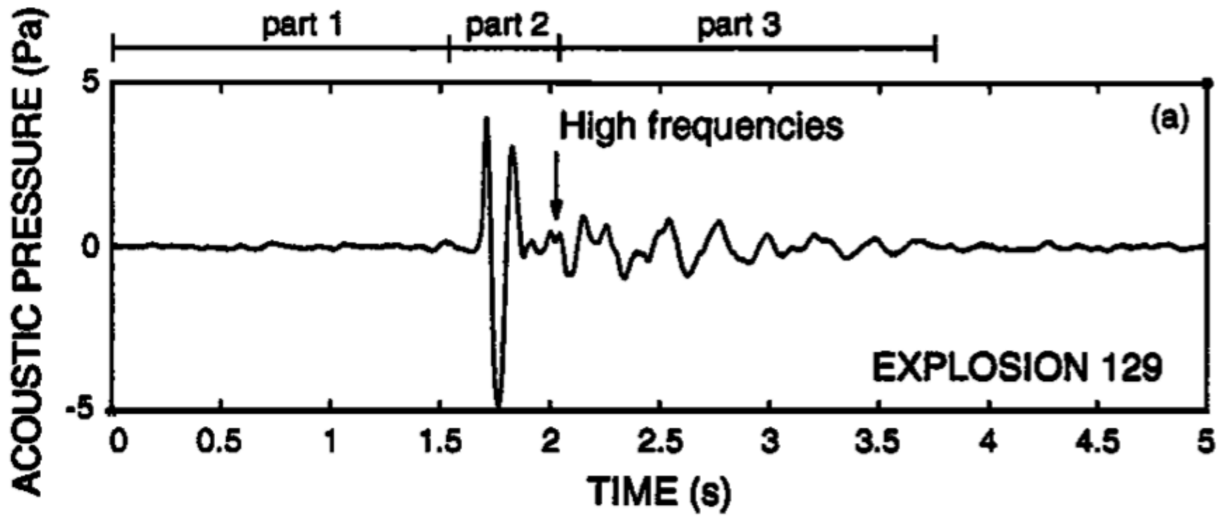

Sakurajima; Sakai et al. [1996]

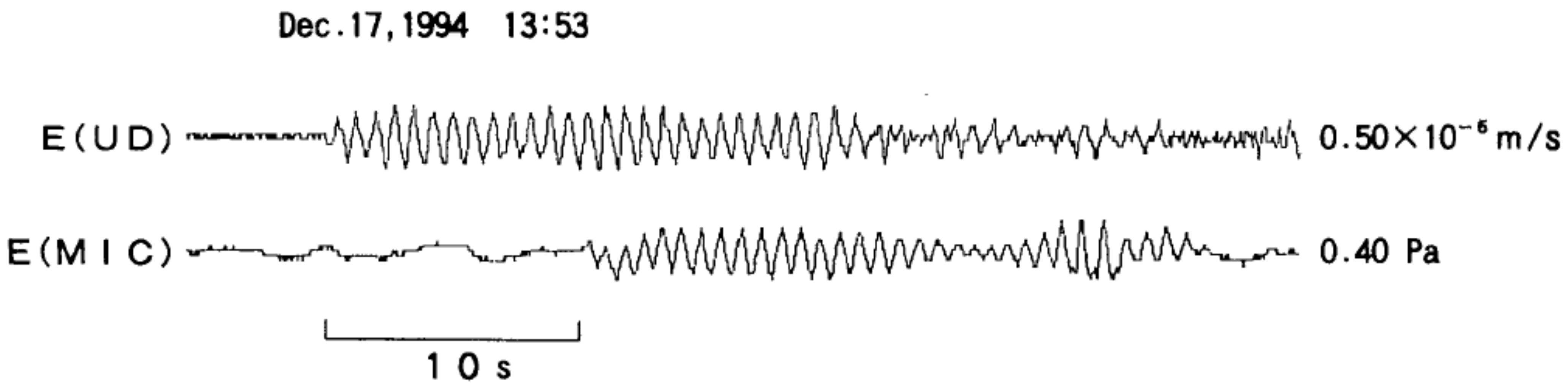

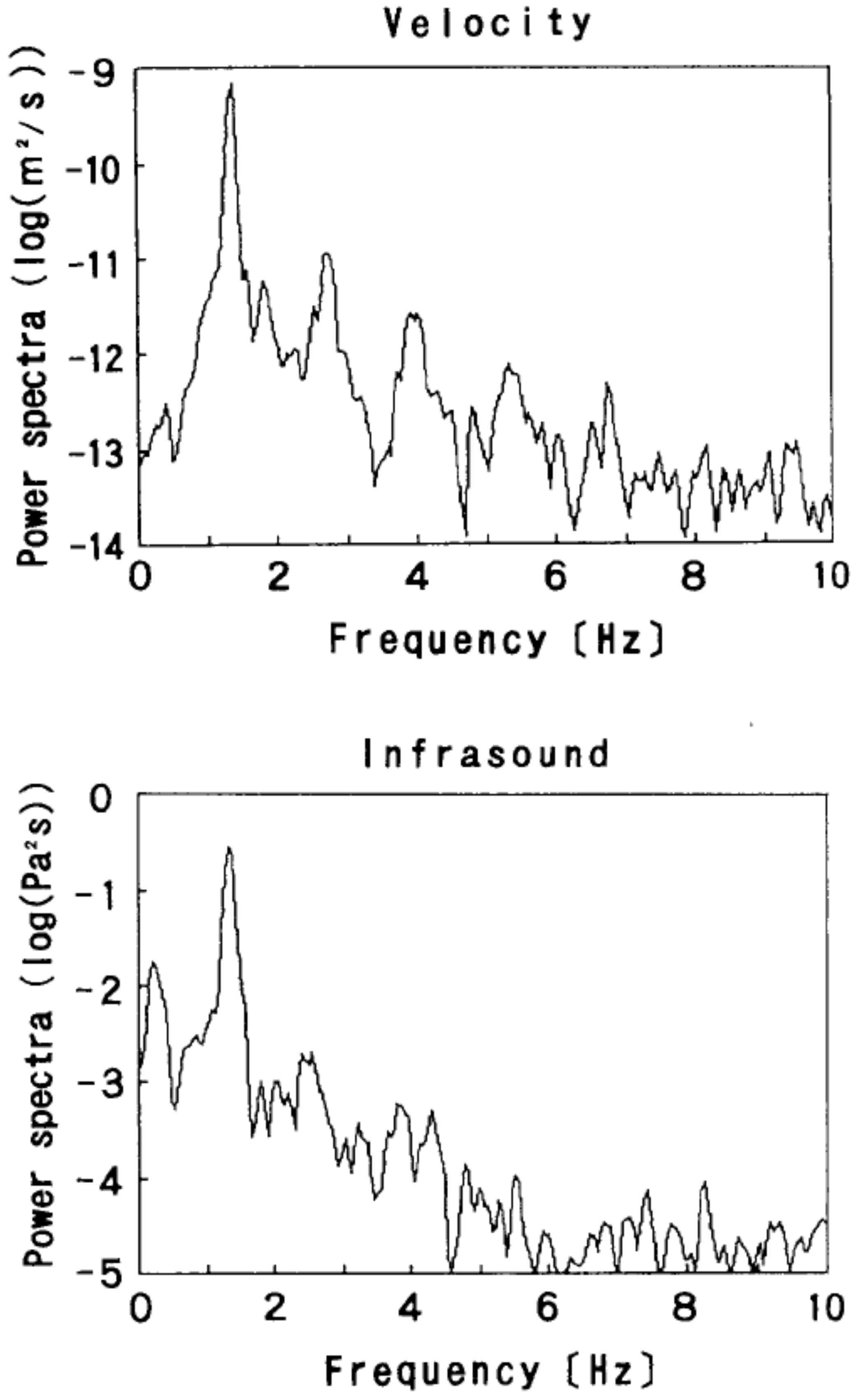

- **1990s:** first deployments of infrasound sensors at volcanoes

Arenal, Costa Rica; Garces et al. [1998]

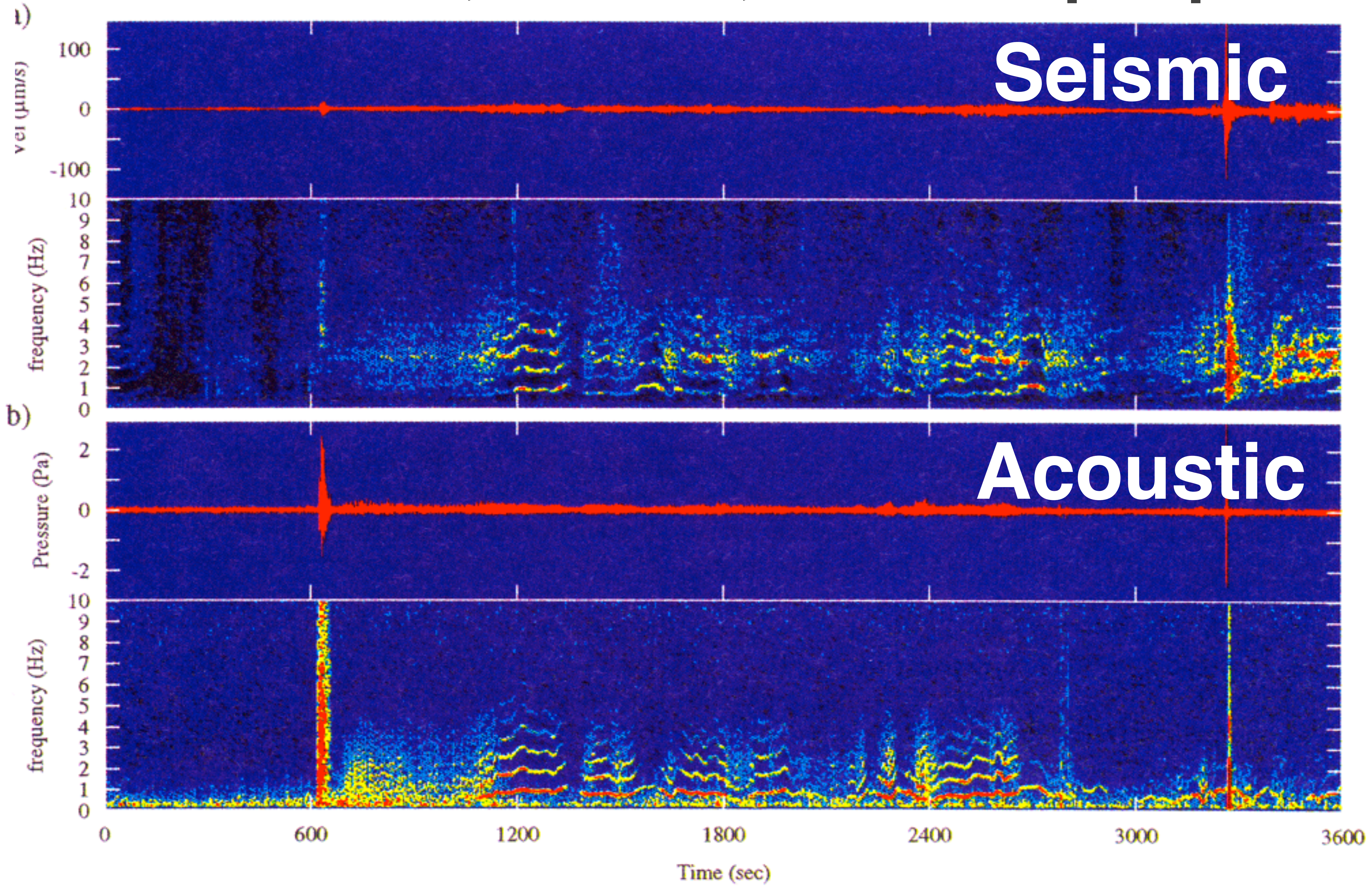

Instrumentation changes 1919–2019

- Increasing seismic network density
- **1990s:** transition from event-triggered to continuous digital waveform data storage; analog to digital telemetry, etc.

Seismic station coverage, Island of Hawai`i 1950

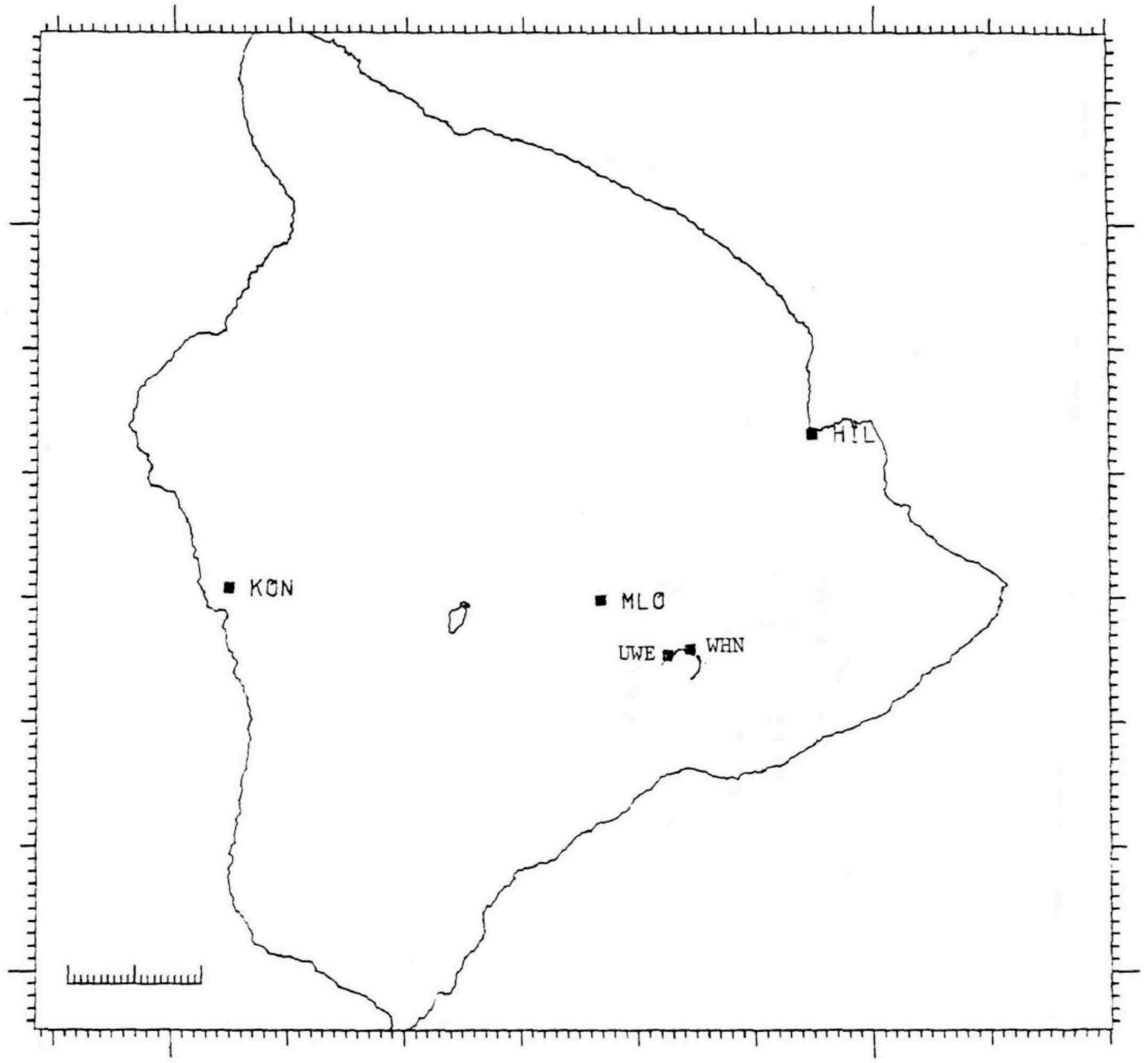

Figure 3. Stations in December 1950.

Klein and Koyanagi [1980]

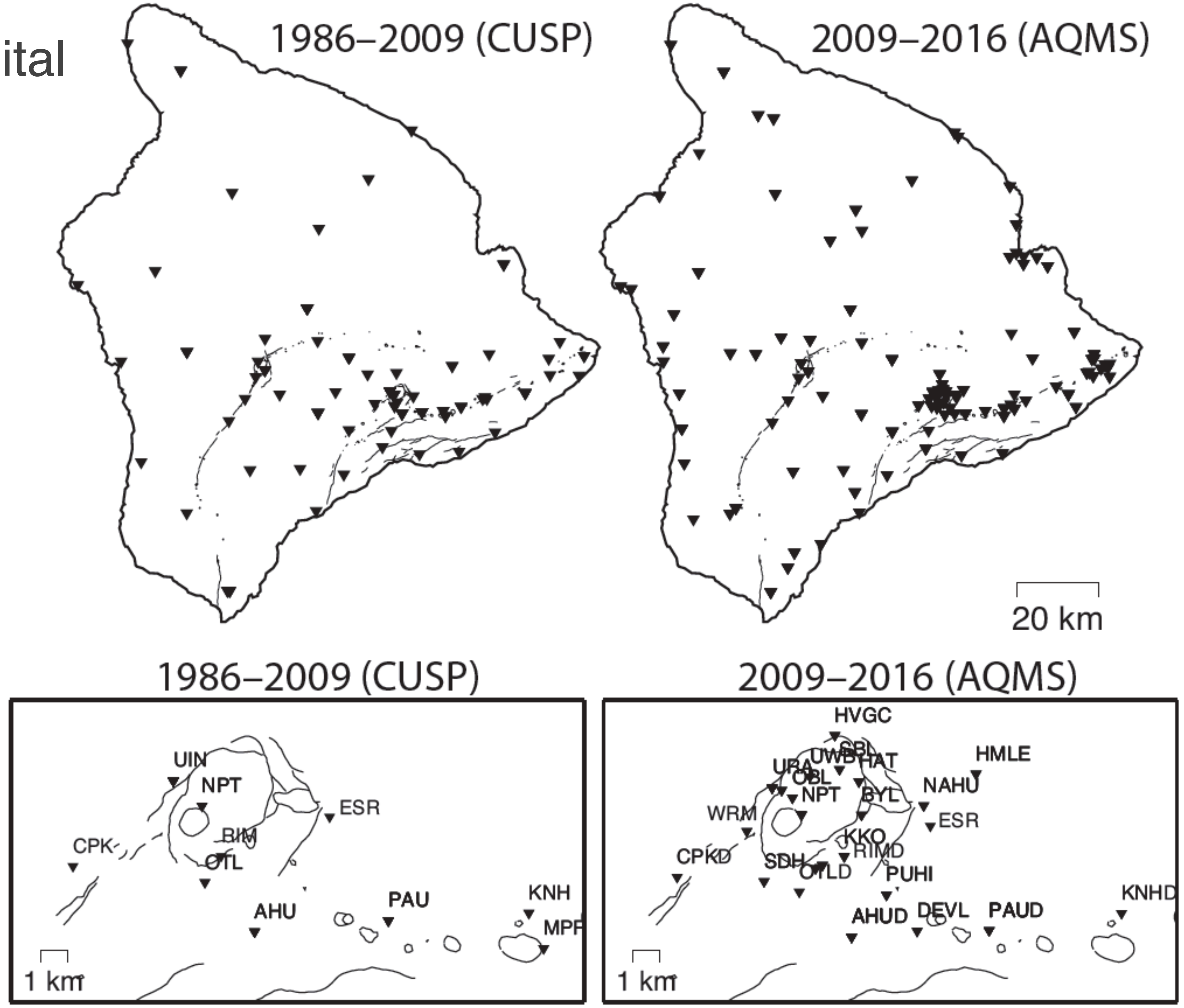

Figure from *Matoza et al.* [2019]

Instrumentation changes 1919–2019

- The computer revolution enabled increasingly sophisticated data processing and source modeling, and facilitated the transition from event-triggered to continuous digital waveform recording by about the 1990s.
- The first deployments of broadband seismic instrumentation and infrasound sensors on volcanoes in the 1990s led to discoveries of new signals and phenomena.

Phreatic explosion, Mount St. Helens, 8 March 2005; recorded by a broadband seismometer and broadband infrasound array

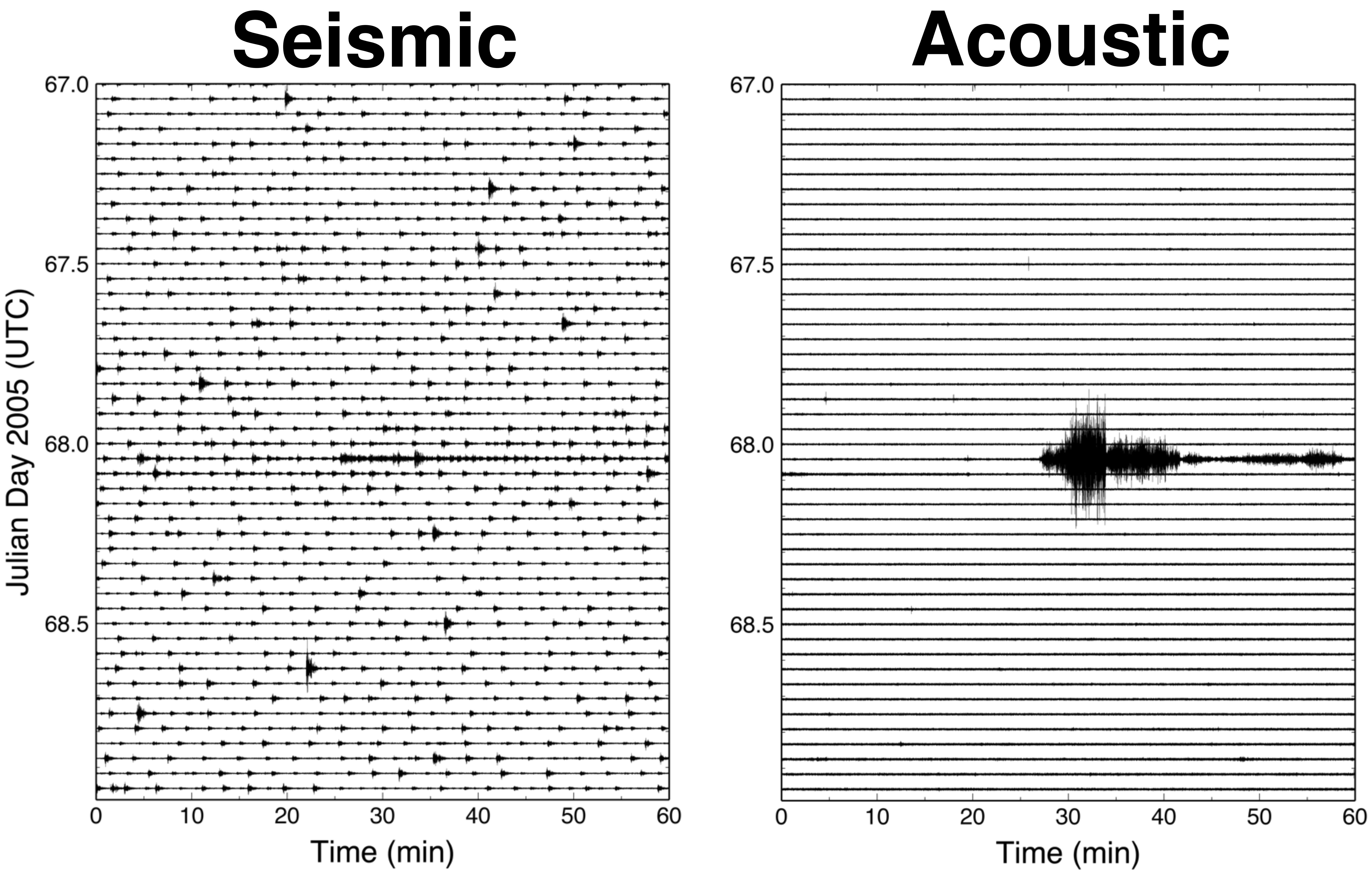

Matoza et al. [2007]

Event Classification

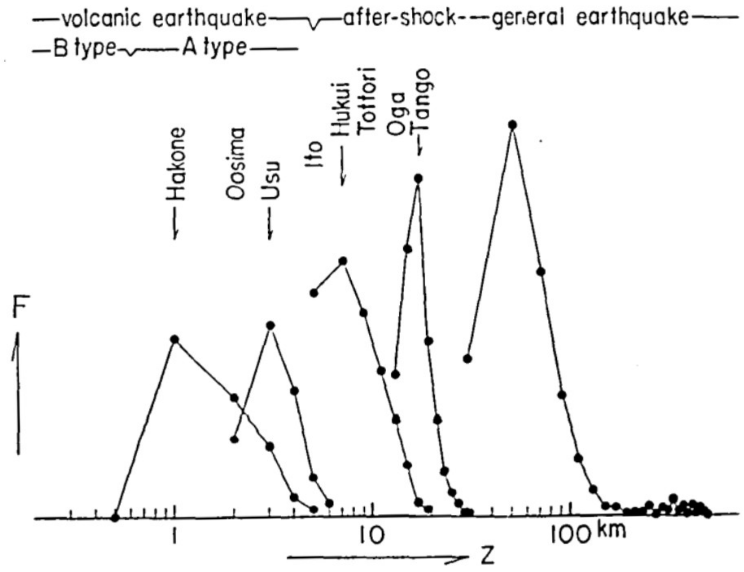

Fig. 4. Comparison of frequency distribution of hypocentral depth for general earthquake, after-shock and volcanic earthquake of the A and B types.

Four classes of volcanic earthquakes: (location of foci, nature of motion)

- A-type (from a depth of 1-10 km, sometimes 20 km)
- B-type (originating in swarms from a shallow depth near the crater)
- Explosion earthquakes accompanying (causing!) explosive eruptions of the Vulcanian type
- Volcanic microtremors accompanying Strombolian eruptions

Minakami [1960]

Event Classification

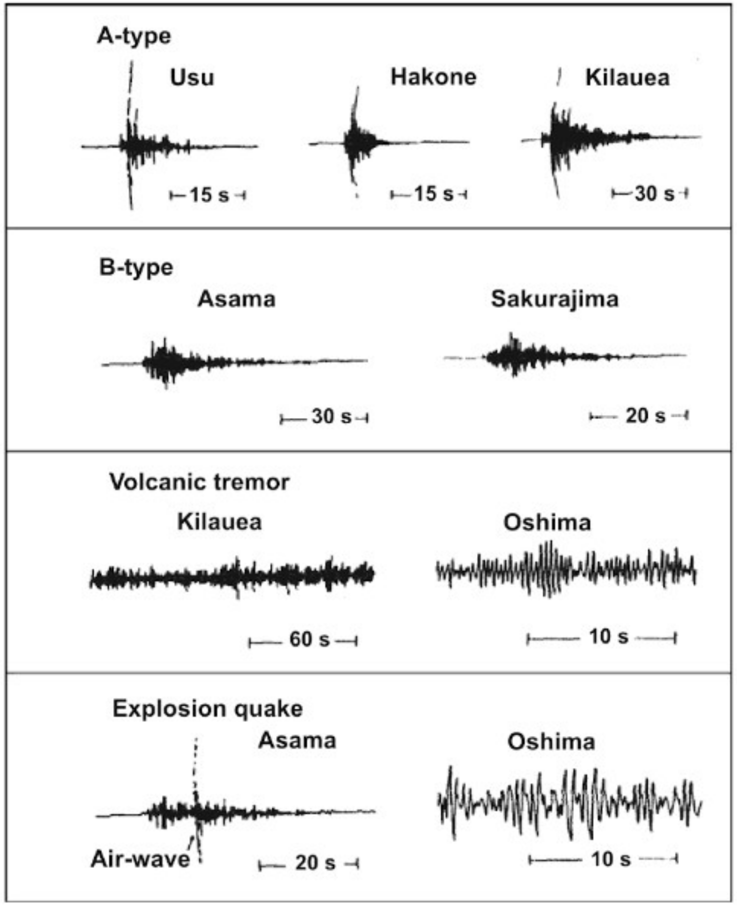

Four classes of volcanic earthquakes: (location of foci, nature of motion)

- A-type (depths of 1-10 km, similar to shallow tectonic quakes, double-couple?)
- B-type (depths of < 1 km, small-magnitude, 1-5 Hz waveform, no clear S-phase, first-motion pattern unresolvable)
- Explosion earthquakes
- Volcanic tremors or pulsations

Minakami [1974]

Event Classification

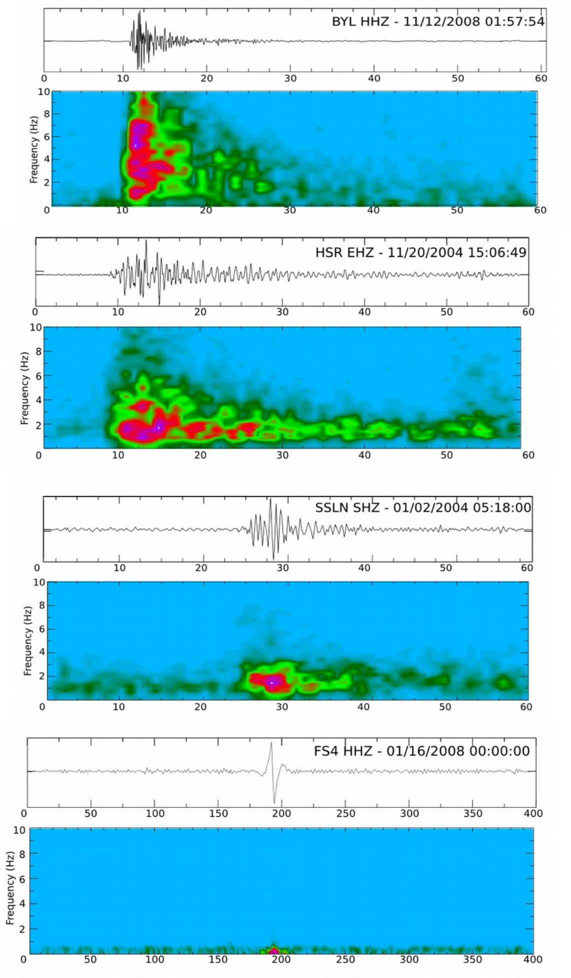

Multiple classes of volcanic earthquakes:

- **Volcano-Tectonic** (VT), or high-frequency (HF) (=A-Type)
- Hybrid events
- **Long-Period** (LP), or low-frequency (LF) (=B-Type)
- Very-Long-Period (VLP)

- Explosion earthquakes
- Volcanic tremor

e.g., Lahr et al. [1994]

High-frequency (VT) earthquakes

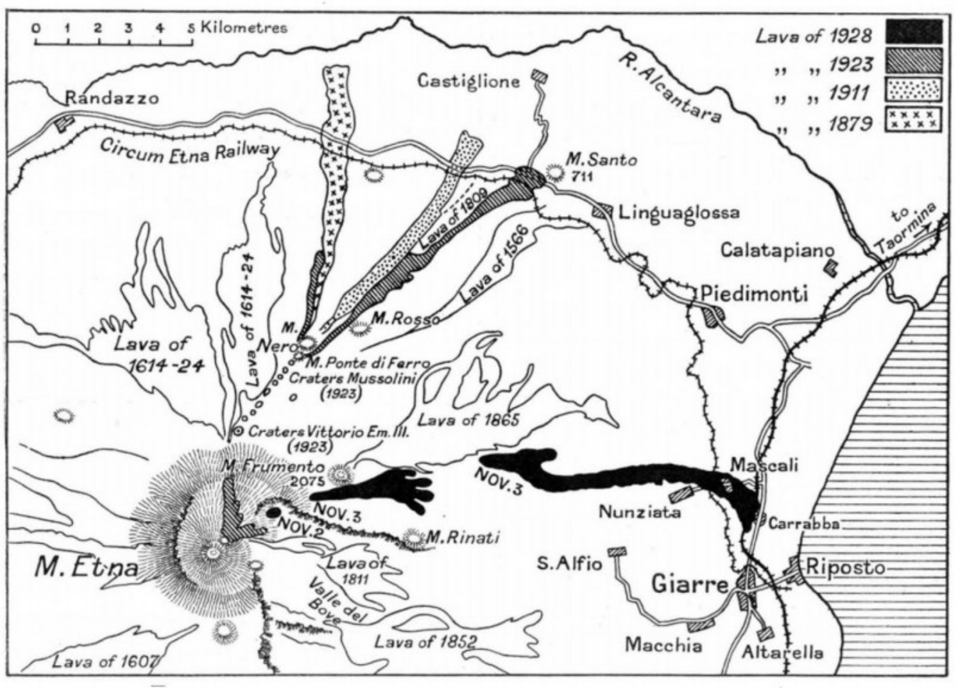

Figure from Di Franco [1928]

"I think the greater number of so-called volcanic earthquakes are due to **tension-cracks.** The pressure caused by upwelling lava must produce cracks, which the lava fills, and which appear later as radial dykes about partially disintegrated volcanoes. The strong but very limited earthquakes that occur on Mt. Etna often follow straight lines along which lava shortly afterwards pours out."

HF Reid [1929]

High-frequency (VT) earthquakes

- Early evidence of double-couple mechanism for some (all?) A-type quakes

● First-motion up
○ First-motion down

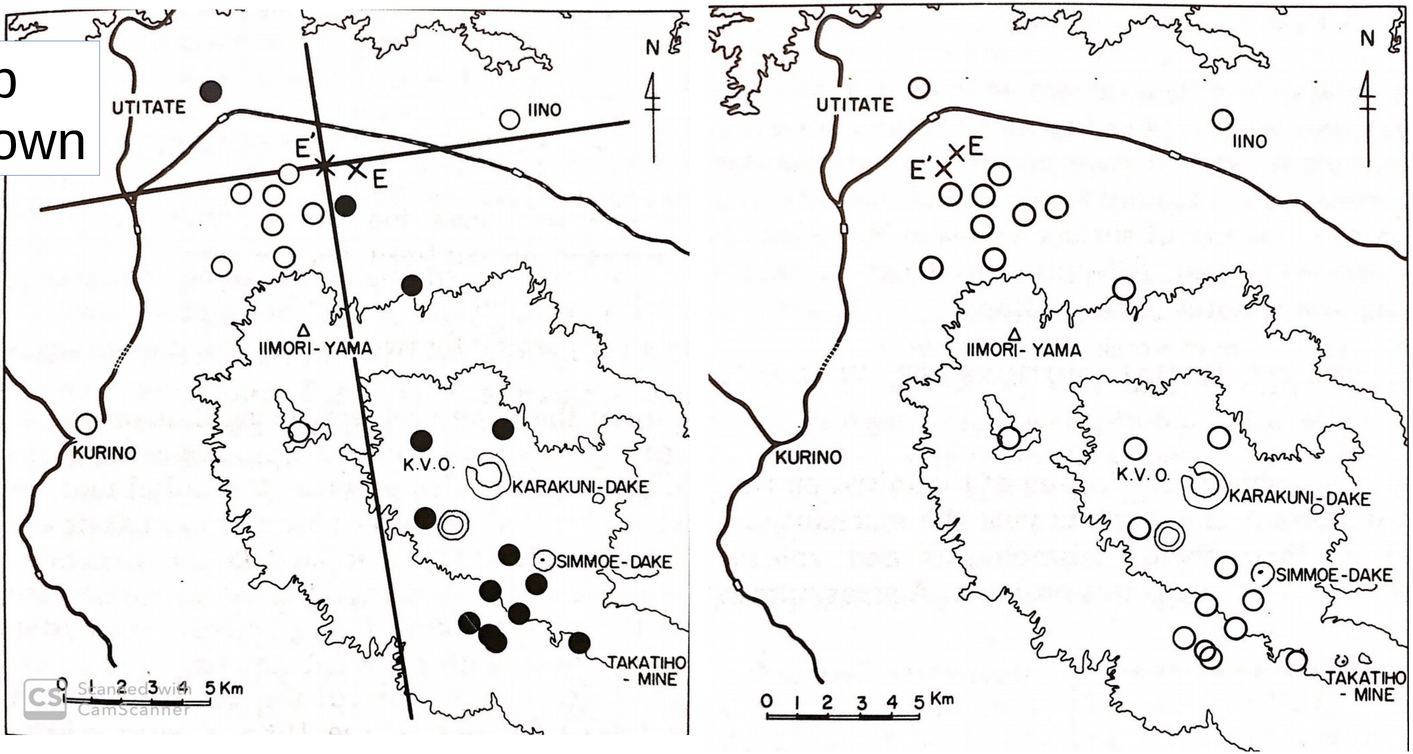

Minakami [1974]

High-frequency (VT) earthquakes

- Earthquake swarms on mid-ocean ridges reflect the breakup and collapse of the central-rift valley floors due to a drop in pressure in the underlying magma chamber

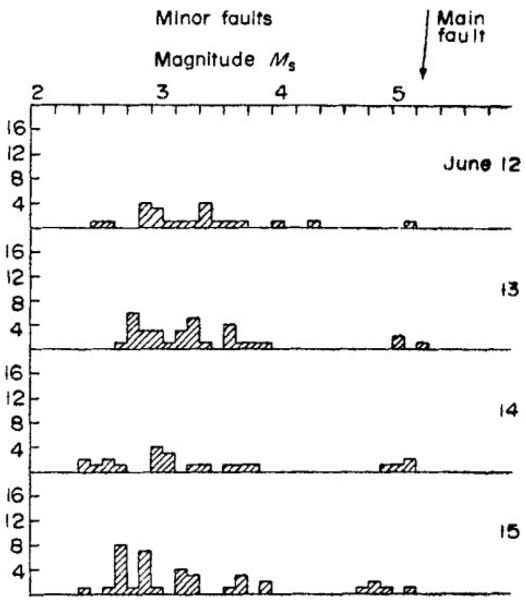

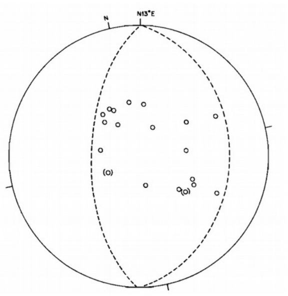

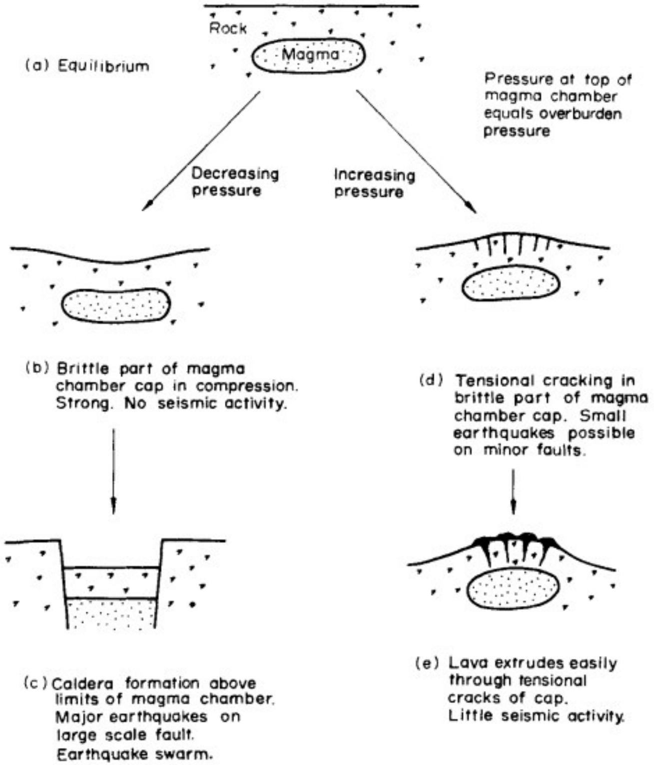

Filson et al. [1973], Francis [1974]

High-frequency (VT) earthquakes

- ‘Hill mesh’ hypothesis – swarms of volcanic earthquakes in transitional regions between spreading centers and transform faults occur on cracks connecting tips of en-echelon, fluid-filled fractures

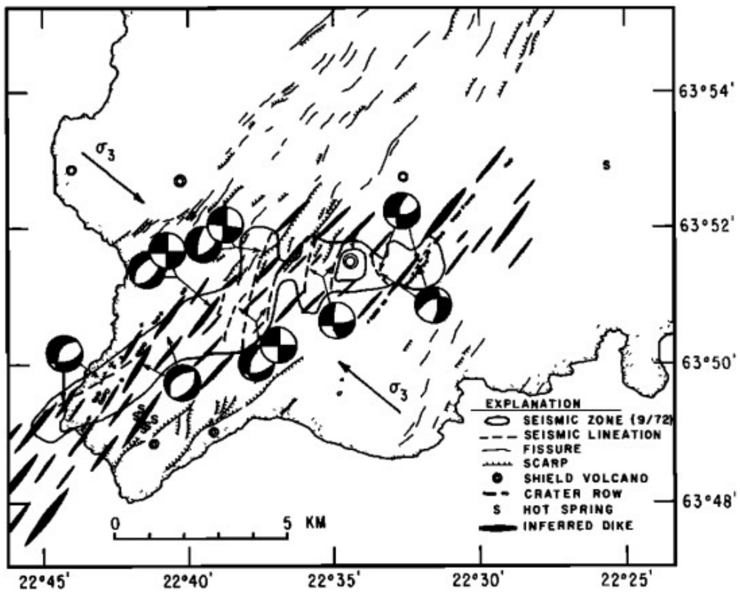

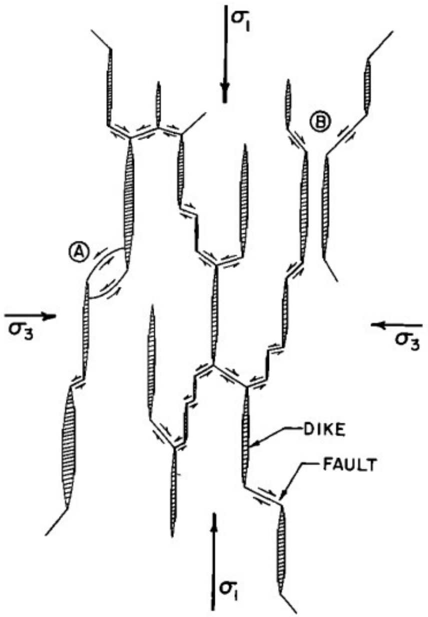

Hill [1977]

High-frequency (VT) earthquakes

- Evidence from Mt. St. Helens that post-eruptive earthquakes occurred in response to stresses from relaxation of emptied conduit

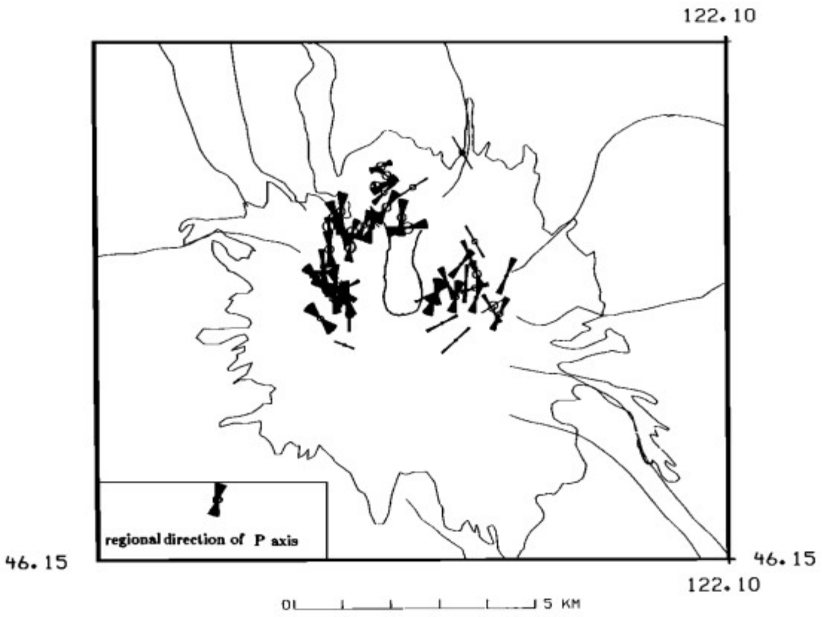

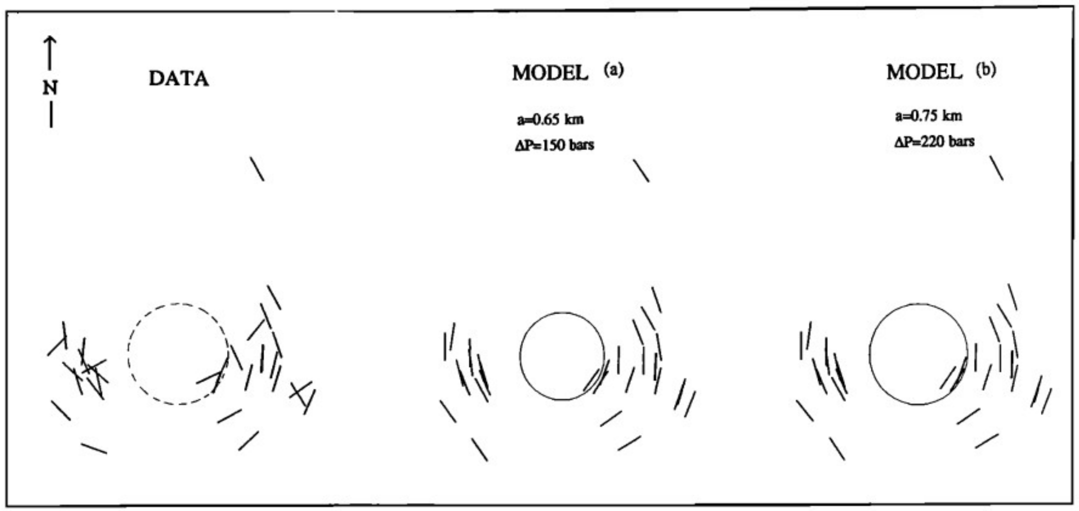

Barker and Malone [1991]

High-frequency (VT) earthquakes

- VT source process/location depends on magma rheology

Low-viscosity magmas

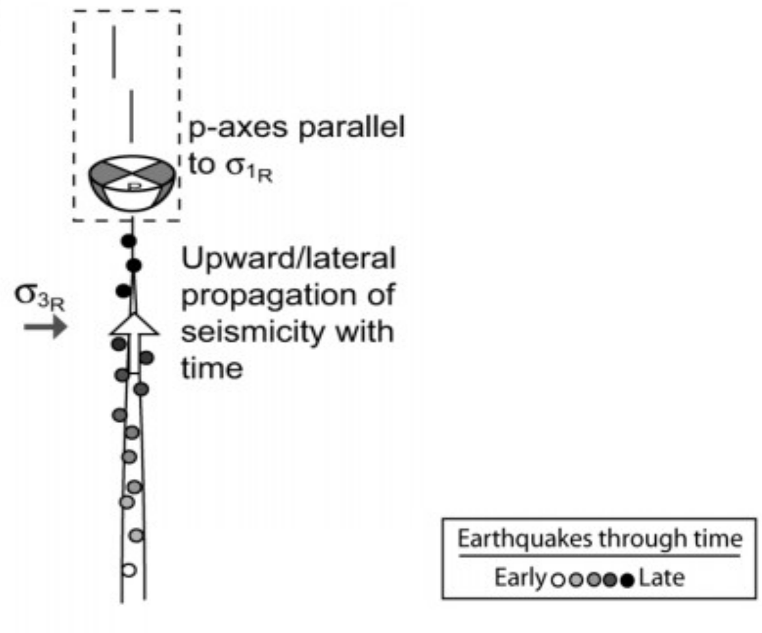

High-viscosity magmas

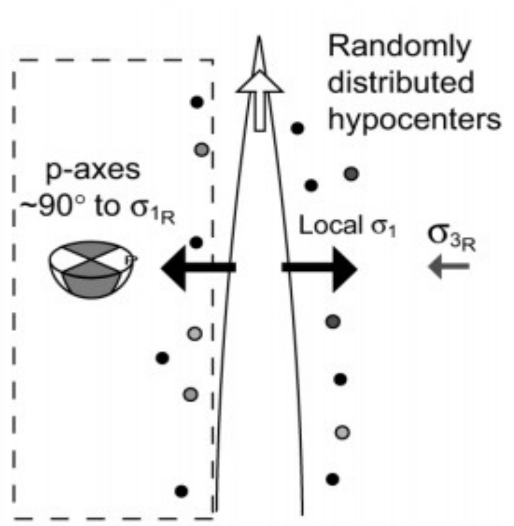

Roman and Cashman [2006]

High-frequency (VT) earthquakes

- Evidence for ‘distal VT’ seismicity due to stress transfer onto regional faults

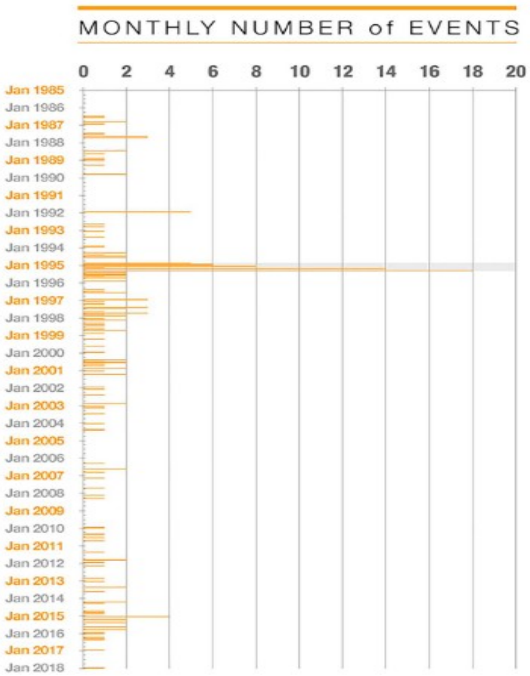

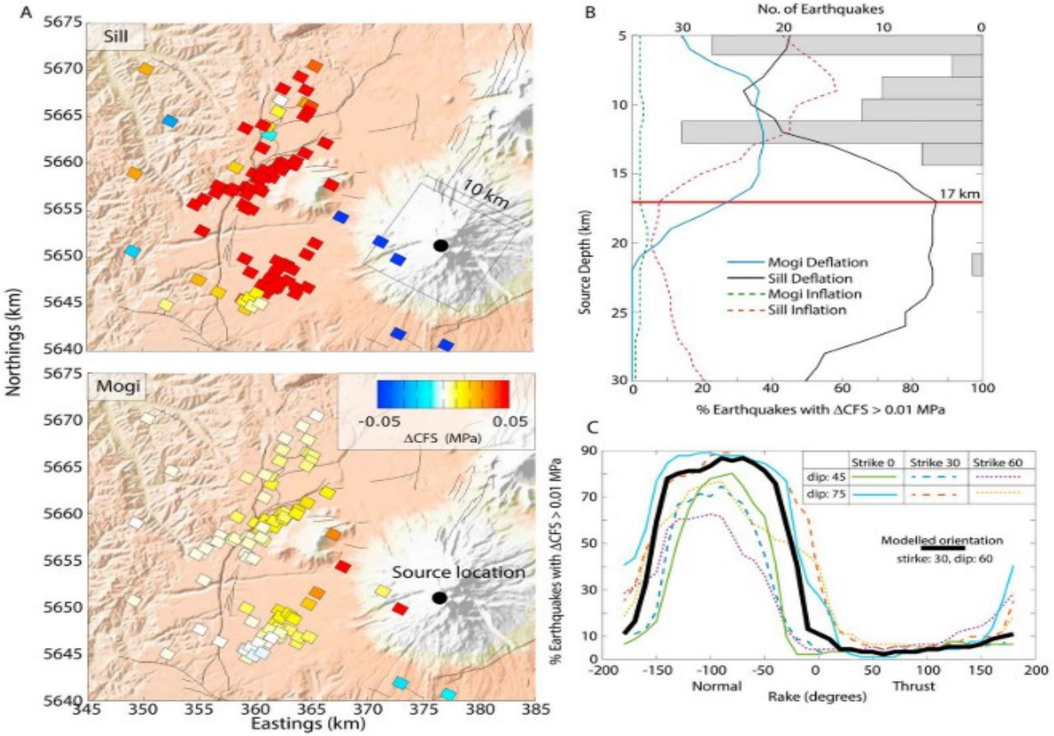

Hurst et al. [2018]

High-frequency (VT) earthquakes

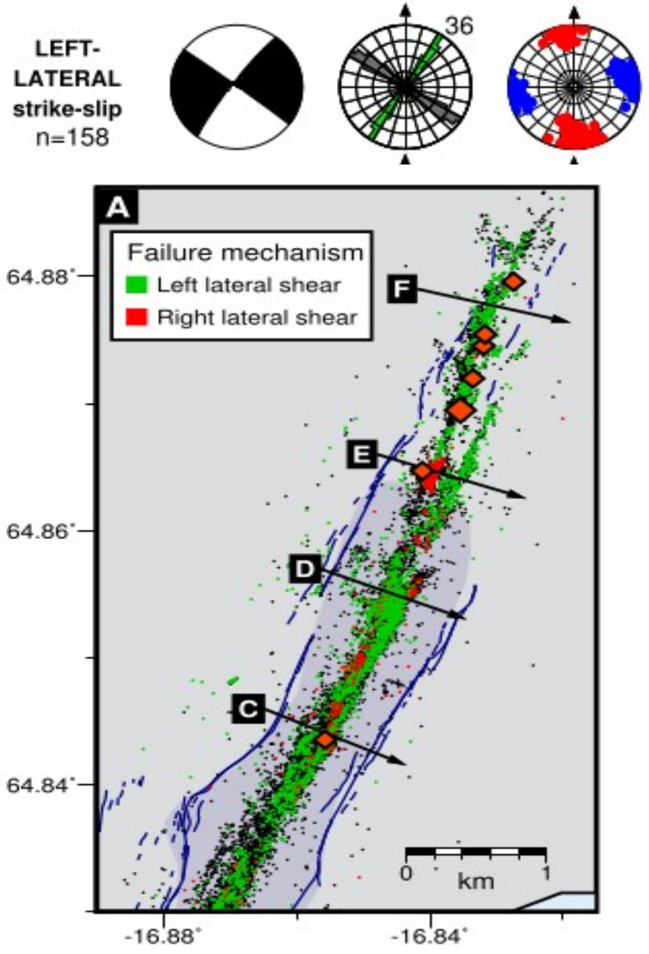

- Propagating VT seismicity at base of laterally-intruding dike, Holuhraun 2014

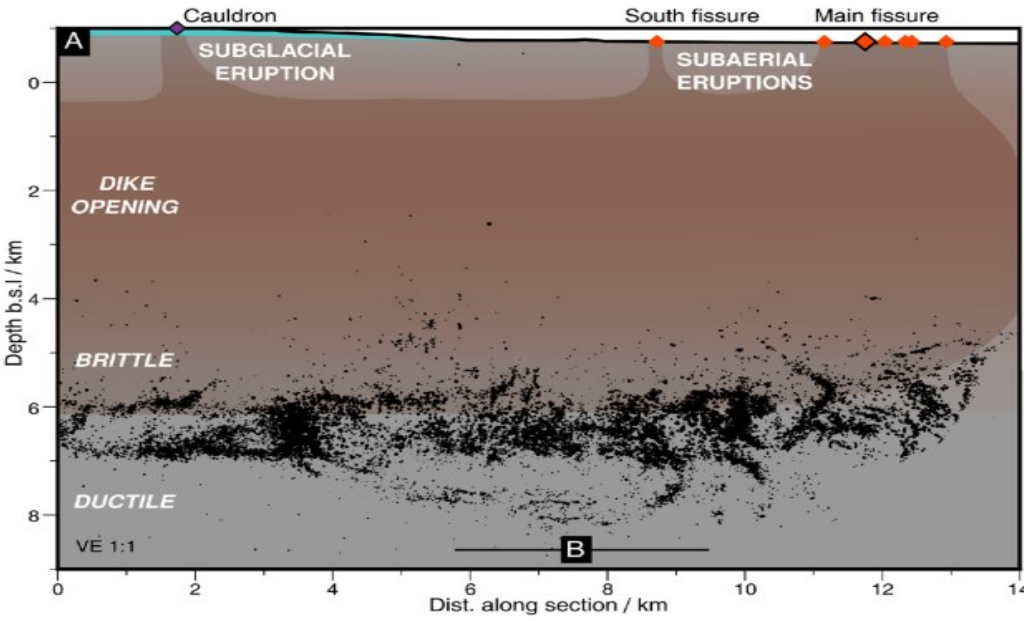

Agustsdottir et al. [2016], Woods et al. [2019]

Volcano seismology: signal classification

Classification based on mechanism

1) **Volcano-tectonic (VT)**
   - Shear/tensile failure in brittle solid
   - e.g., intrusions, loading and deformation

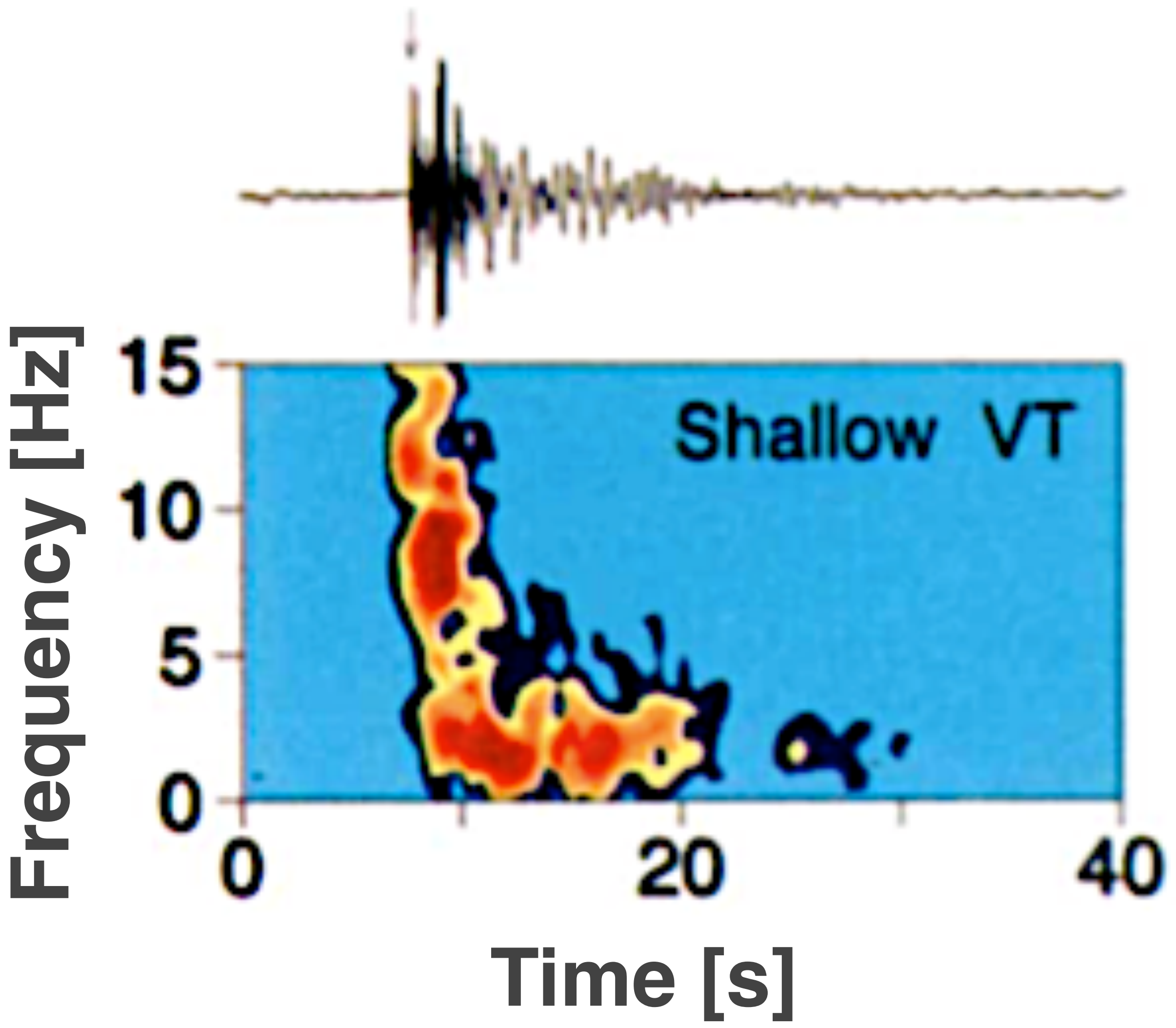

2) **Long-period (LP)** [0.5-5 Hz]
   - Actively involve a fluid

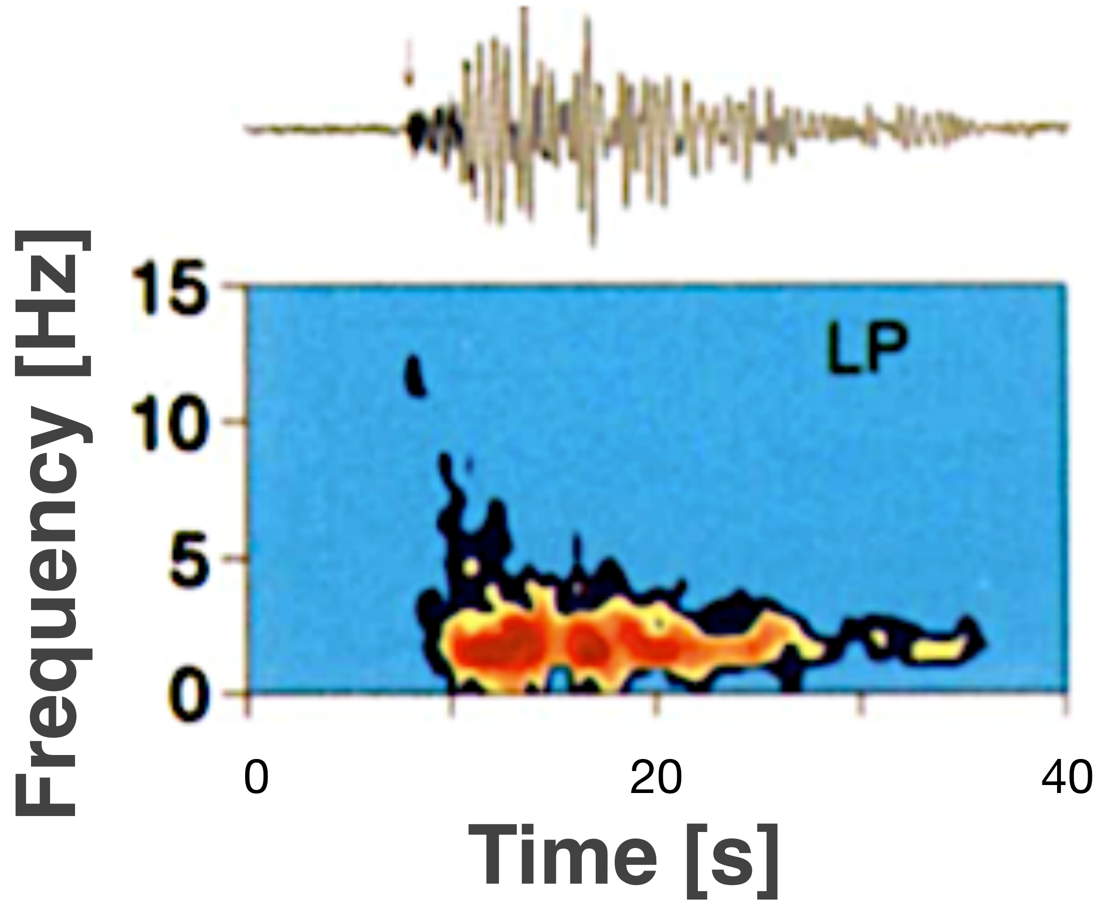

Lahr et al. [1994]; *Chouet* [1996]

Volcano seismology: signal classification

Classification based on mechanism

1) **Volcano-tectonic (VT)**
- Shear/tensile failure in brittle solid
- e.g., intrusions, loading and deformation

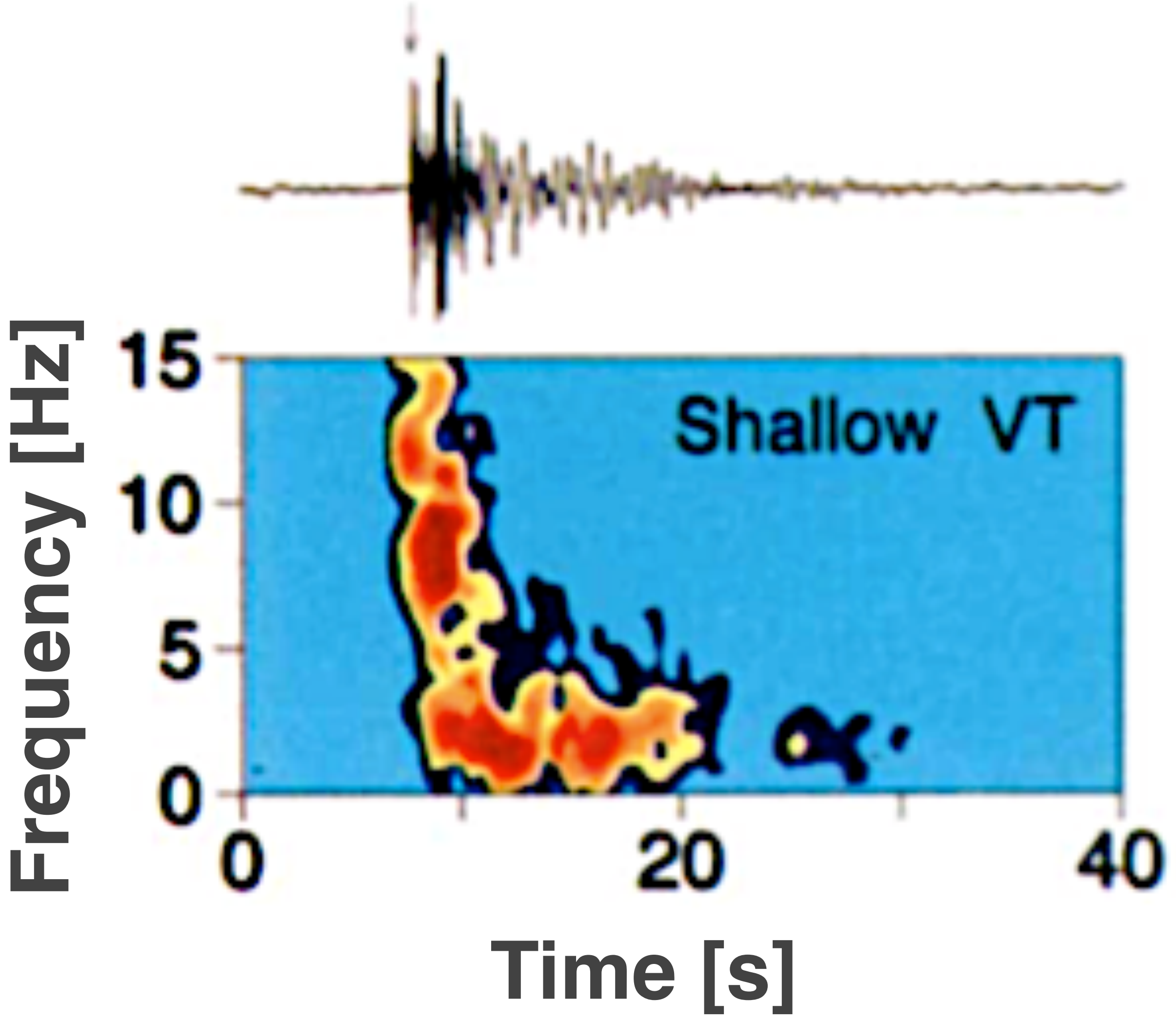

2) **Long-period (LP)** [0.5-5 Hz]
- Actively involve a fluid
- Includes **LP events** and **tremor**

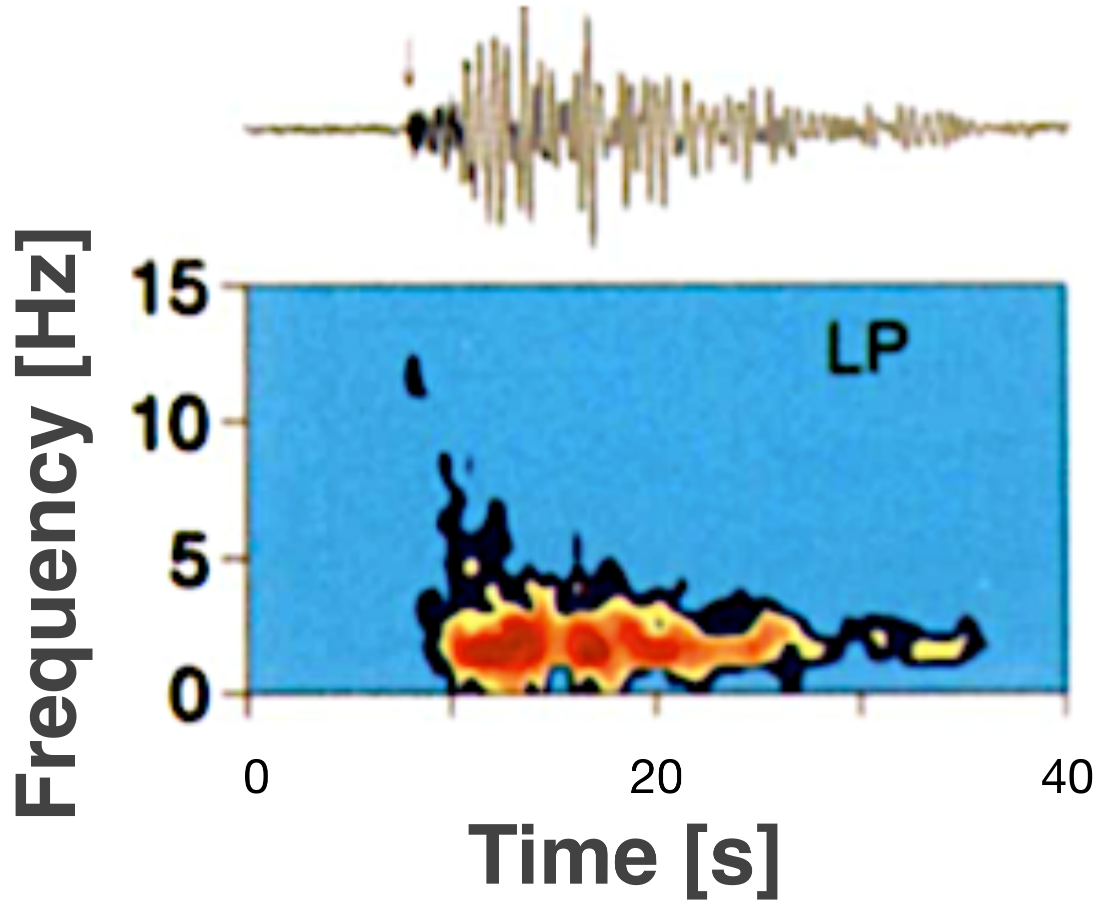

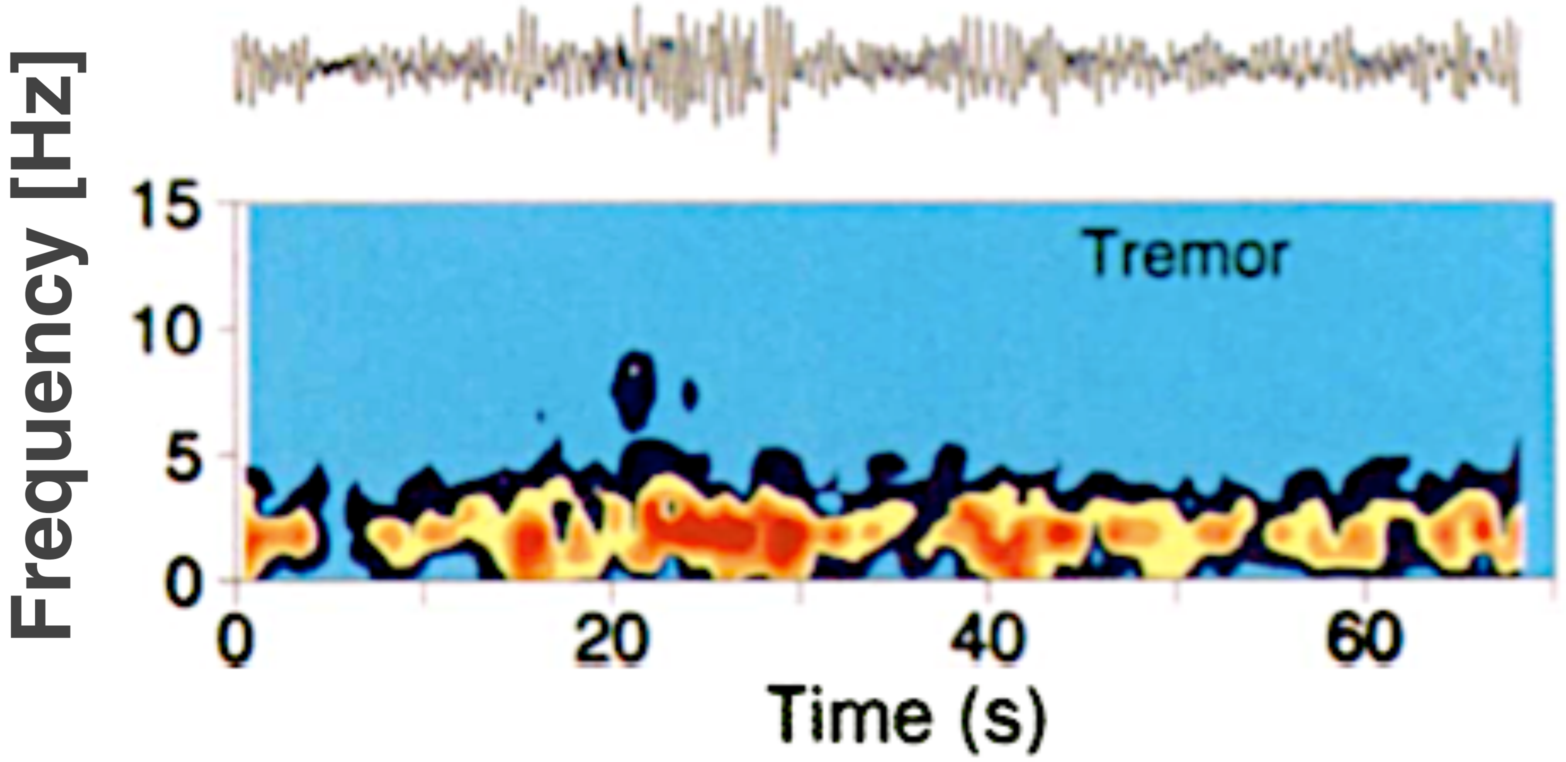

Lahr et al. [1994]; *Chouet* [1996]

Volcanic tremor

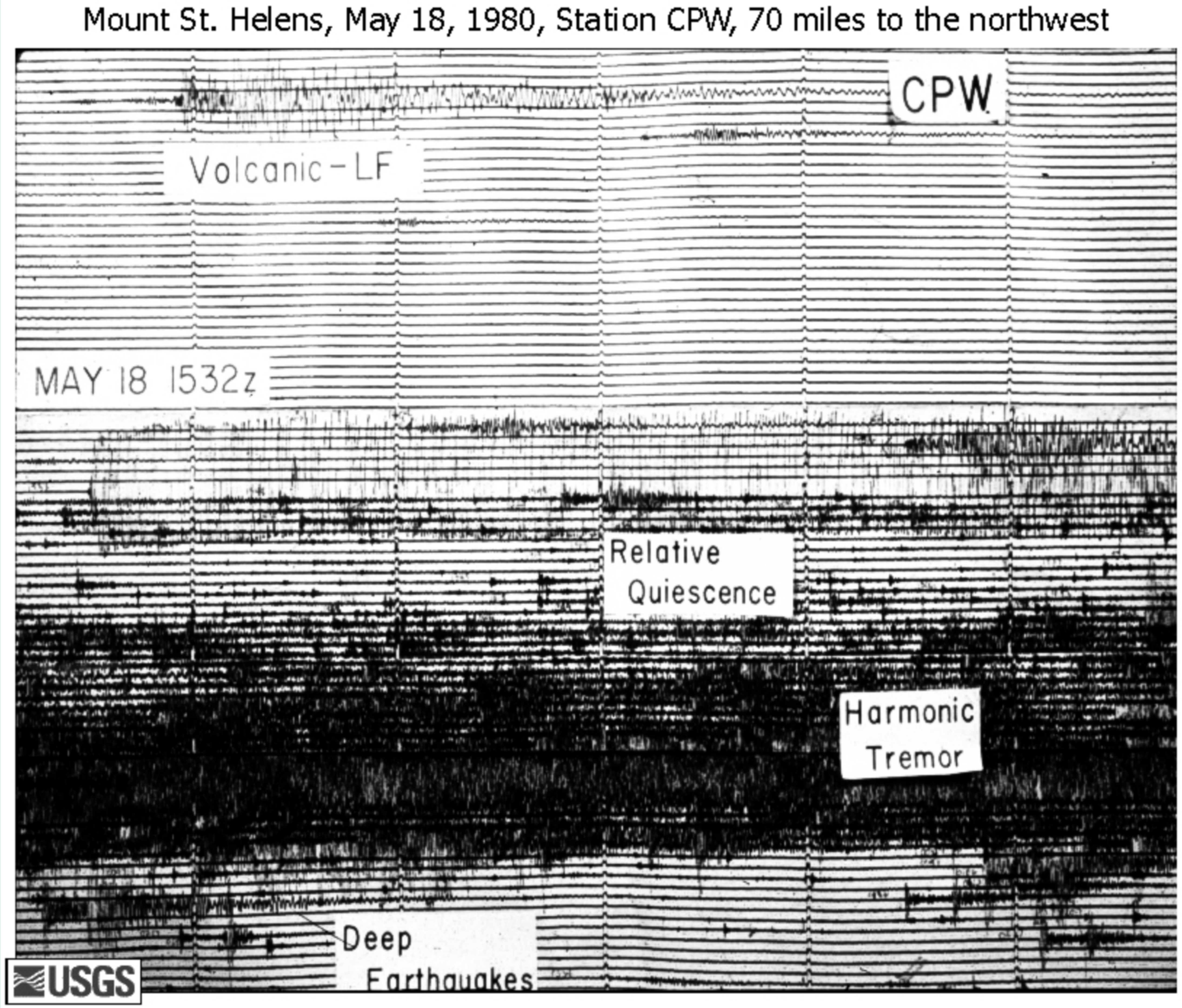

Volcanic tremor a catch-all term for *sustained* seismic and acoustic signals associated with a wide range of volcanic activity

multifarious : many and of various types; having or occurring in great variety

- Harmonic
- Monotonic/monochromatic
- Spasmodic
- Eruption
- Banded
- Tremor storm

etc.? ...

e.g., Mcnutt [1992], Konstantinou and Schlindwein [2002]

Spasmodic vs. harmonic tremor

Jaggar/Omori: early 20th Century

Spasmodic tremor:
irregular vibrations

Harmonic tremor:
more rhythmic vibrations

Spasmodic vs. harmonic tremor

Jaggar/Omori: early 20th Century

Spasmodic tremor:
irregular vibrations

Harmonic tremor:
more rhythmic vibrations

Seismograms from Galeras, Colombia, *Gil Cruz* [1999]

Spasmodic tremor

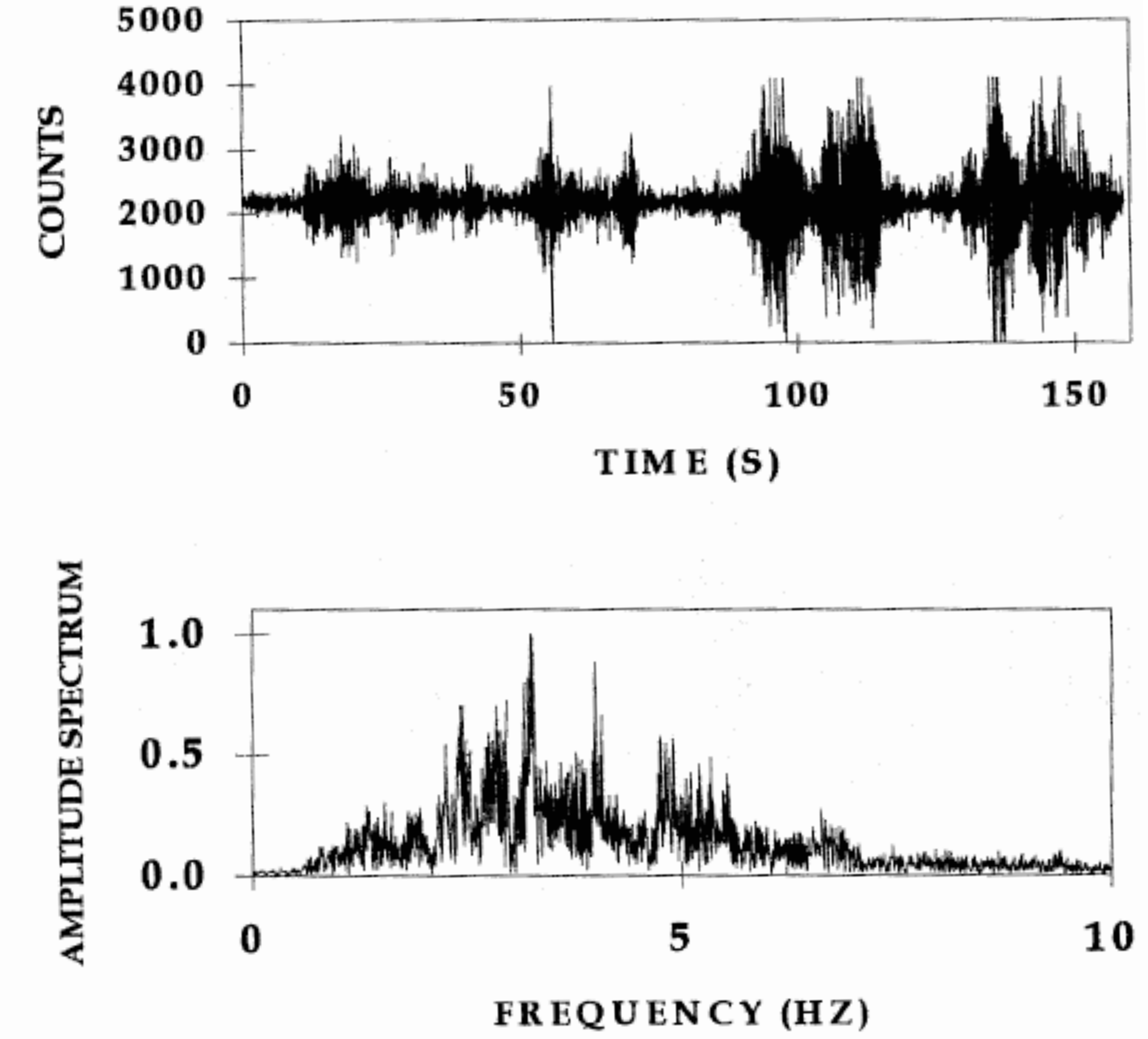

Harmonic tremor

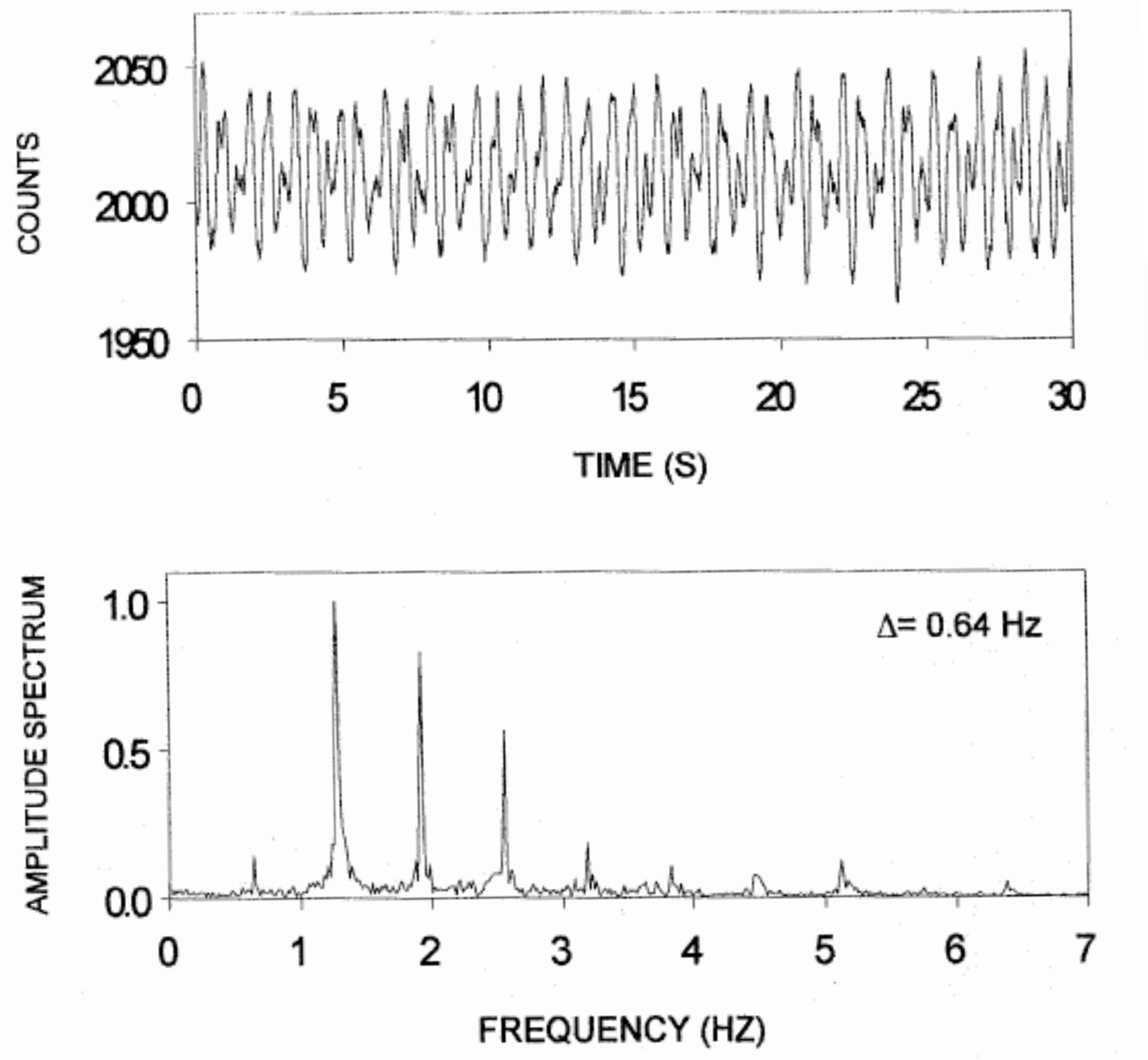

Volcanic tremor mechanisms

- *Omer* [1950] attributes tremor to a path effect: the reverberation of volcanic strata excited into motion by lava moving though feeding conduits.

VOLCANIC TREMOR*

(PART TWO: THE THEORY OF VOLCANIC TREMOR)

BY GUY C. OMER, JR.

ABSTRACT

IT IS proposed that volcanic tremor originates in the vibration of laminae which are partly freed by the differential tilting of the surface of the earth around a volcanic vent during an eruption. The topographic evidence around Kilauea caldera is examined and a probable range of the free vibrating lengths is determined. The various possible modes of vibration are considered and it is concluded that longitudinal vibration would best explain the observed seismograms.

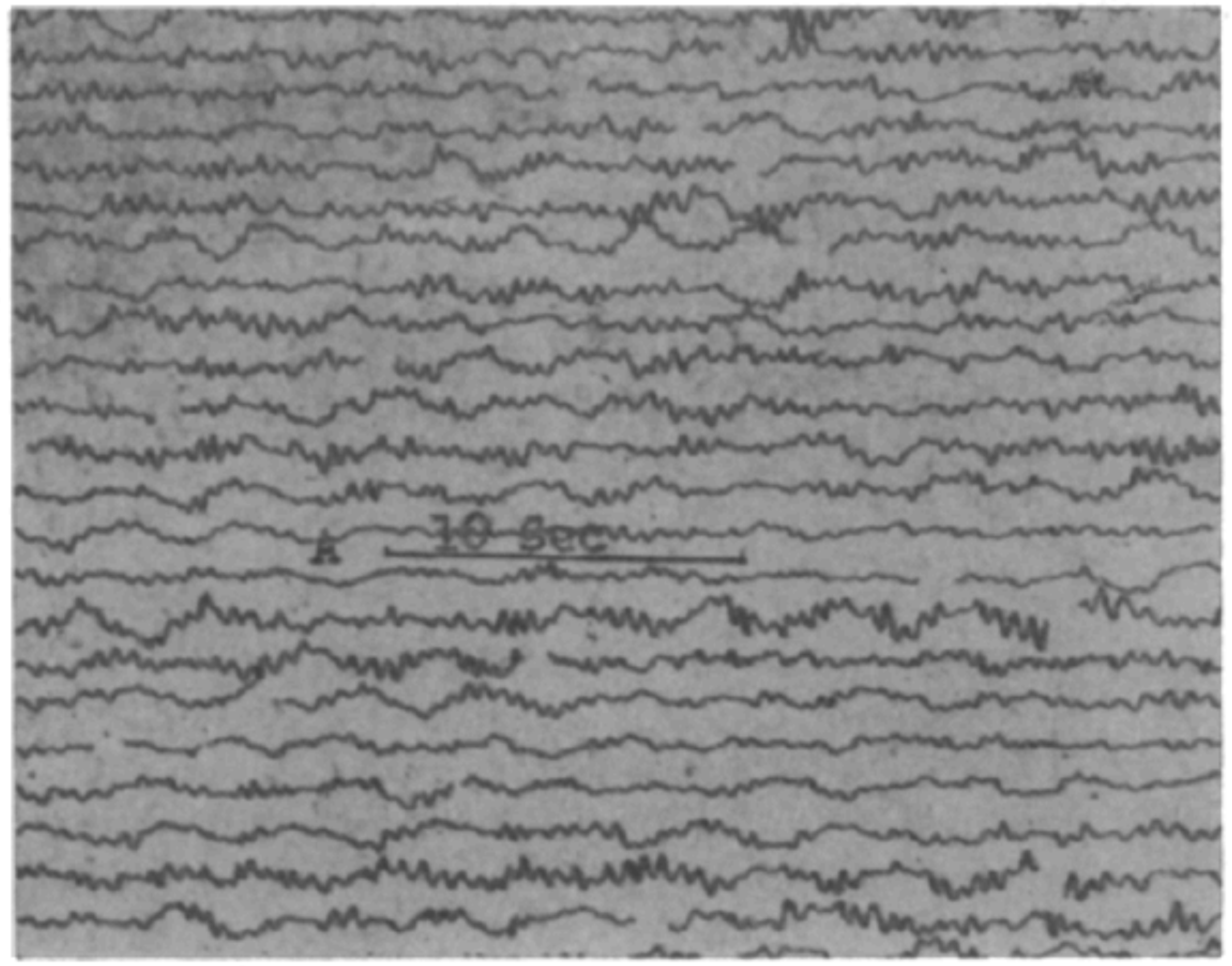

A.

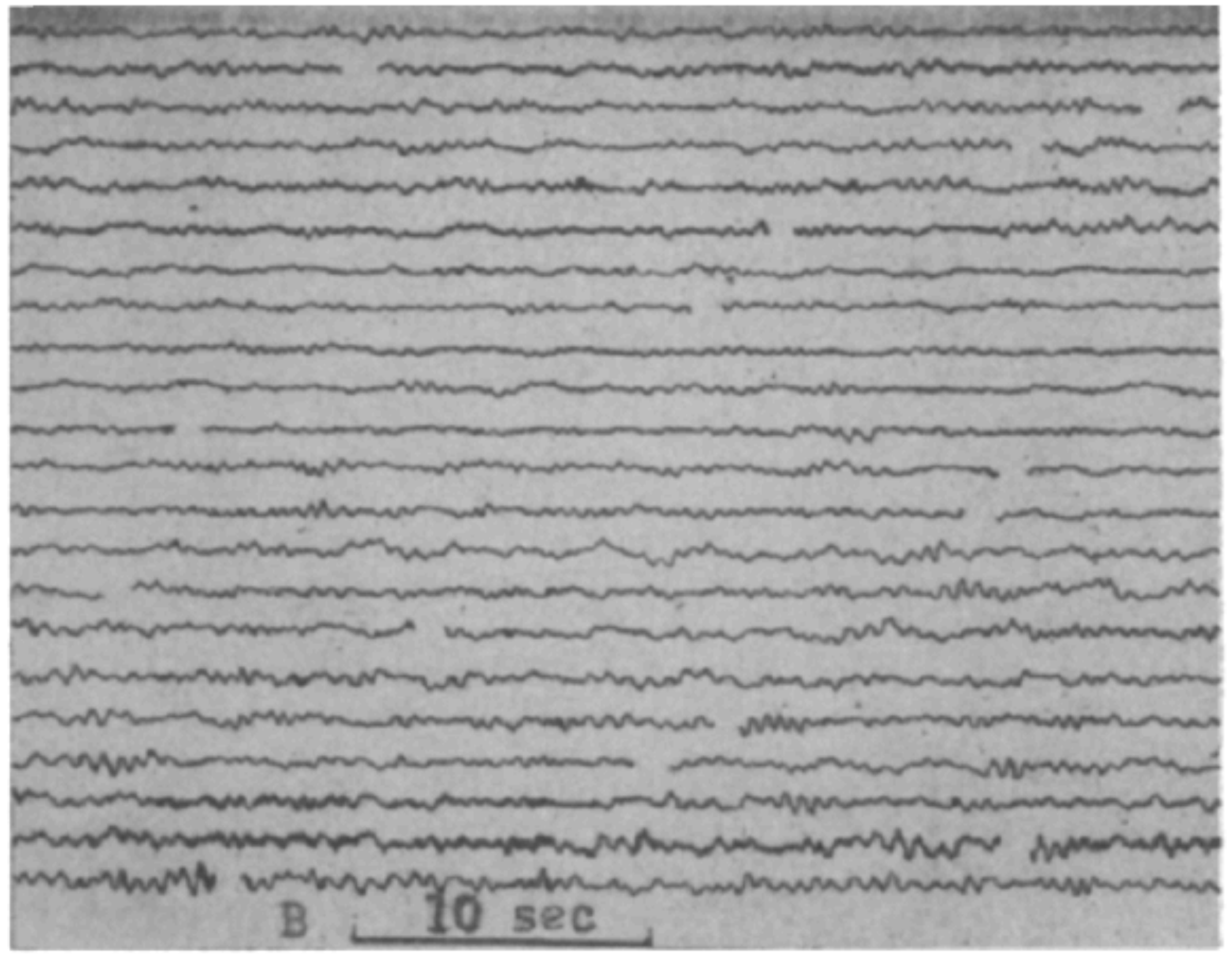

B.

Fig. 1. Volcanic tremor as recorded on the Bosch-Omori seismograph, 2.1 miles from Halemaumau, with a static magnification of about 115.

A. March 21, 1921. This is typical of the record when lava is high in Halemaumau. Some microseisms present. Record magnified 3 times.

B. May 8, 1924. Record when no lava is visible in Halemaumau but underground movement of lava in the Puna Rift probable. Magnified 2 times.

Finch [1949]; *Omer* [1950]

Volcanic tremor mechanisms

- *Shima* [1958] and *Kubotera* [1974]: peaked tremor spectrum at Aso modeled as free oscillations of a spherical magma chamber
- *Shimozuru* [1961]: longitudinal resonance of a cylindrical magma column

- However, these early models required implausibly large dimensions for the resonating cavities
- e.g., *Kubotera* [1974] determined the source of 3.5–7 s period tremor at Mount Aso to be a resonating spherical magma chamber of 4–6 km radius.

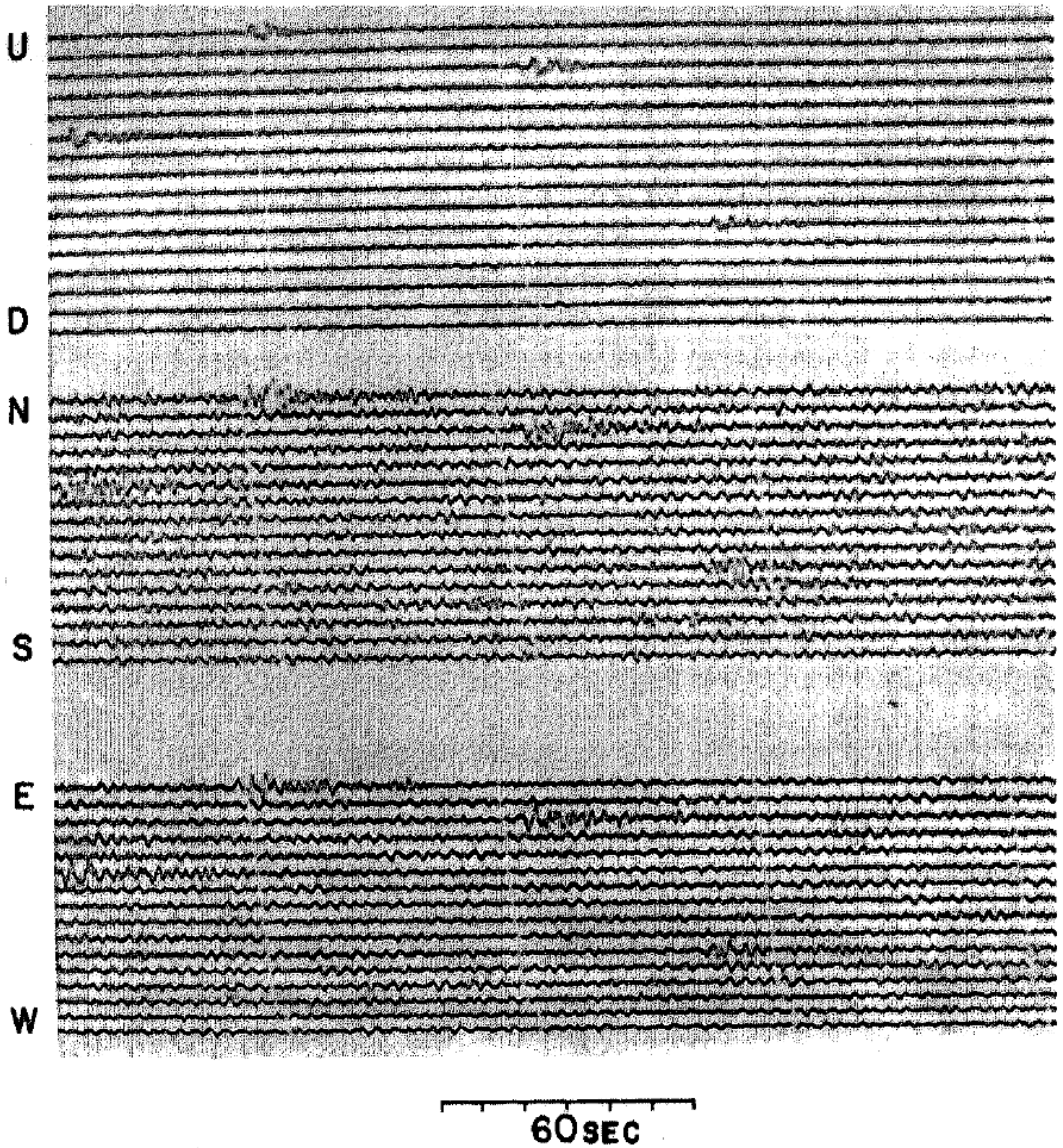

Fig. 2. Seismograms obtained at the volcanological laboratory.

Kubotera [1974]
“Volcanic tremors at Aso Volcano”

LPs as the impulse response of the resonant tremor system

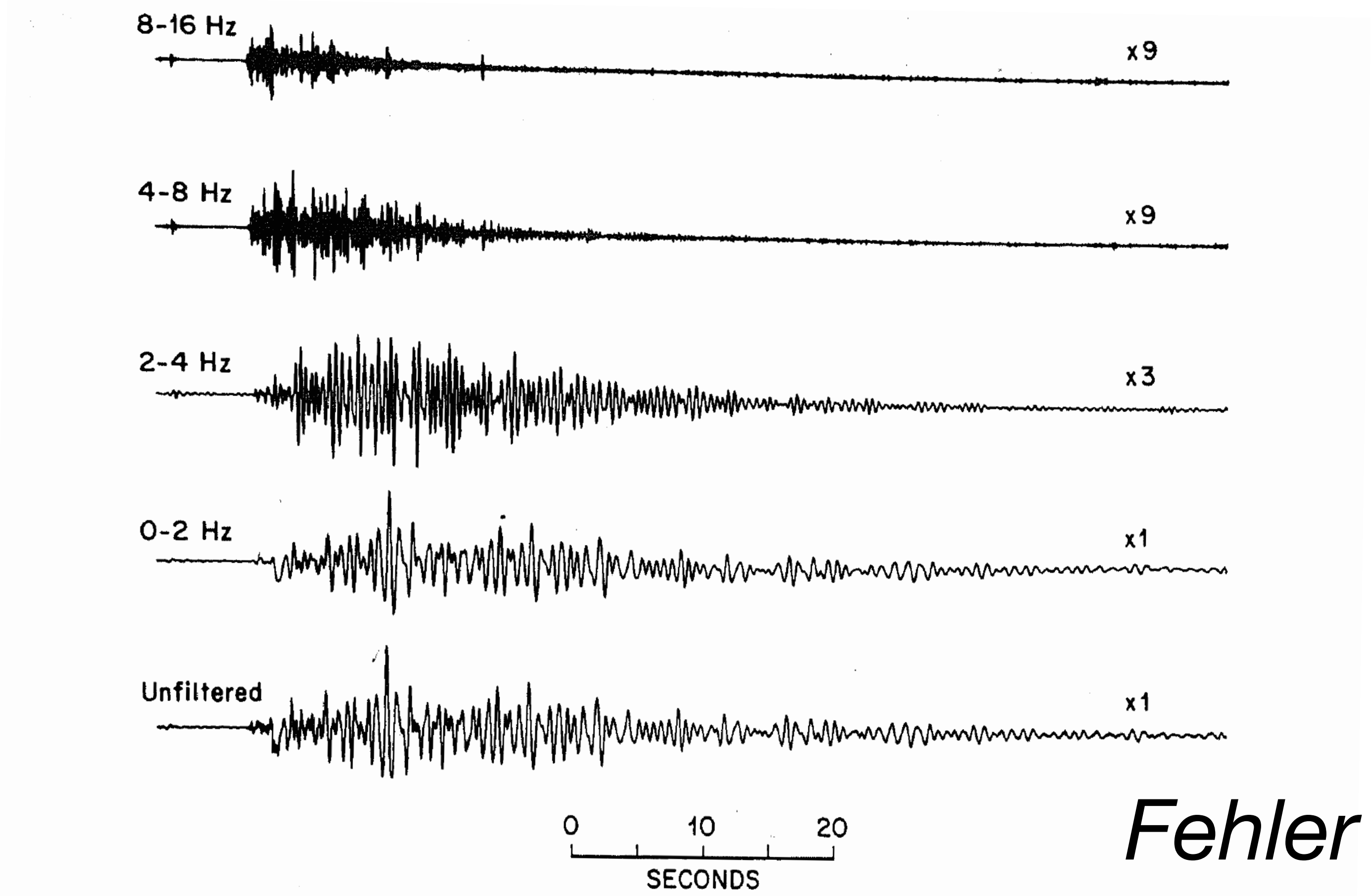

Fig. 9. Waveform of a typical long-period earthquake recorded at Mount St. Helens in October 1980 (lower trace). Upper traces show the result when the waveform is filtered with a band pass filter. The passband of the filter is labeled next to each trace. Note that some of the filtered traces have been magnified compared to the original traces.

Fehler [1983]

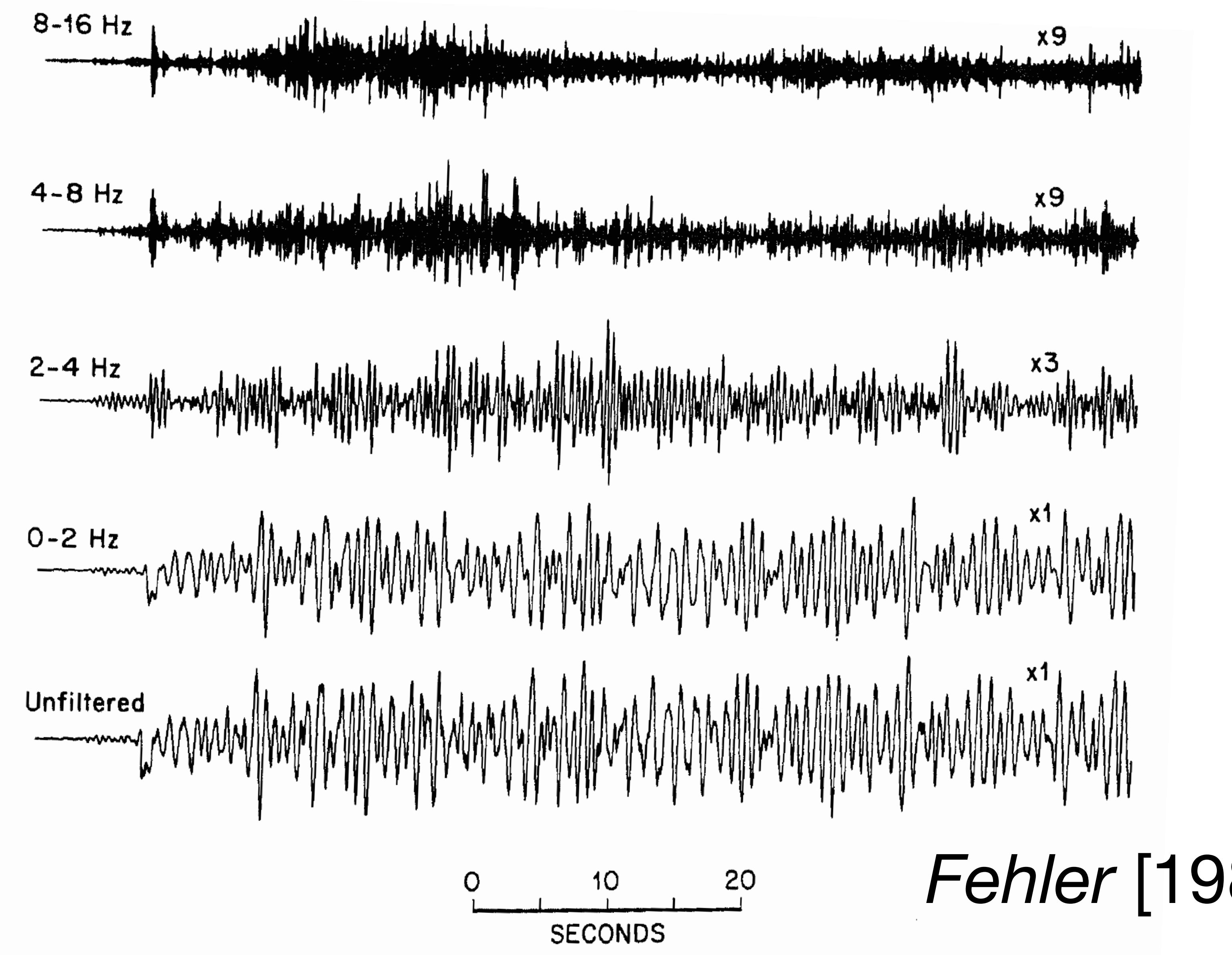

Fig. 10. Waveform of a tremor event and filtered traces.

Fehler [1983]

- Individual LP events (transients) and certain types of tremor are closely linked
- LPs merge into tremor

[e.g., *Latter*, 1979; *Fehler*, 1983; *Neuberg*, 2011; *Hotovec et al.*, 2012]

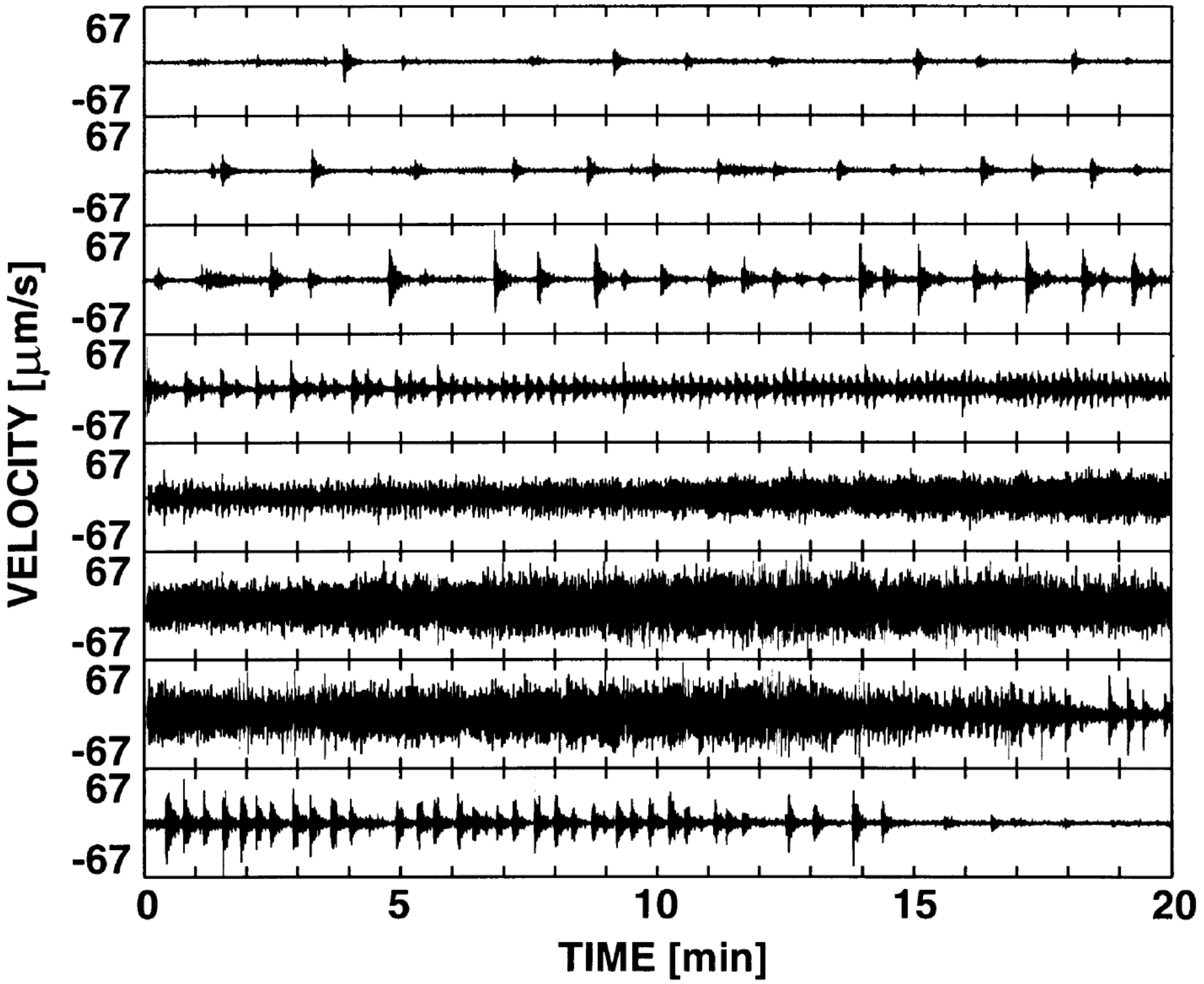

Soufrière Hills Volcano, Montserrat, February 12th 1997
[*Neuberg et al.*, 2000]

LP events: repetitive waveforms

Soufrière Hills Volcano, Montserrat, 1997

- LP waveform families or multiplets

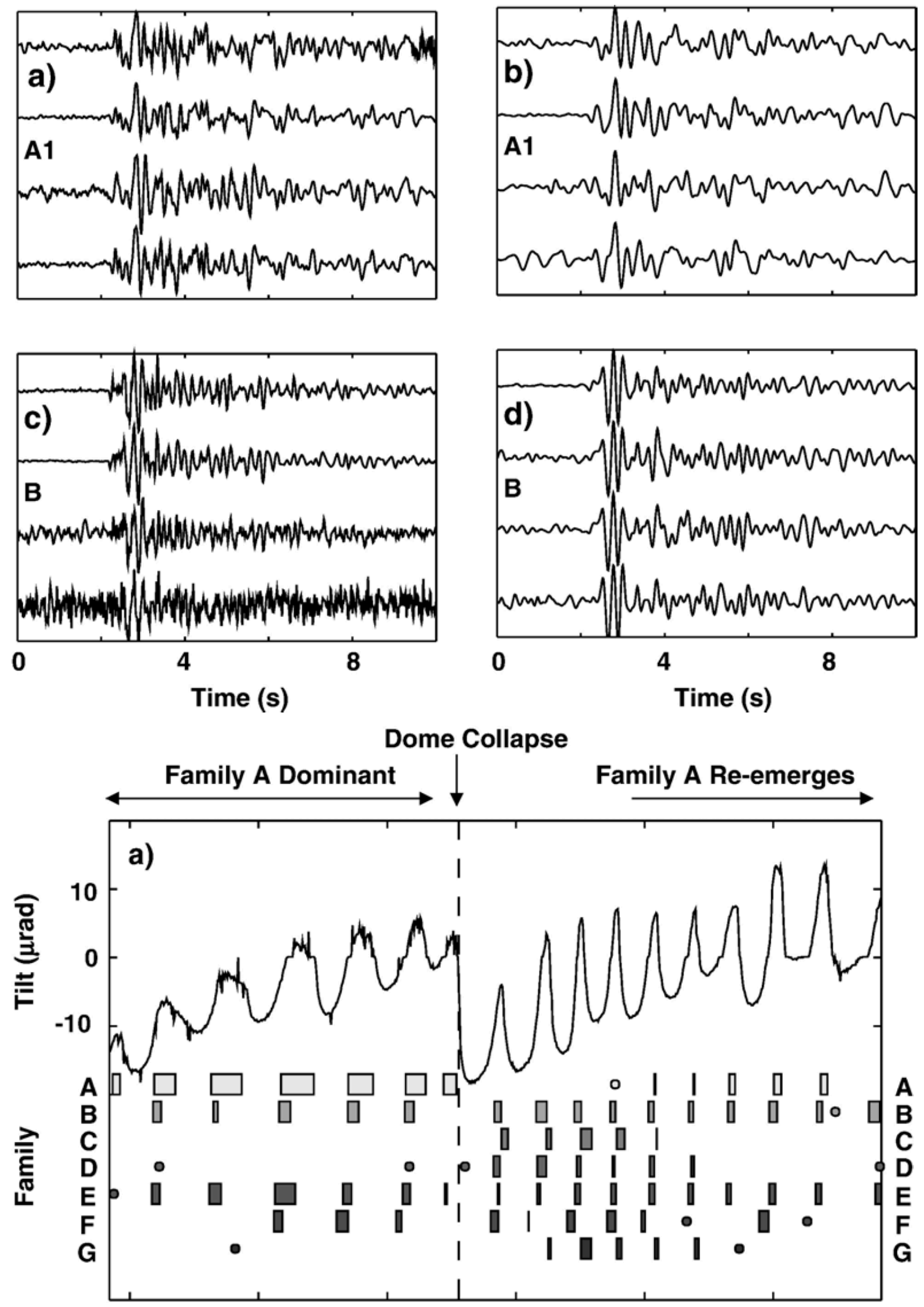

Green and Neuberg [2006]

Redoubt 1989

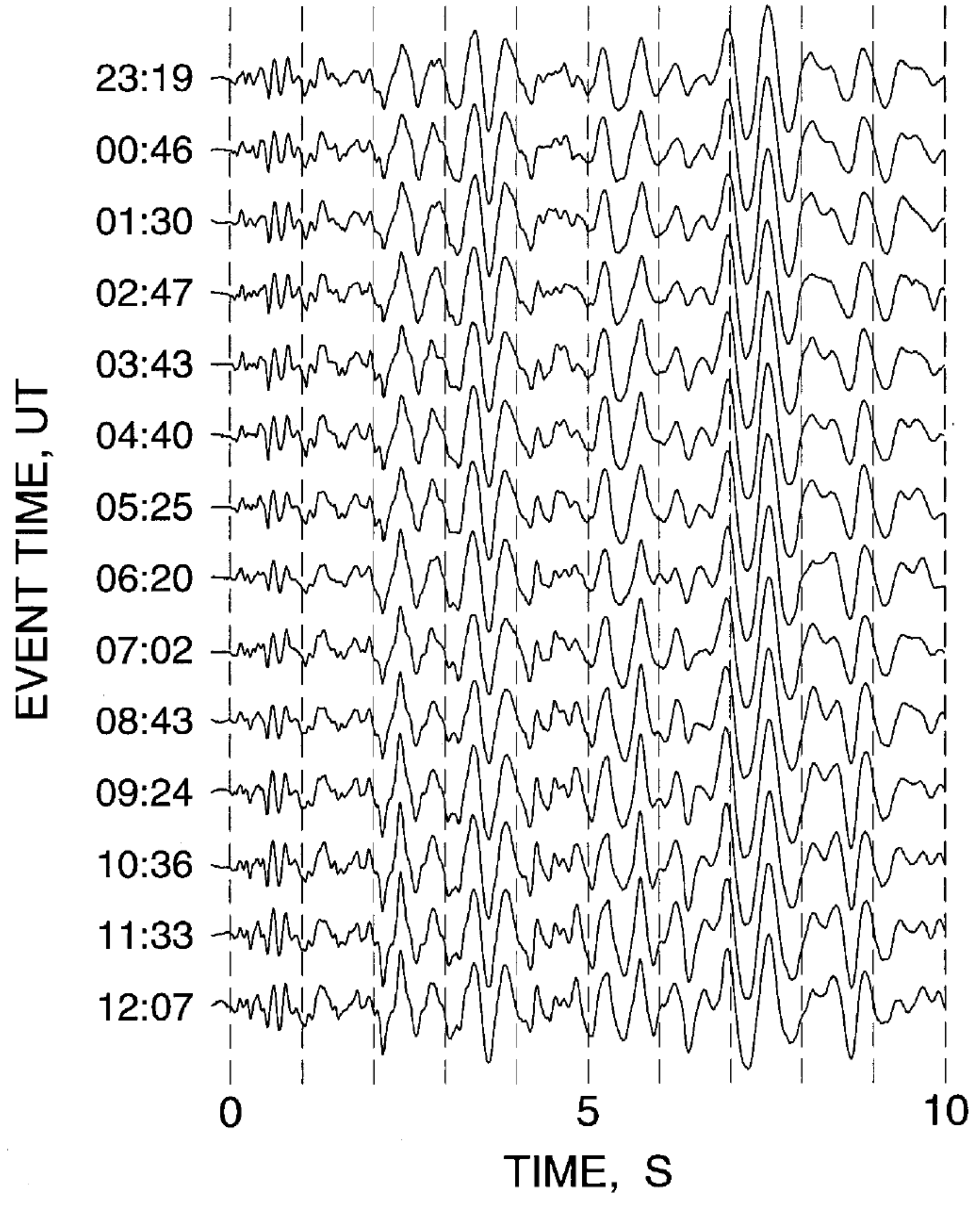

Stephens and Chouet [2001]

Small LP events at Mount St. Helens, 2005

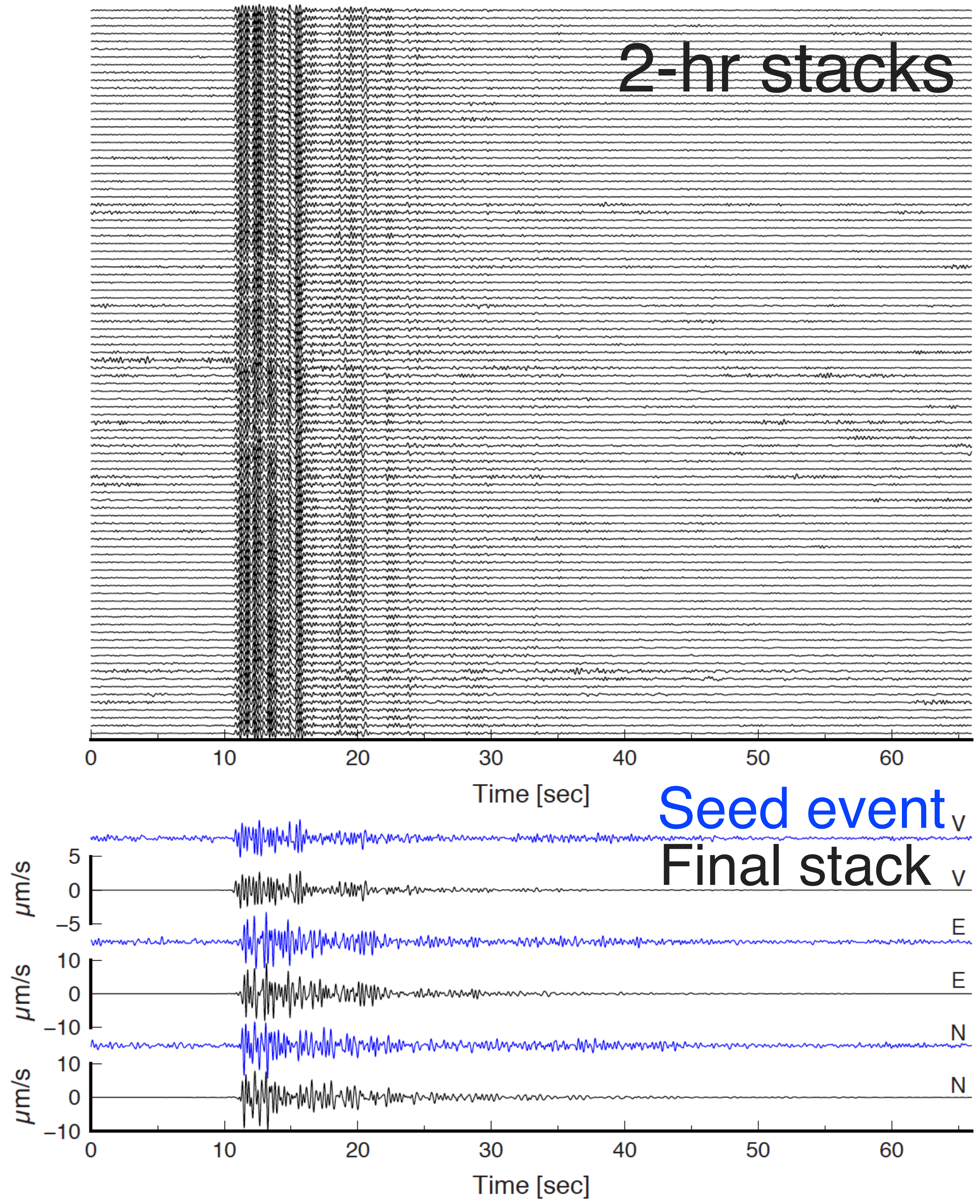

Matoza et al. [2015]

LPs as the impulse response of the resonant tremor system

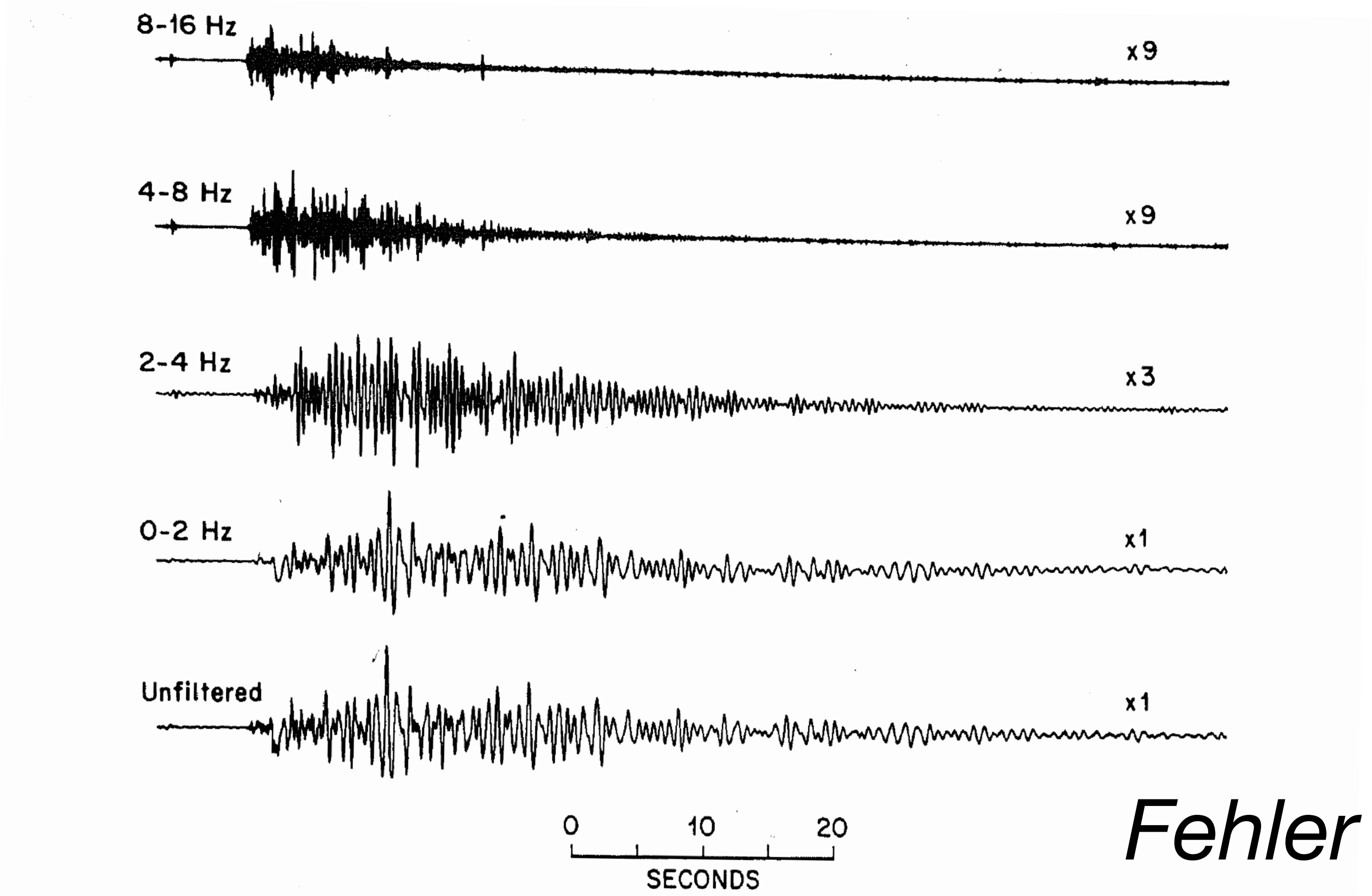

Fig. 9. Waveform of a typical long-period earthquake recorded at Mount St. Helens in October 1980 (lower trace). Upper traces show the result when the waveform is filtered with a band pass filter. The passband of the filter is labeled next to each trace. Note that some of the filtered traces have been magnified compared to the original traces.

Fehler [1983]

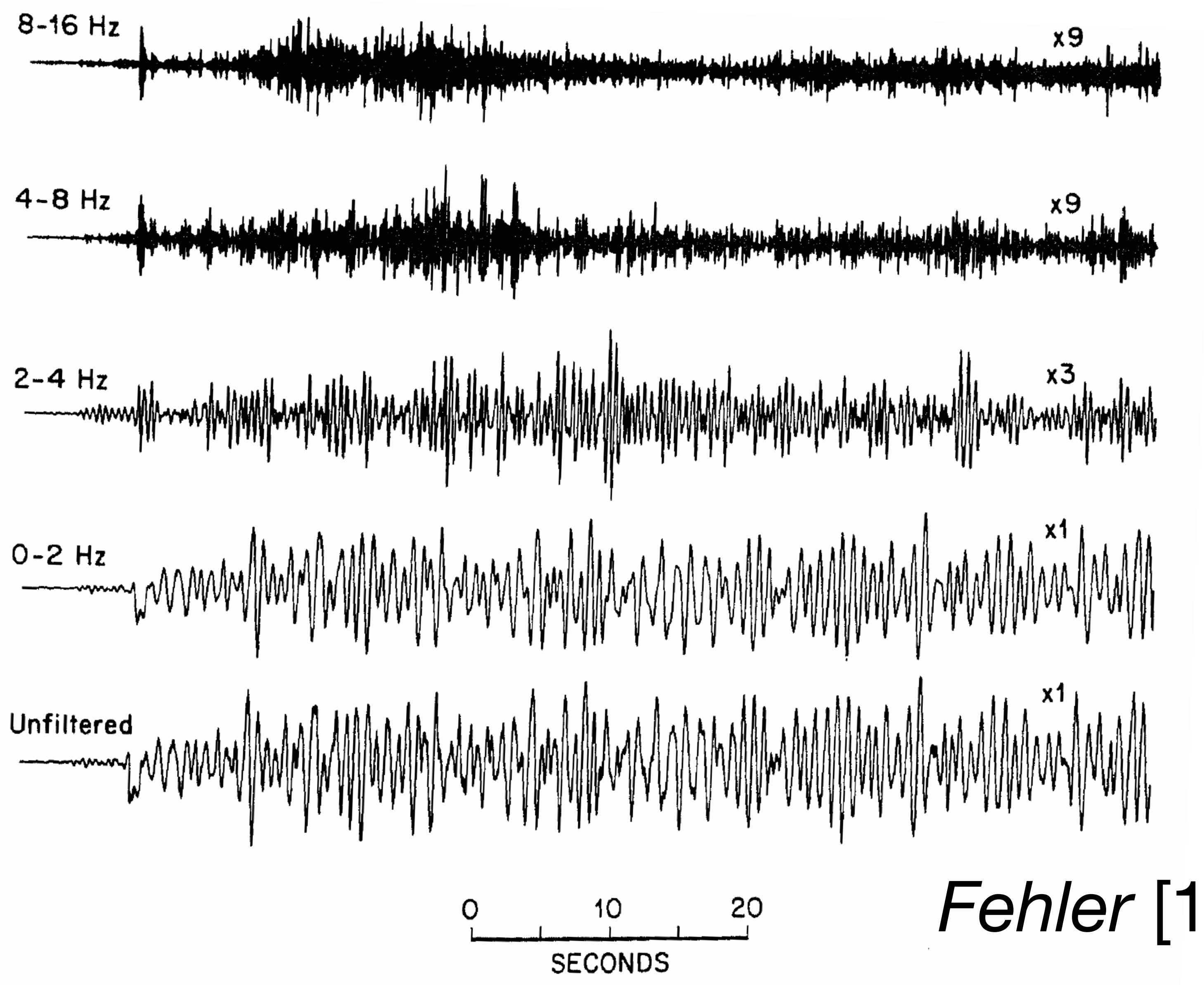

Fig. 10. Waveform of a tremor event and filtered traces.

Fehler [1983]

- LPs interpreted as the impulse response of a resonant tremor-generating system

Resonance of a fluid-filled conduit

JOURNAL OF GEOPHYSICAL RESEARCH, VOL. 90, NO. B2, PAGES 1881–1893, FEBRUARY 10, 1985

Excitation of a Buried Magmatic Pipe: A Seismic Source Model for Volcanic Tremor

BERNARD CHOUET

U.S. Geological Survey, Menlo Park, California

Recent observations of seismic events at various volcanoes suggest that harmonic tremor results from the sustained occurrence of so-called long-period or low-frequency events. Accordingly, we can view the long-period volcanic event as the elementary process of tremor and interpret it as the impulse response of the tremor-generating system. We present a seismic model in which the source of tremor is the acoustic resonance of a fluid-filled volcanic pipe triggered by excess gas pressure. The model consists of three elements, namely, a triggering mechanism, a resonator, and a radiator.

Chouet [1985]

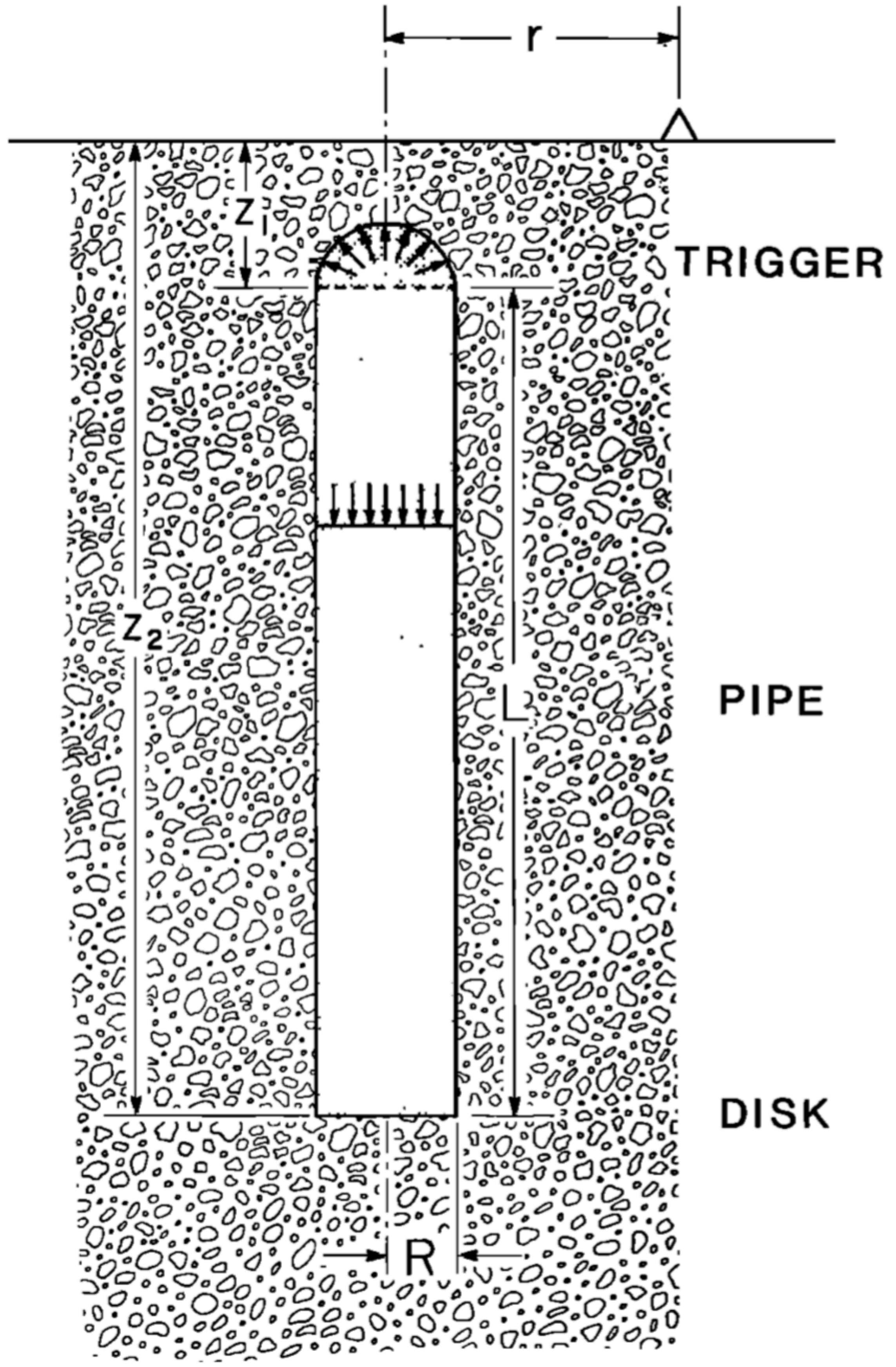

Fig. 1. Configuration of the source, medium, and receiver used in the computation of the ground motion produced by the excitation of a fluid-filled pipe. The composite source consists of a vertical conduit of radius R and length L capped by a hemisphere and shut by a horizontal disk at the bottom. The pipe is filled with a liquid while the hemispherical cap contains a gas. The depth to the pipe inlet is z_1, and the receiver is located at the epicentral distance r.

see also *Jousset et al.* [2003]; finite-difference solution of conduit resonance

LPs as the impulse response of the resonant tremor system

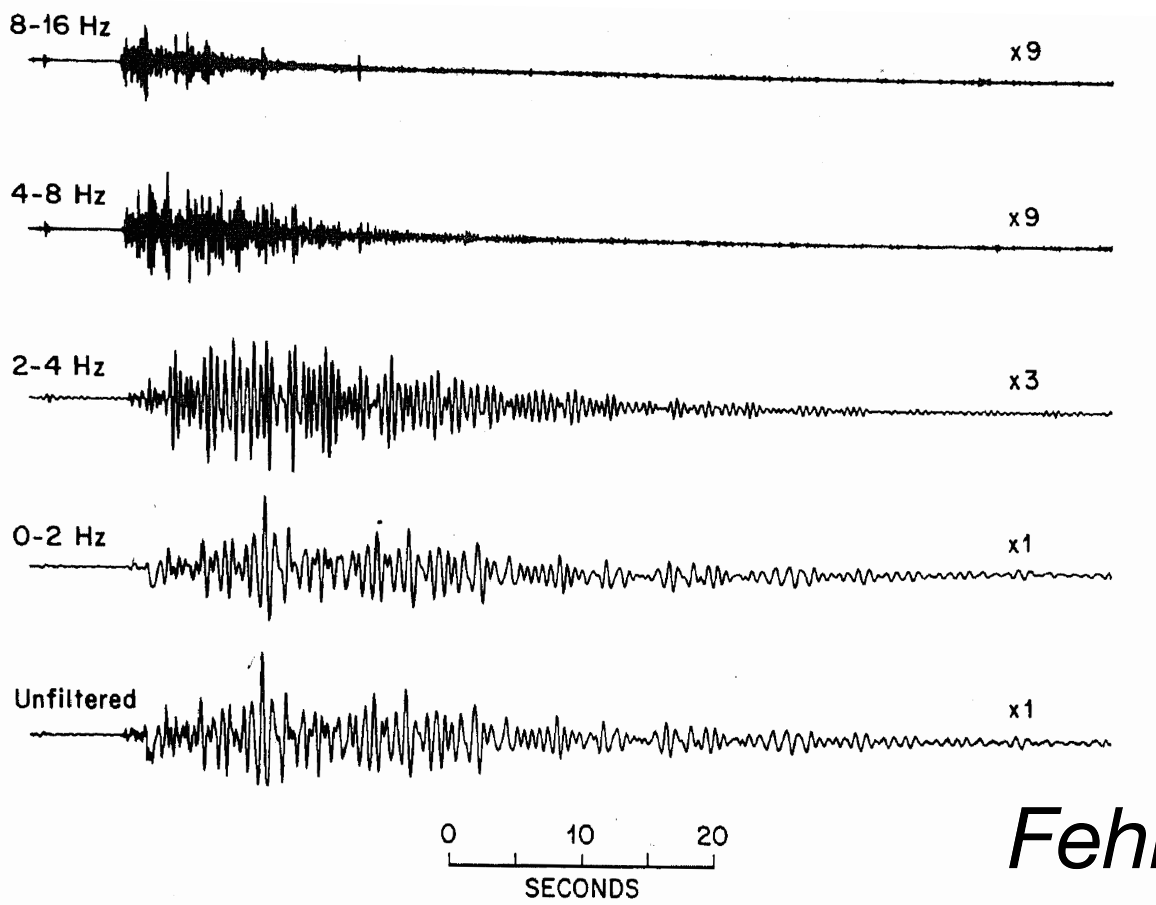

Fehler [1983]

Fig. 9. Waveform of a typical long-period earthquake recorded at Mount St. Helens in October 1980 (lower trace). Upper traces show the result when the waveform is filtered with a band pass filter. The passband of the filter is labeled next to each trace. Note that some of the filtered traces have been magnified compared to the original traces.

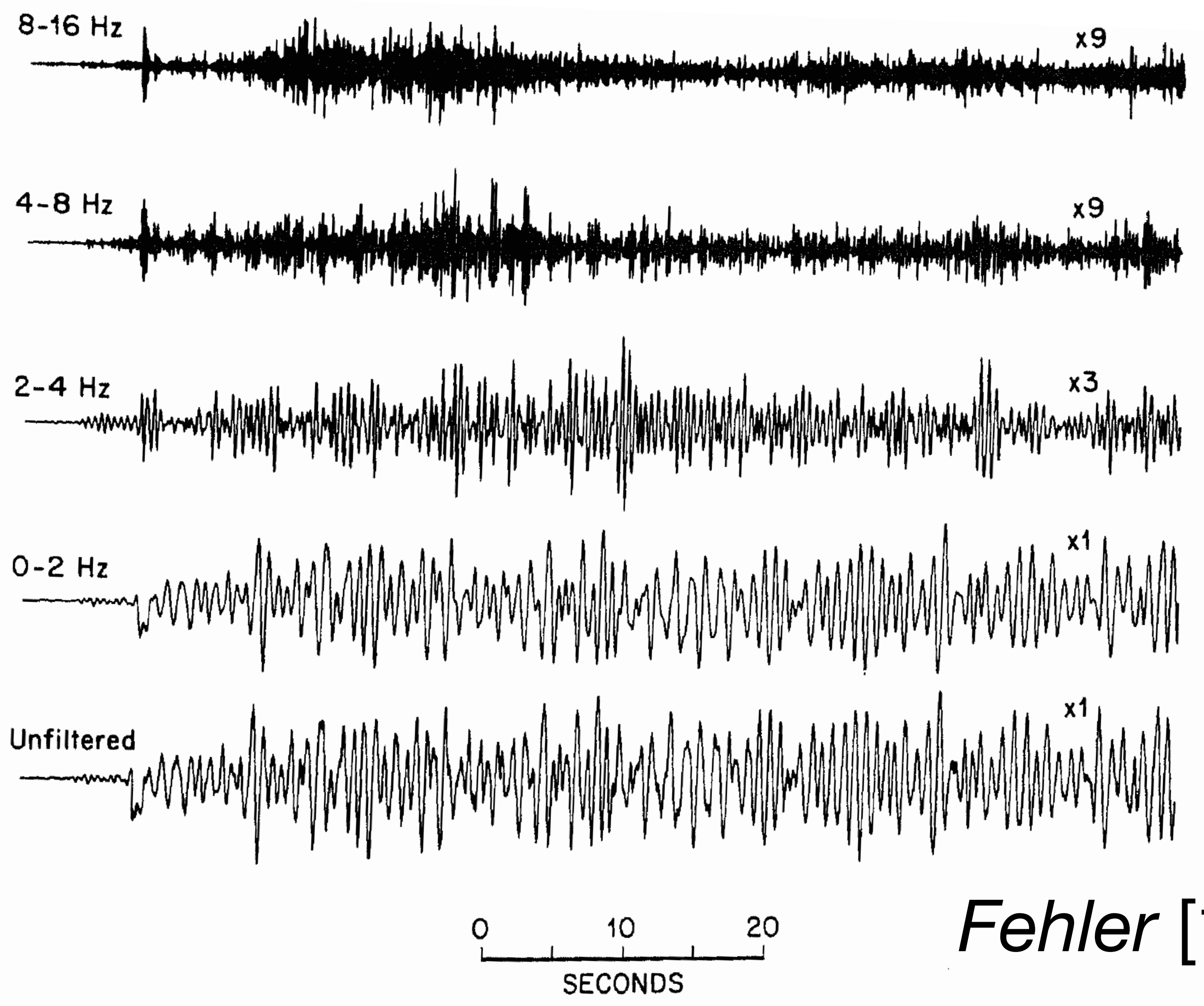

Fehler [1983]

Fig. 10. Waveform of a tremor event and filtered traces.

Resonance of a fluid-driven crack

JOURNAL OF GEOPHYSICAL RESEARCH, VOL. 93, NO. B5, PAGES 4375–4400, MAY 10, 1988

Resonance of a Fluid-Driven Crack: Radiation Properties and Implications for the Source of Long-Period Events and Harmonic Tremor

BERNARD CHOUET

U.S. Geological Survey, Menlo Park, California

A dynamic source model is presented, in which a three-dimensional crack containing a viscous compressible fluid is excited into resonance by an impulsive pressure transient applied over a small area ΔS of the crack surface. The crack excitation depends critically on two dimensionless parameters called the crack stiffness, $C = (b/\mu)(L/d)$, and viscous damping loss, $F = (12\eta L)/(\rho_f d^2 \alpha)$, where b is the bulk modulus, η is the viscosity, ρ_f is the density of the fluid, μ is the rigidity, α is the compressional velocity of the solid, L is the crack length, and d is the crack thickness. ---

Chouet [1988]

SOURCE MECHANISM OF VOLCANIC TREMOR: FLUID-DRIVEN CRACK MODELS AND THEIR APPLICATION TO THE 1963 KILAUEA ERUPTION

KEIITI AKI, MIKE FEHLER and SHAMITA DAS

Department of Earth and Planetary Sciences, Massachusetts Institute of Technology, Cambridge, Mass. 02139 (U.S.A.)

(Received November 1, 1976; revised version accepted March 17, 1977)

Aki, Fehler, and Das [1977]

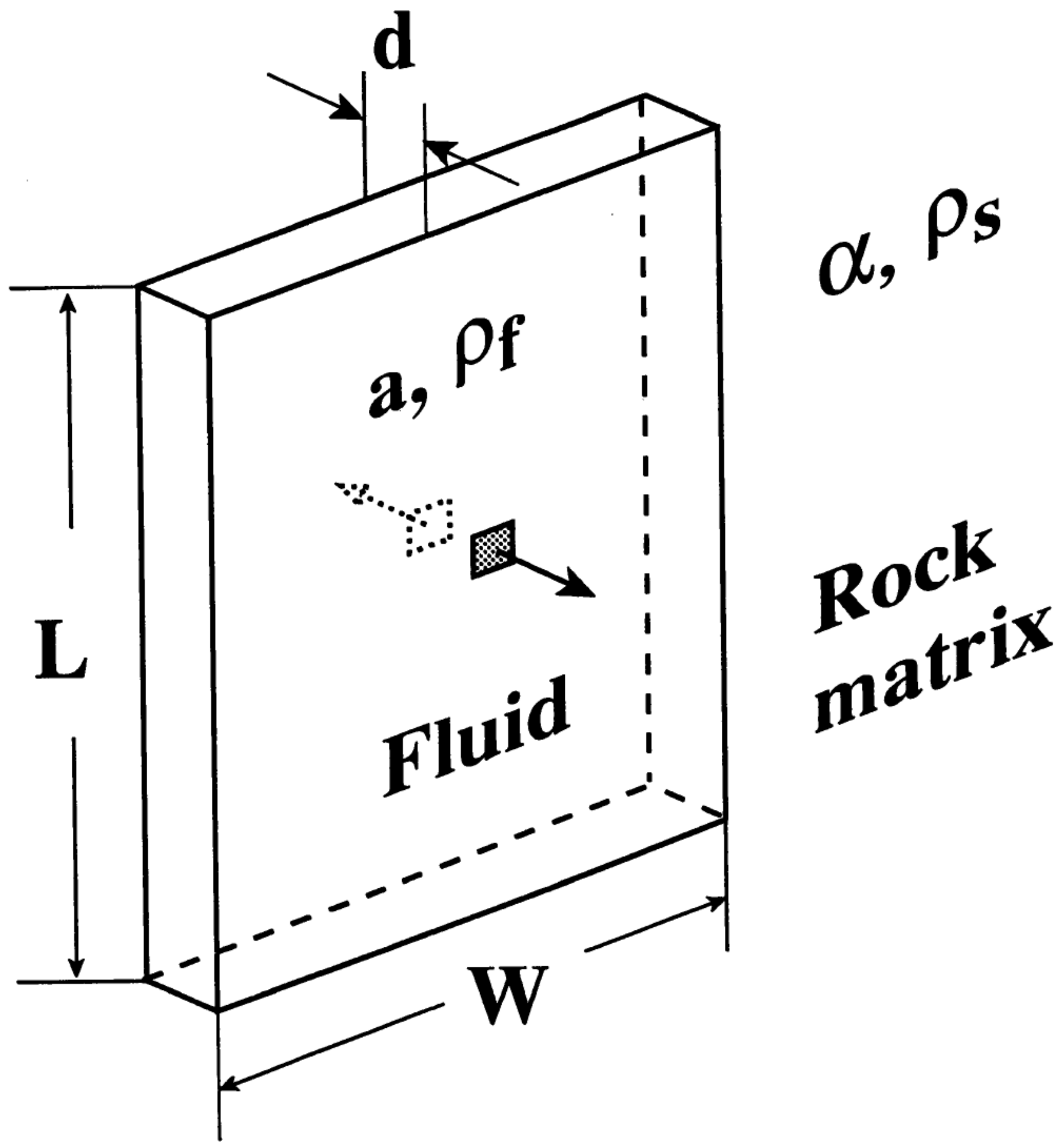

Figure 1. Geometry of the crack model. L, W, and d are the length, width, and aperture of the crack, respectively; a is the sound speed of the fluid in the crack and α is the P wave velocity of the rock matrix, and ρ_f and ρ_s are the densities of the fluid and rock matrix, respectively. We use $W/L = 0.5$, $L/d = 10^4$, and a step increase in pressure applied at the center of the crack as the crack excitation throughout this study.

figure: *Kumagai and Chouet* [2000]

LPs: the fluid-driven crack model

broadband onset

long-duration coda oscillation

$$s(t) * l(t)$$

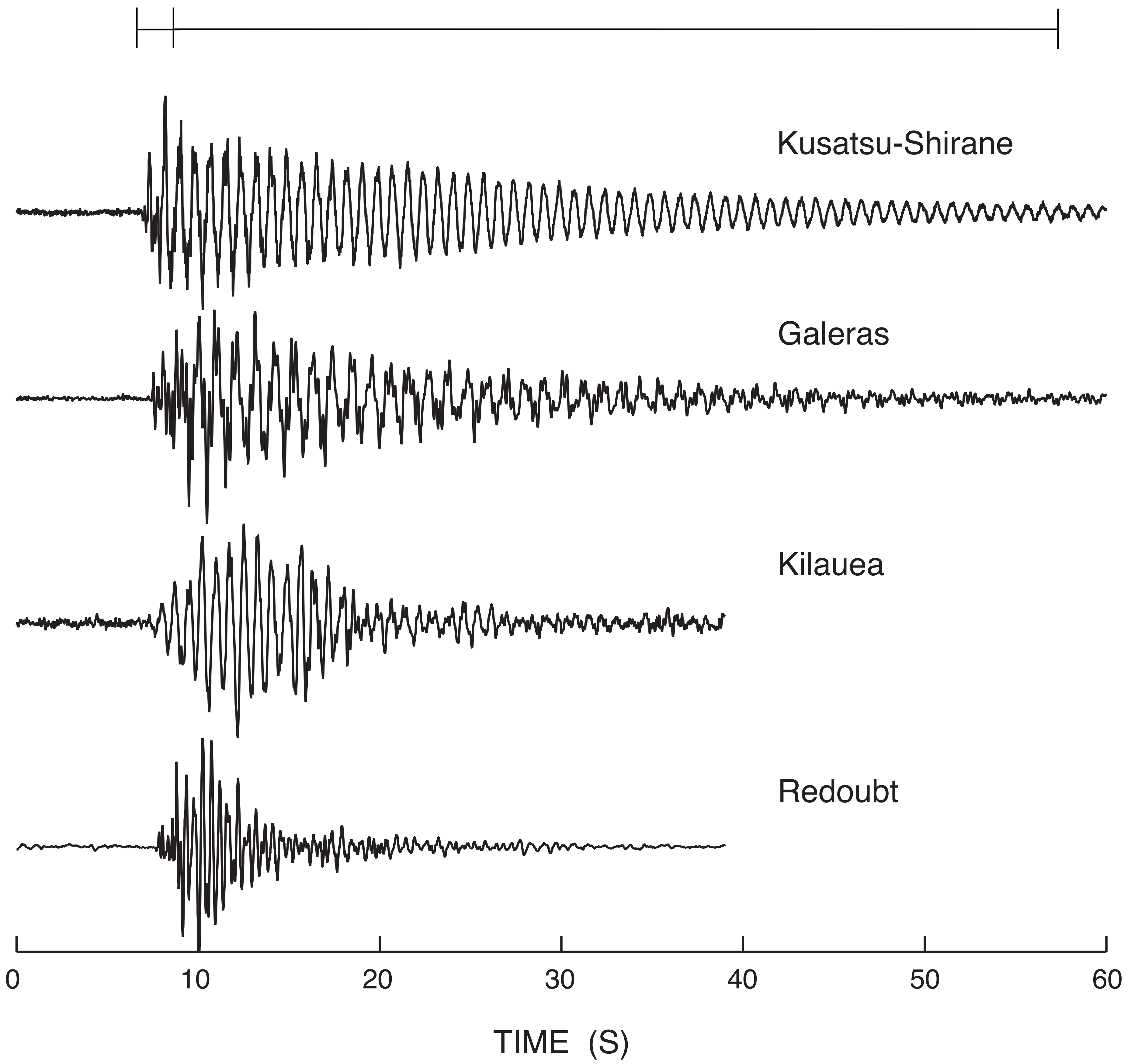

Chouet [1996]

LPs: the fluid-driven crack model

trigger/excitation → fluid response

$$s(t) * l(t)$$

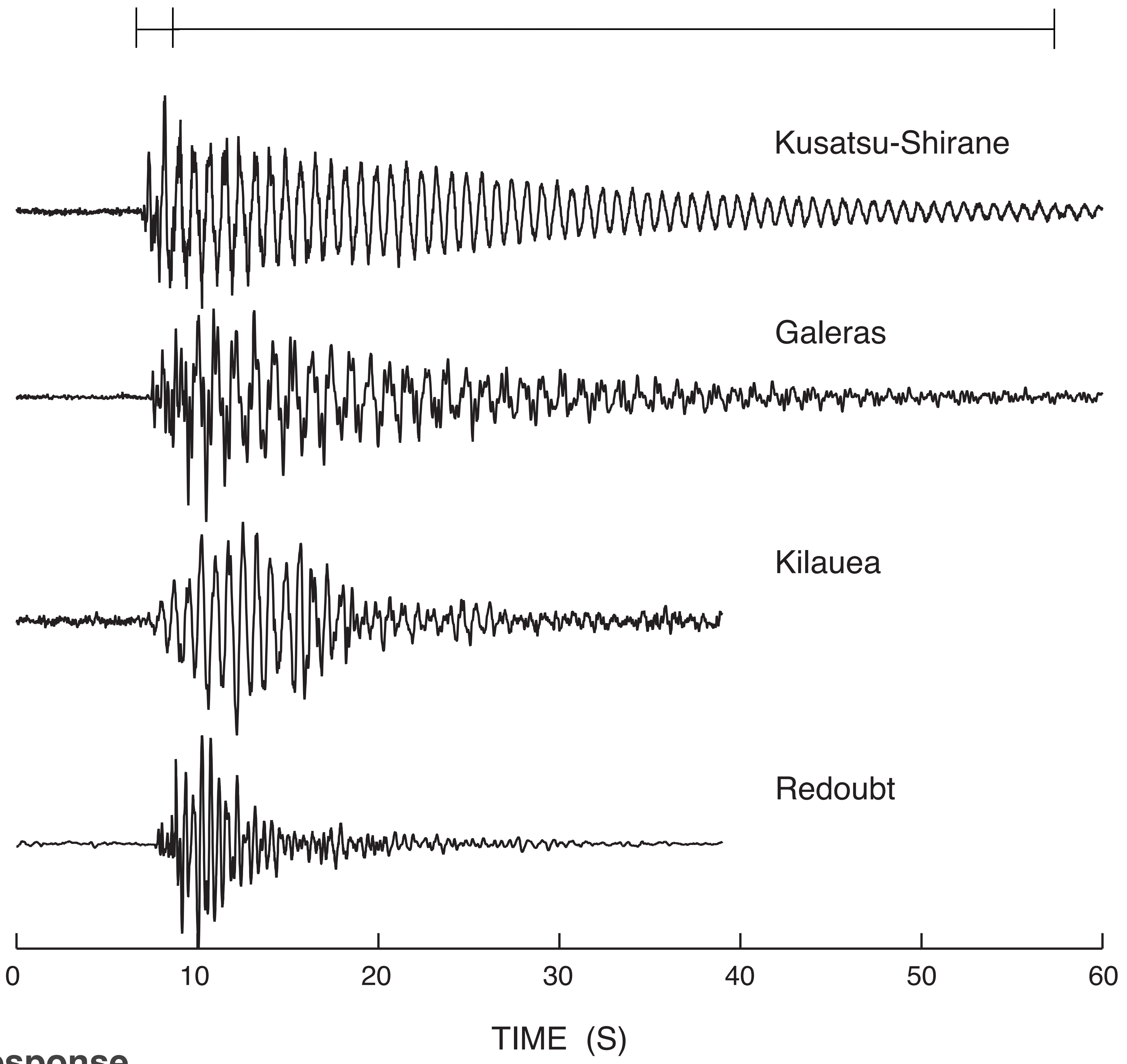

Resonant response

- Fluid-filled crack or conduit
- Bubbly magma, water, steam, dusty gas

Chouet [1996]

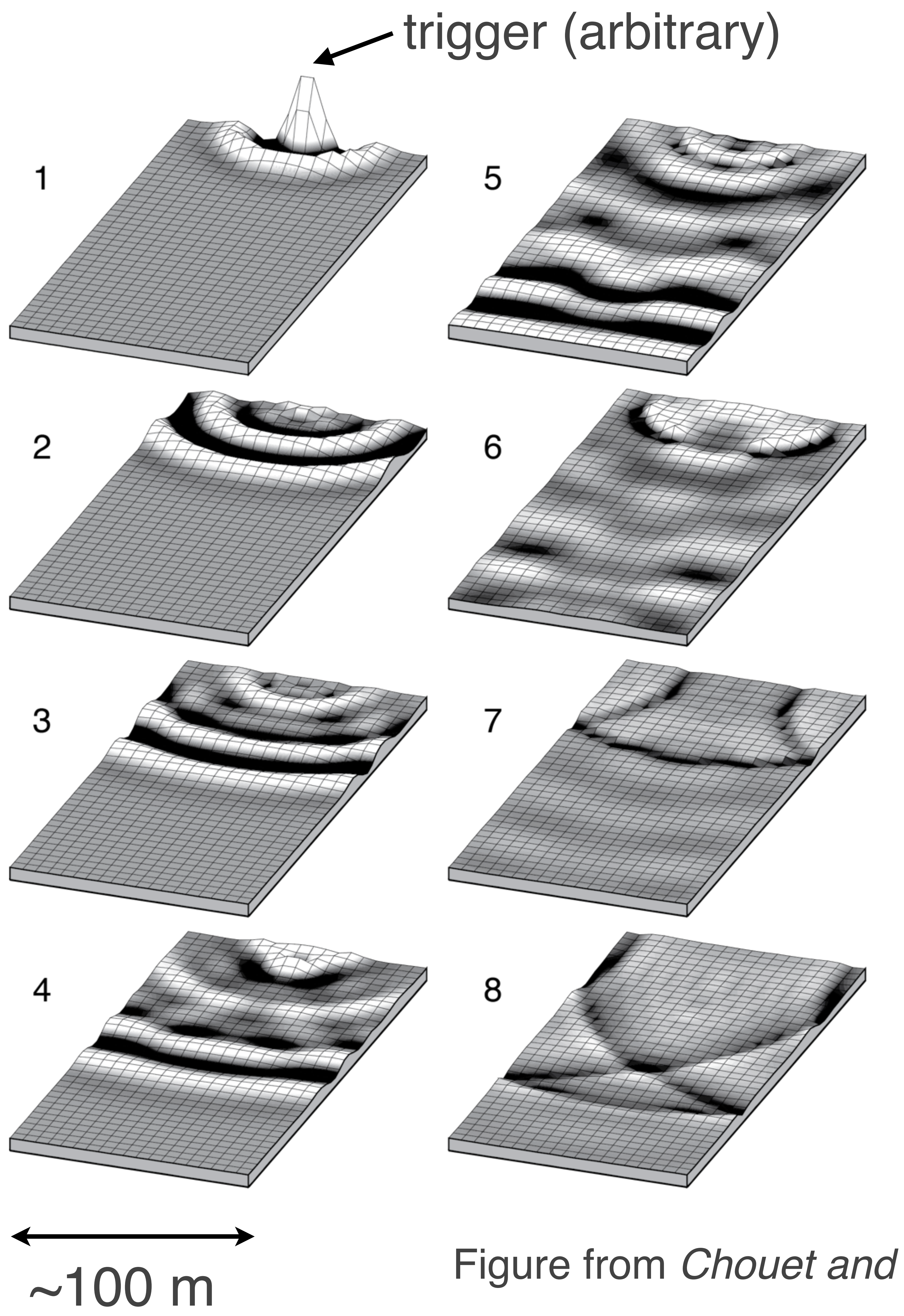

Figure from *Chouet and Matoza* [2013]

"Crack waves" Solid-fluid interface waves; fluid-filled crack in elastic solid

Chouet [1986, 1988, 1992]

Ferrazzini and Aki [1987]: analytic expressions of the crack waves, considering normal modes in a fluid layer sandwiched between two homogeneous half-spaces.

LPs: the fluid-driven crack model

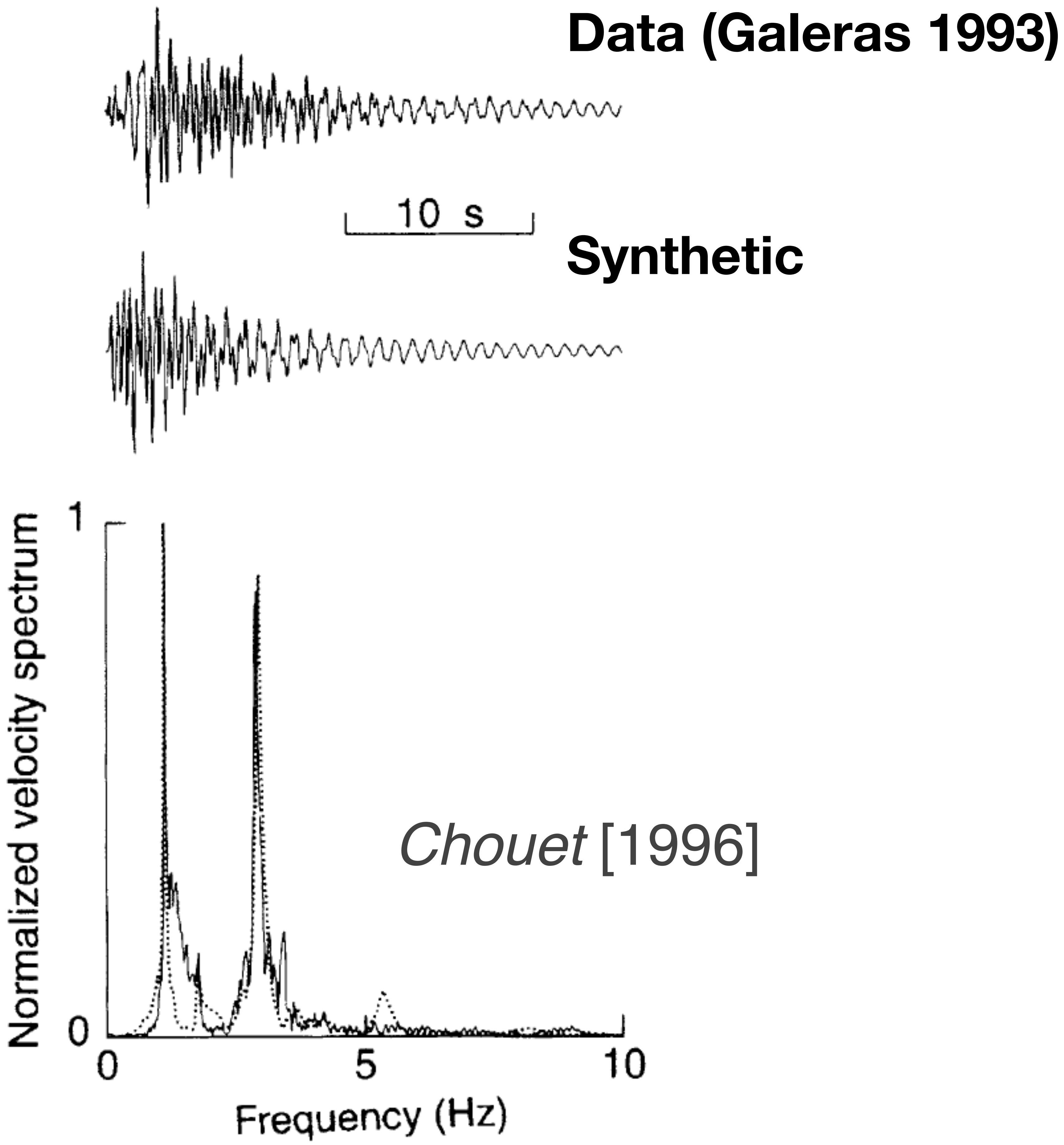

Chouet [1996]

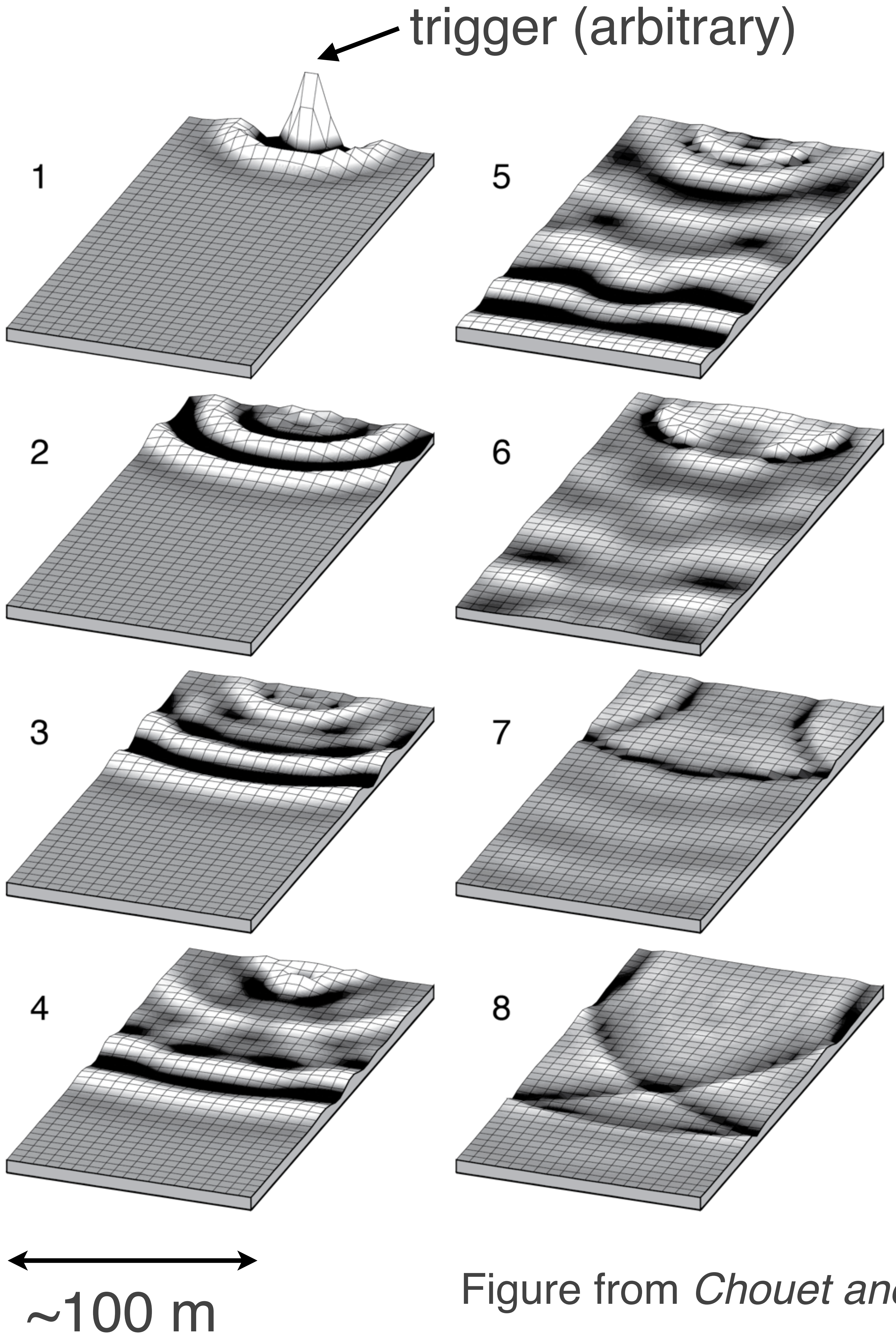

"Crack waves" Solid-fluid interface waves; fluid-filled crack in elastic solid

Chouet [1986, 1988, 1992]

Ferrazzini and Aki [1987]: analytic expressions of the crack waves, considering normal modes in a fluid layer sandwiched between two homogeneous half-spaces.

Figure from *Chouet and Matoza* [2013]

Resonant response

- Fluid-filled crack or conduit
- Bubbly magma, water, steam, dusty gas

LPs: the fluid-driven crack model

trigger/excitation → fluid response

$$s(t) * l(t)$$

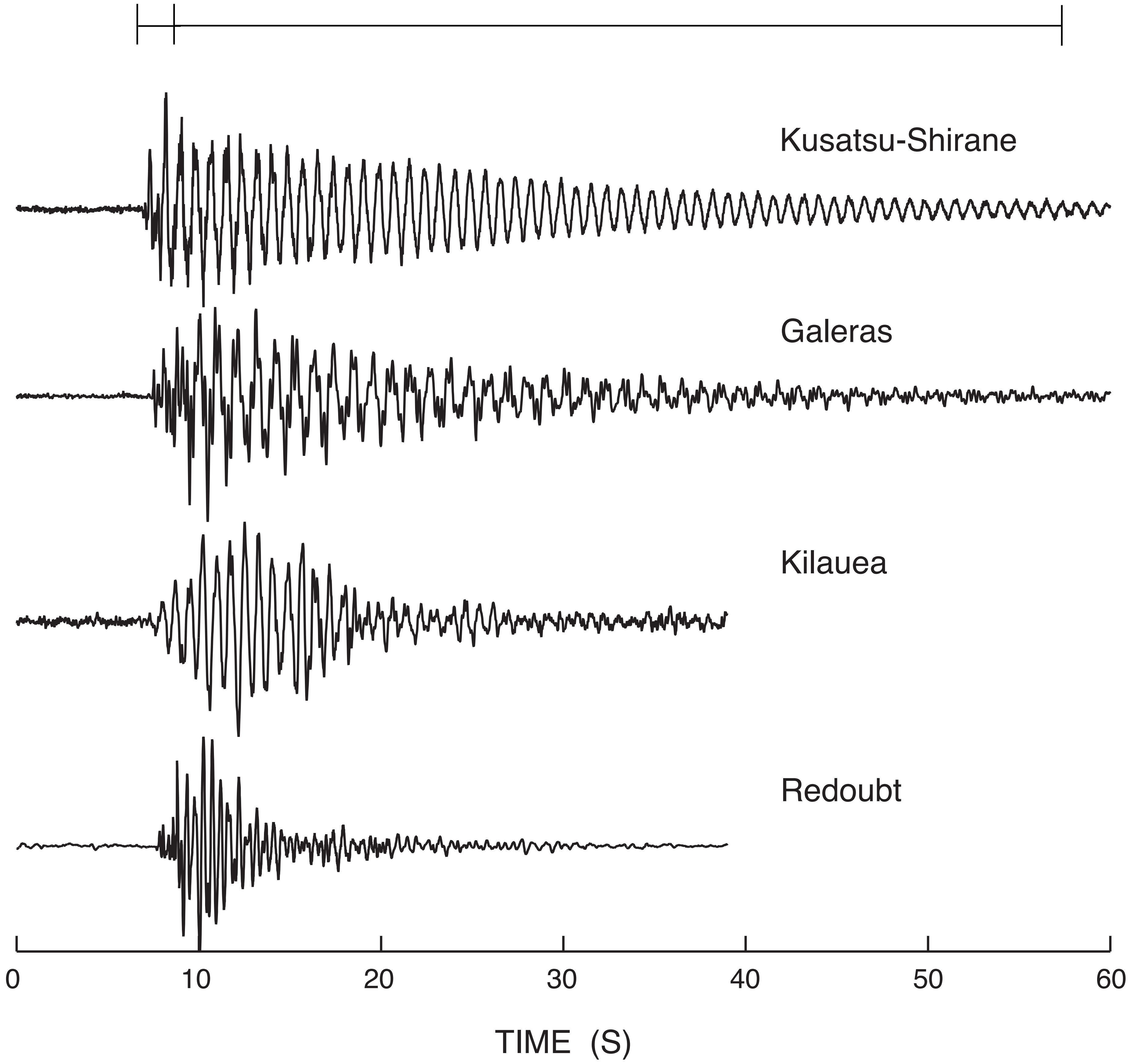

Chouet [1996]

The trigger mechanism

- What excites the resonance?
- Impulsive trigger: discrete LP event
- Sustained trigger: tremor

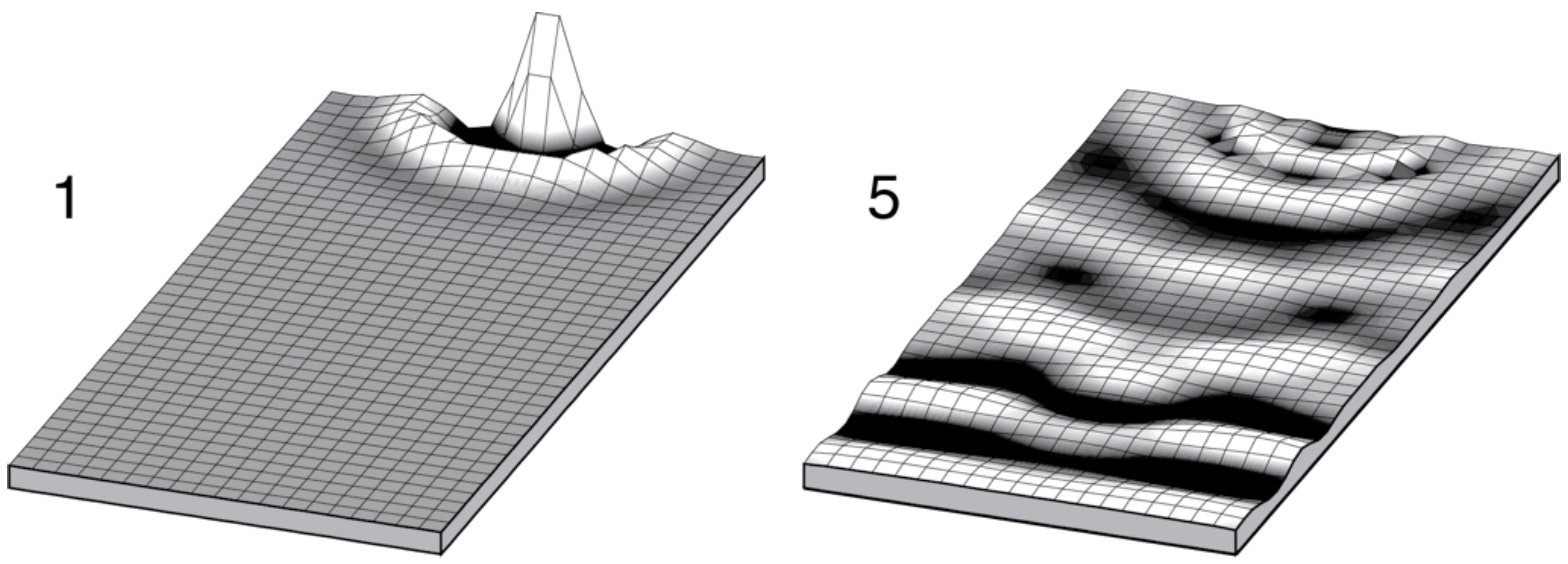

LPs: trigger mechanism in magmatic-hydrothermal systems

Cyclic recharge-collapse of a hydrothermal crack

Mount St. Helens
2152:37 UTC, 9 November 2005

S04 HHZ
distance 1.1 km

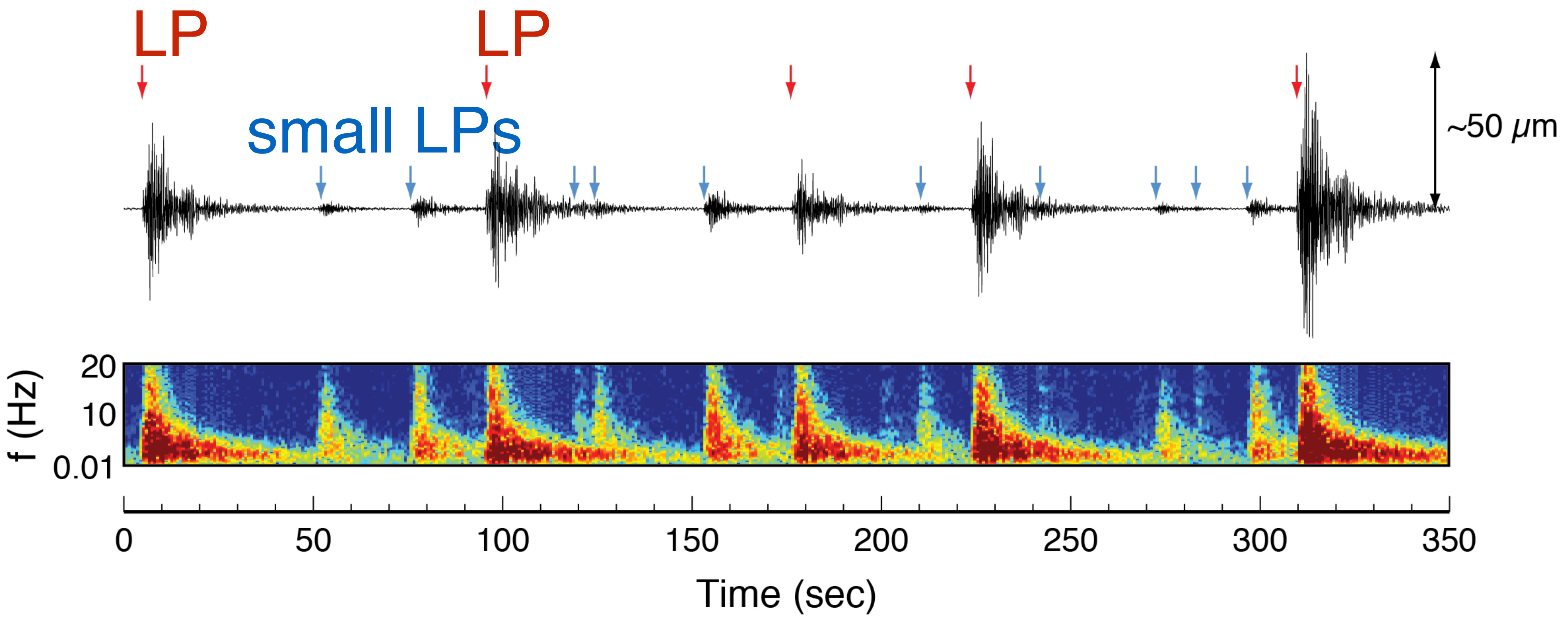

e.g., *Matoza and Chouet* [2010]

Schematic of Kusatsu-Shirane, Japan
Nakano et al. [2003]

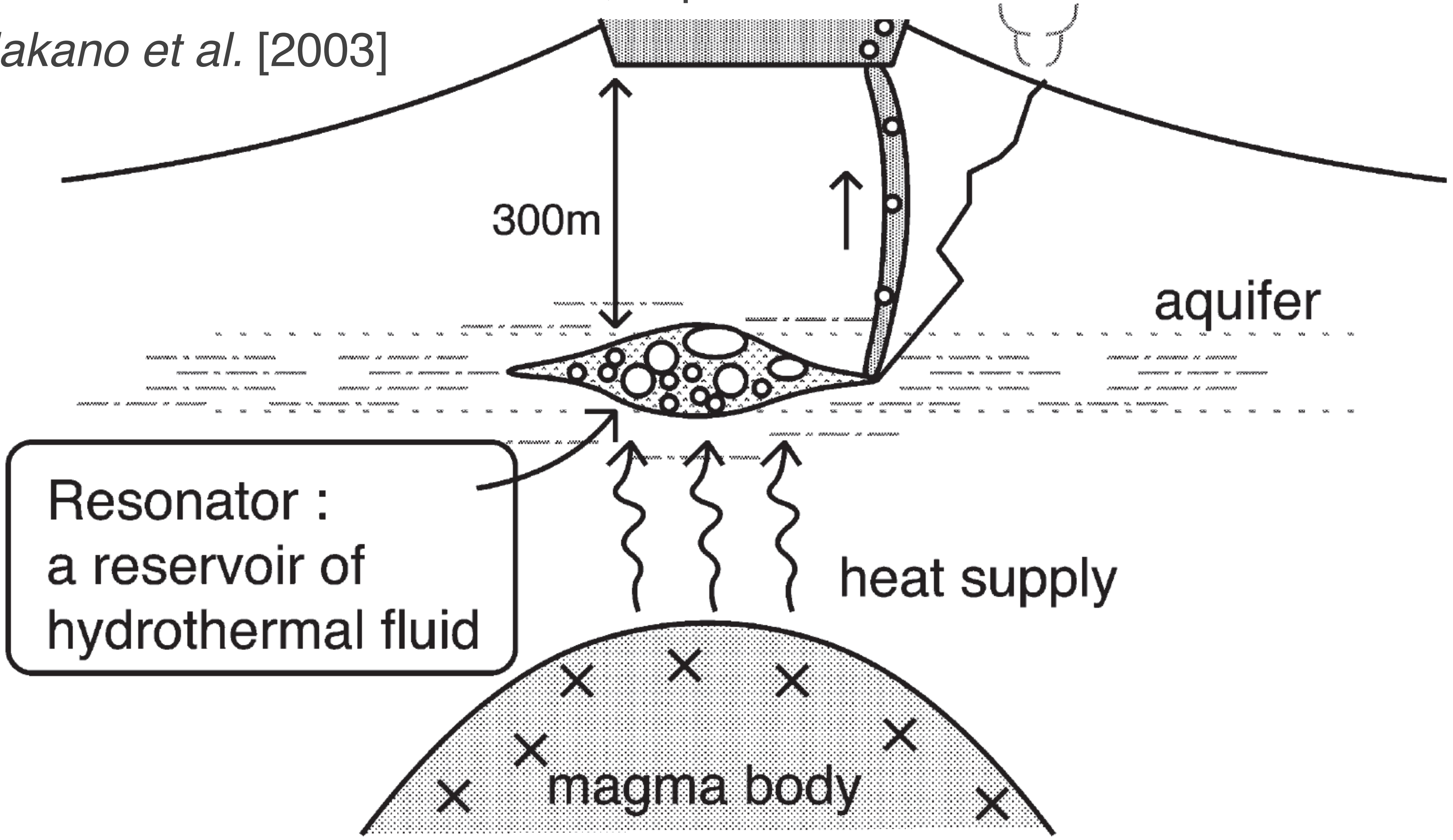

e.g., *Kumagai et al.* [2005]; *Ohminato* [2006]; *Waite et al.* [2008]; *Matoza and Chouet* [2010]; *Maeda et al.* [2013]

Mount St. Helens 2004–2008 eruption

Solid extrusion, plug stick-slip

Iverson et al. [2006]

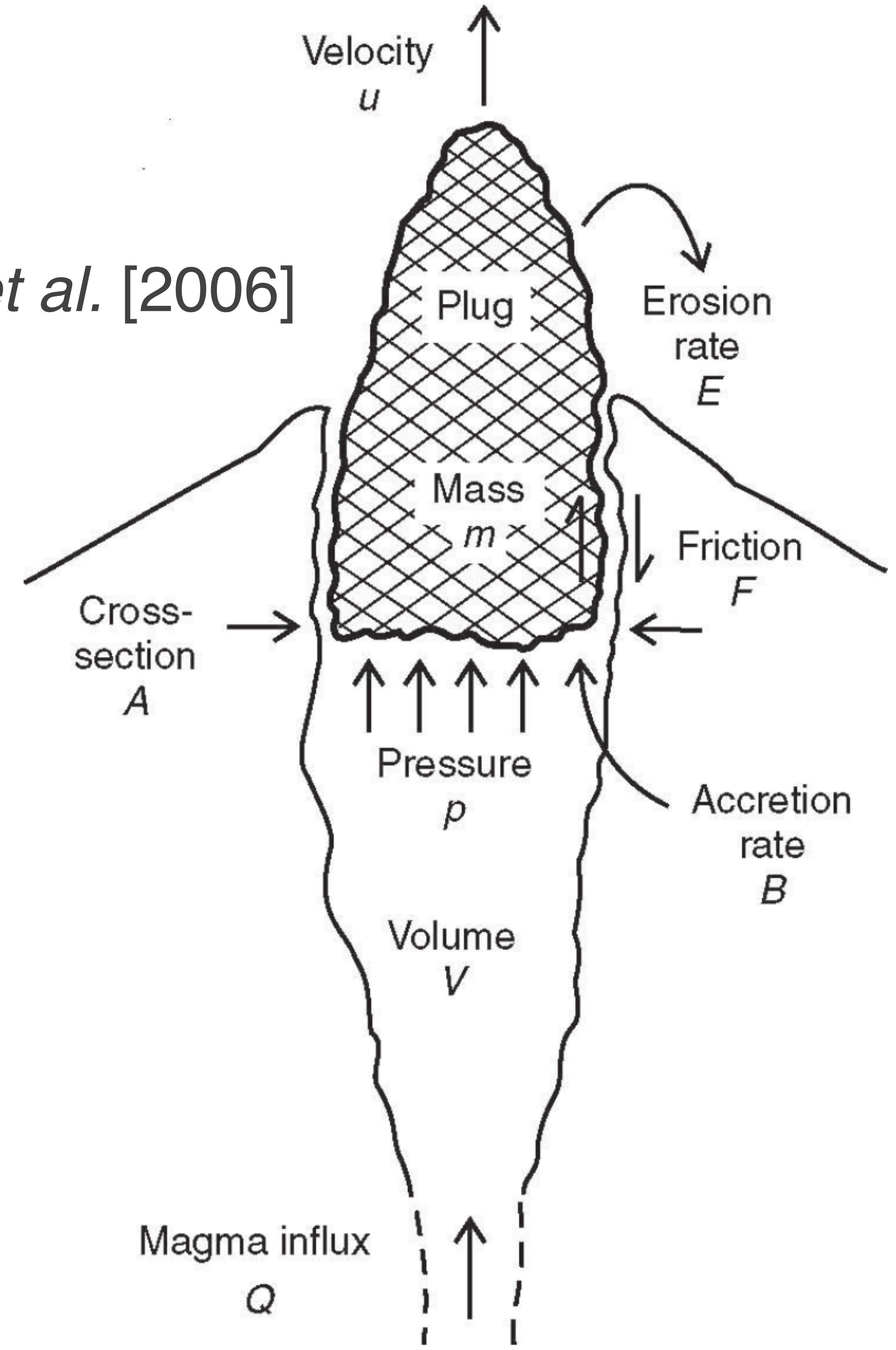

e.g., *Iverson et al.* [2006]; *Harrington and Brodsky* [2007]; *Iverson* [2008]; *Kendrick et al.* [2014]

Cyclic recharge-collapse of a hydrothermal crack

Schematic of Kusatsu-Shirane, Japan

Nakano et al. [2003]

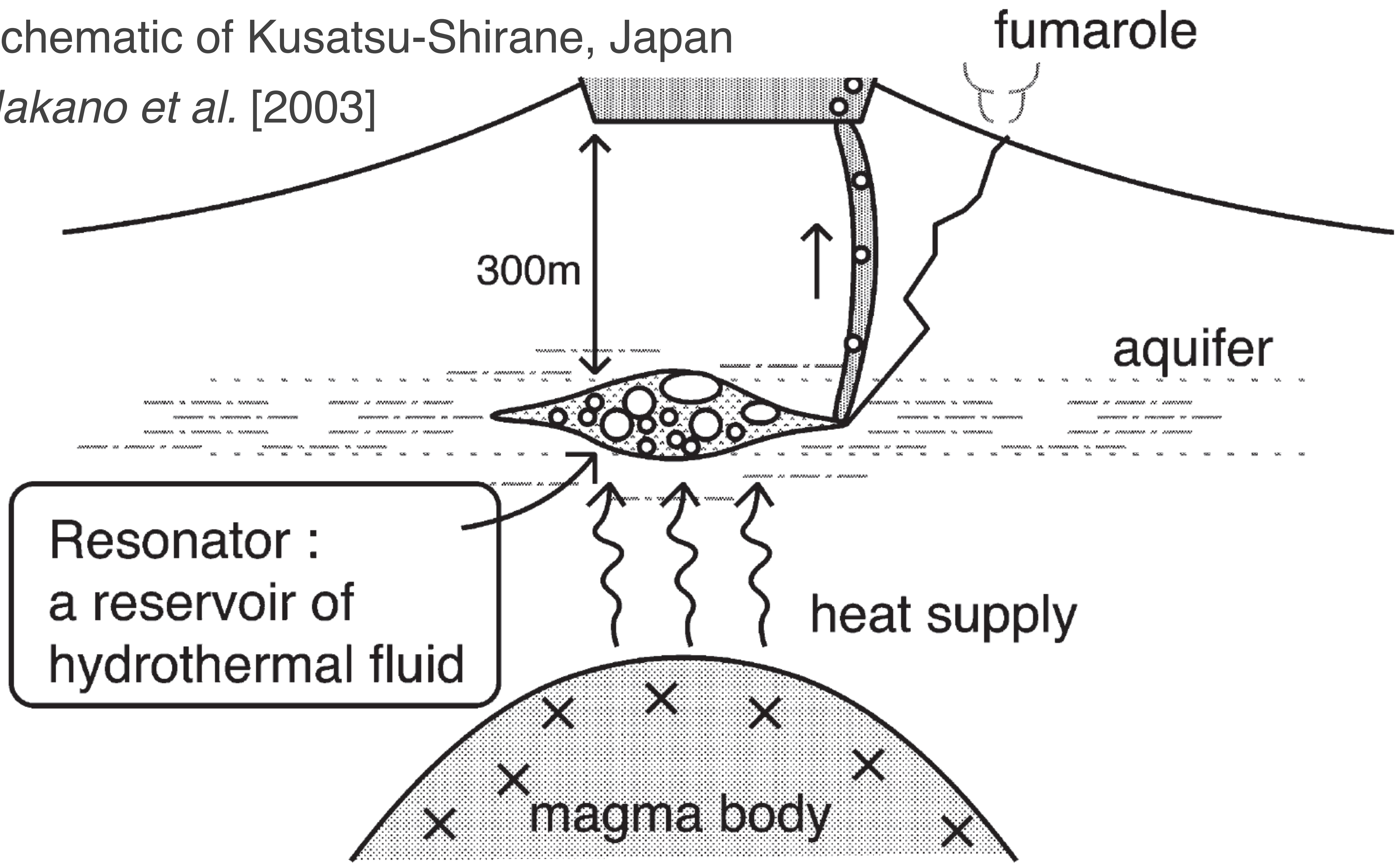

e.g., *Kumagai et al.* [2005]; *Ohminato* [2006]; *Waite et al.* [2008]; *Matoza and Chouet* [2010]; *Maeda et al.* [2013]

Brittle failure of melt

- Brittle failure of melt in the glass transition
- Multiplets: repeated fracture and heal or ascent through a depth-limited seismogenic window

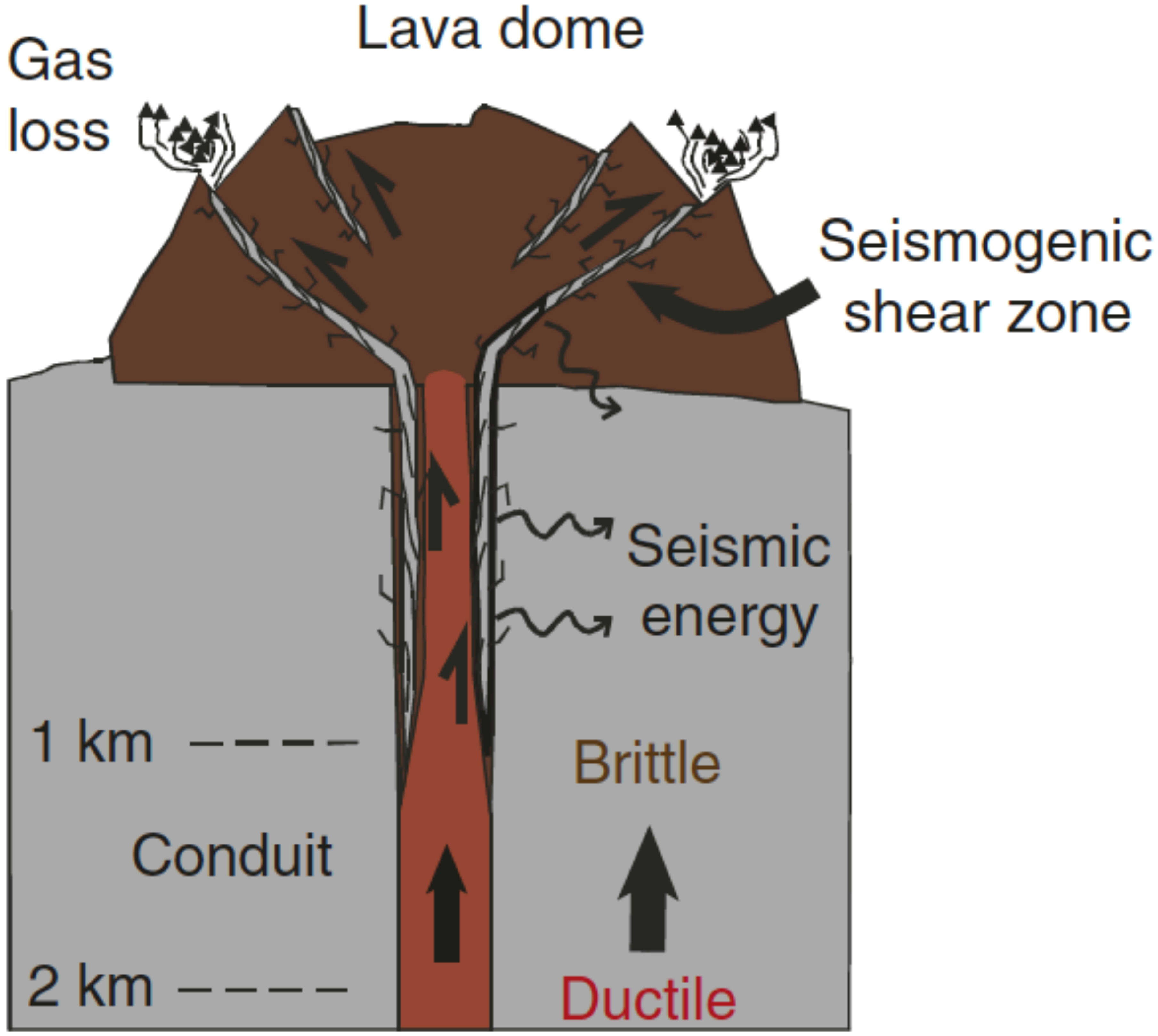

Tuffen et al. [2008]

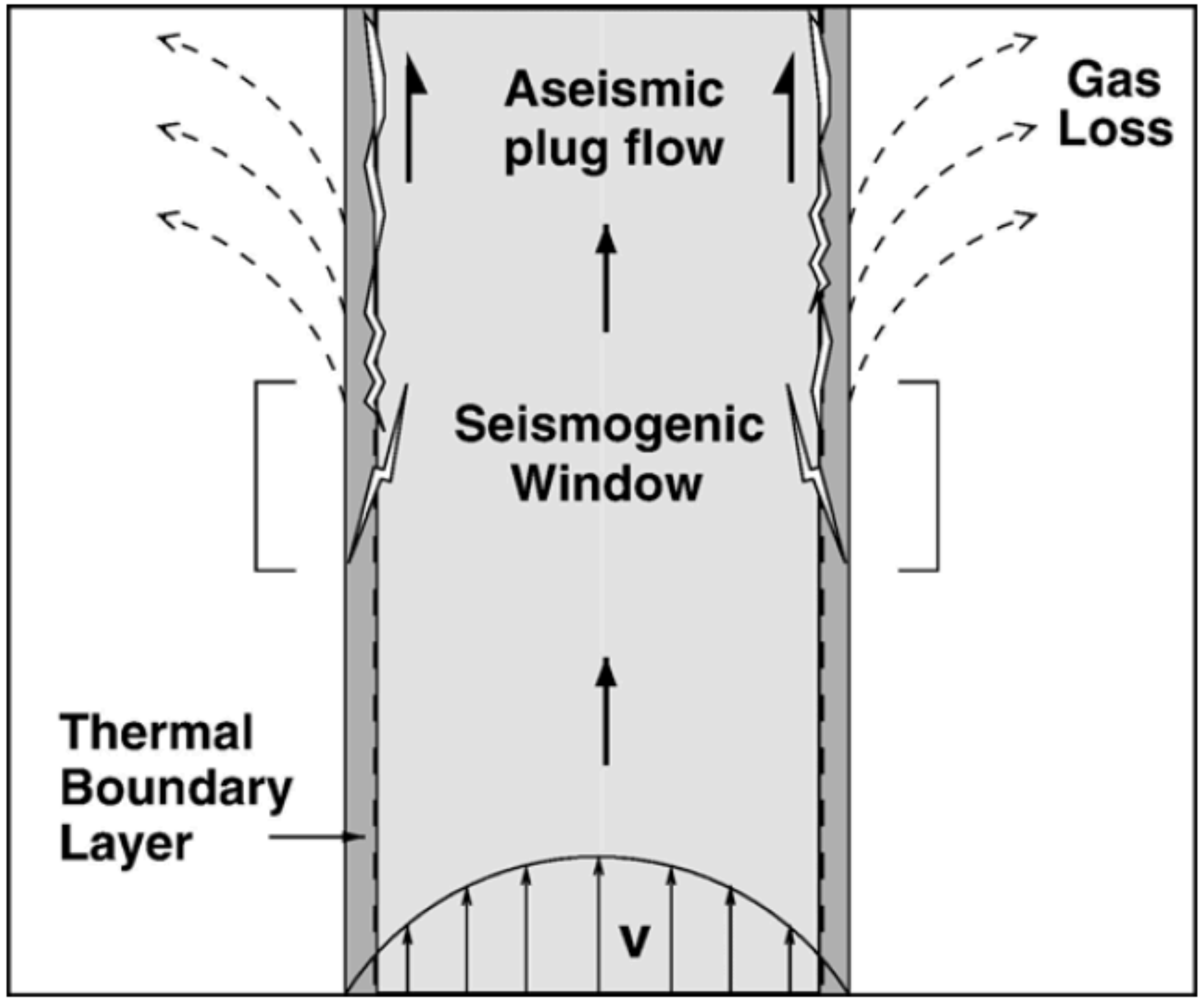

Neuberg et al. [2006]

Eruption cycles and forecasting

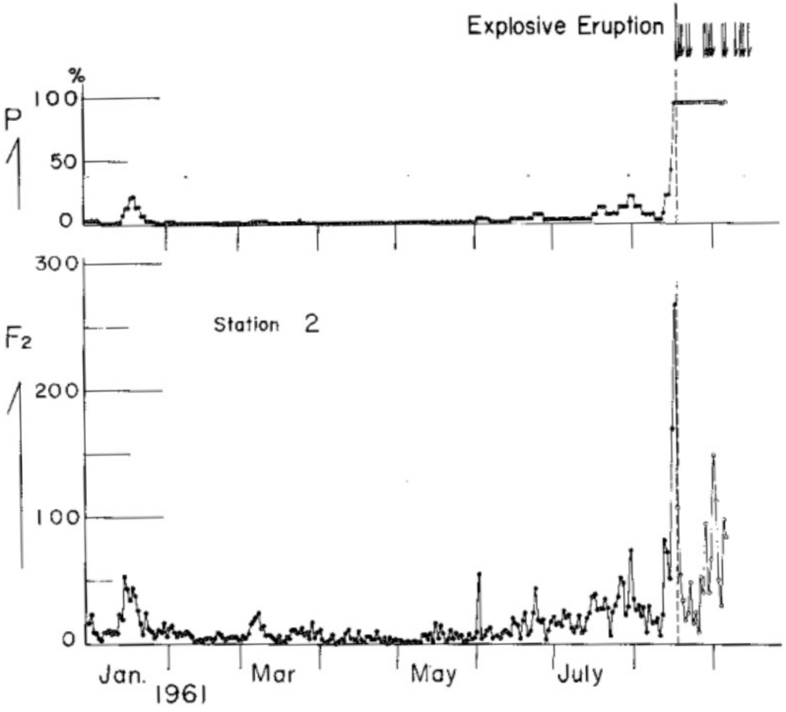

Fig.8. The practical application of the 1960 formula to eruptions which took place in 1961, based on the daily frequency of B-type quakes. Arrows = eruptions; P = probability of eruption given from the 1960 formula; F_2 = seismic daily frequency of B-type quakes originating in Asama.

- Probability of eruptions based on the occurrence rate of B-type earthquakes (=explosion quakes)
- Increase in rate leads to increased probability of a B-type earthquake large enough to cause an explosion

Minakami [1960, 1974]

Eruption cycles and forecasting

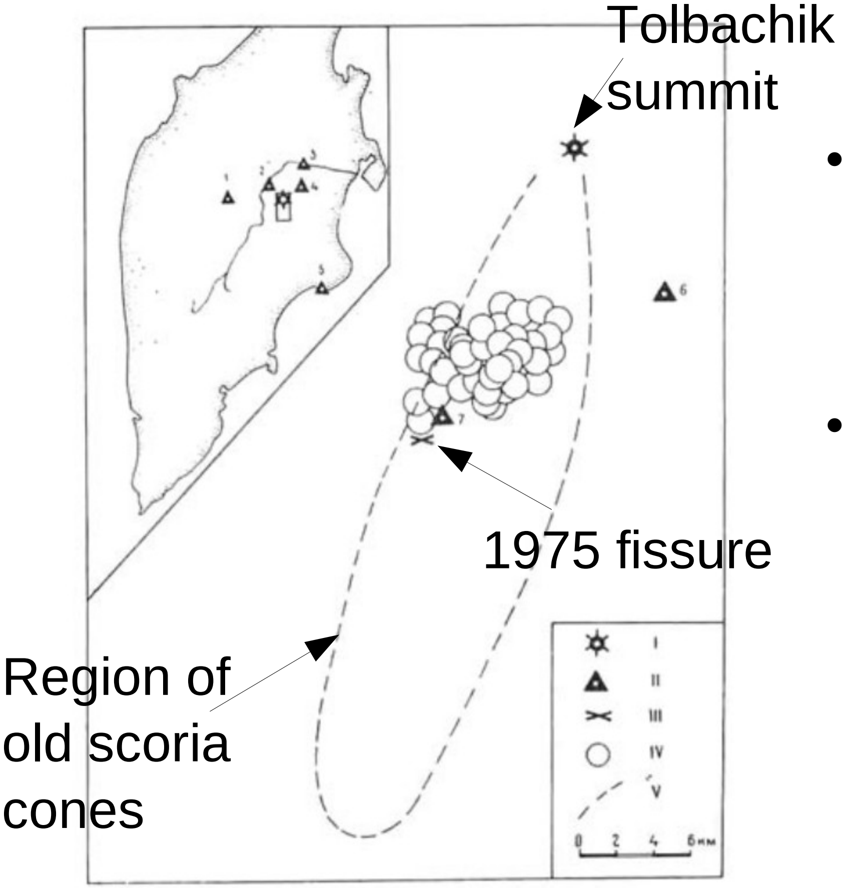

- Location and time of Tolbachik 1975 eruption forecast 3 days beforehand on the basis of epicenter locations
- Rapid deployment of additional seismometers for earthquake location

Tokarev [1978]

Eruption cycles and forecasting

- Quantitative forecasting of eruption time at Mt. St. Helens based on event rate acceleration (‘Failure Forecast Method’)

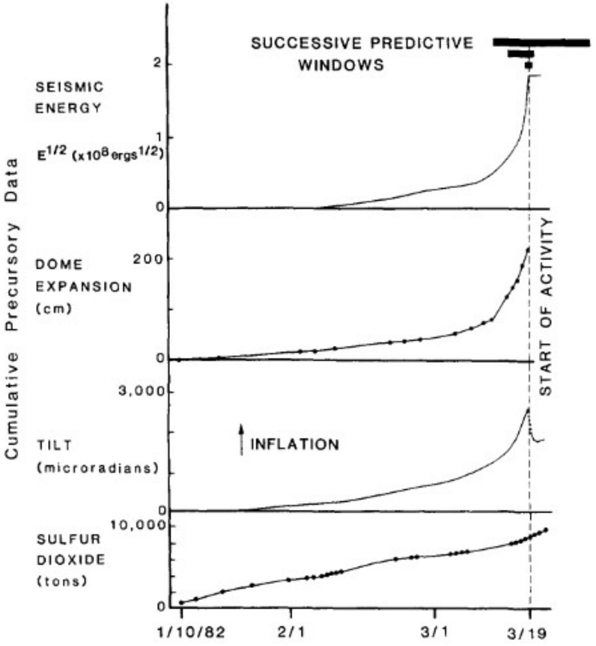

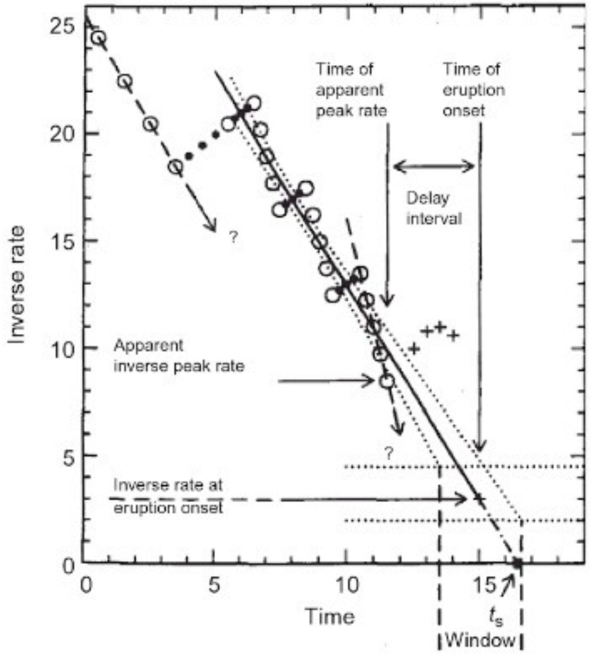

Swanson et al. [1985], Cornelius and Voight [1994]

Eruption cycles and forecasting

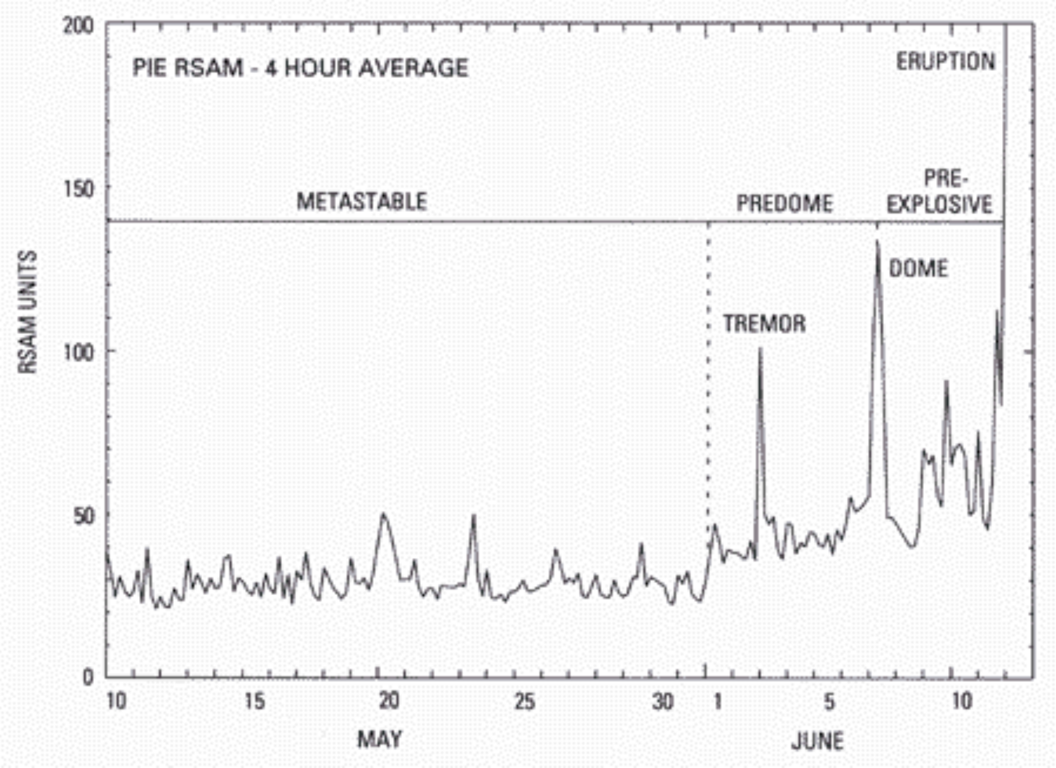

- Use of RSAM (Real-time Seismic Amplitude Measurement) for rapid assessment of eruption potential at Pinatubo (1991)

Harlow et al. [1996]

Eruption cycles and forecasting

- Eruption forecasting without a local seismo-acoustic network at Bogoslof (2016-17)

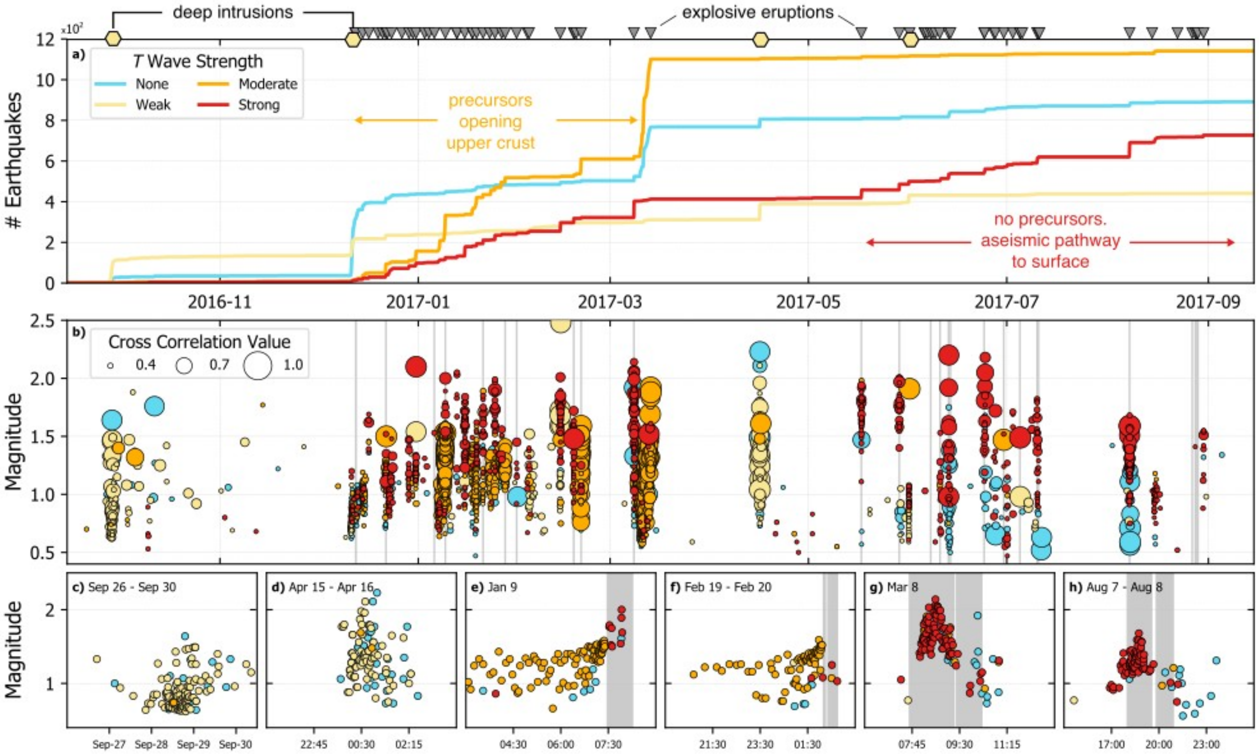

Wech et al. [2018]

Eruption cycles and forecasting

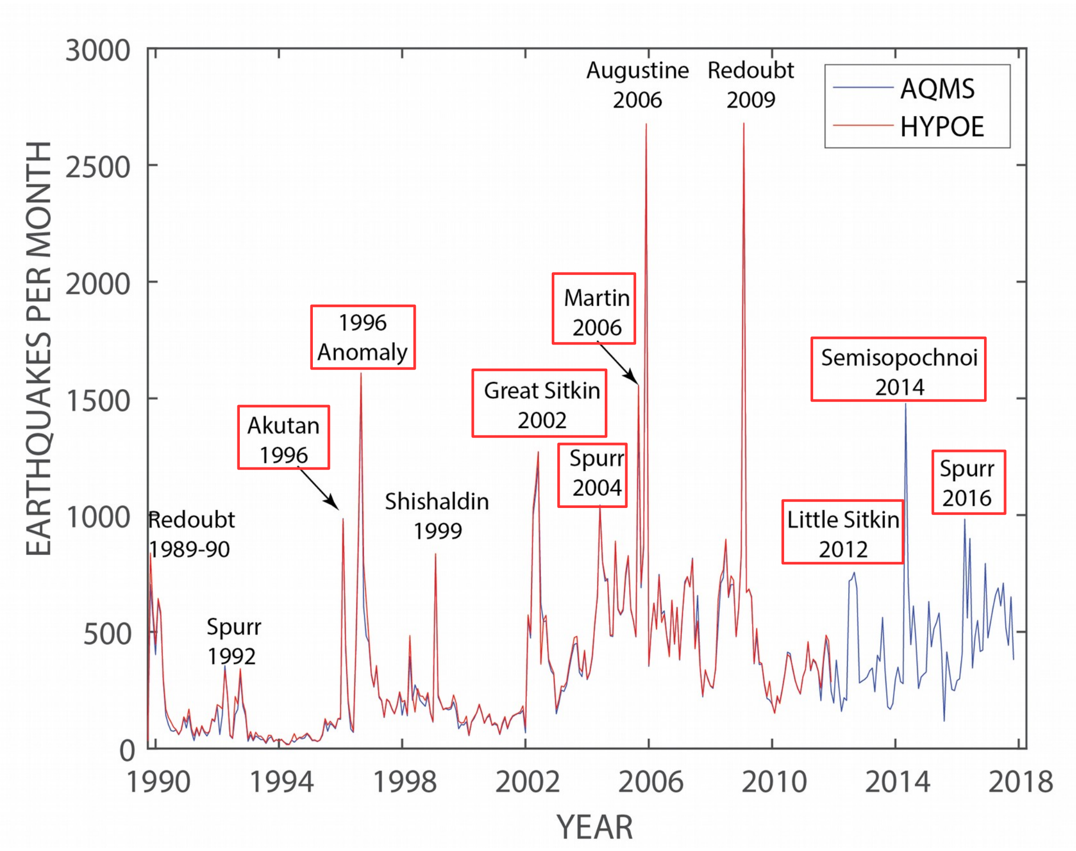

- Most volcanic earthquake swarms do not culminate in eruption

After Power et al. [2019]

Eruption cycles and forecasting

- Full-eruption-cycle records are key to understanding volcanic seismicity

Mt. St. Helens earthquakes 1981-2017

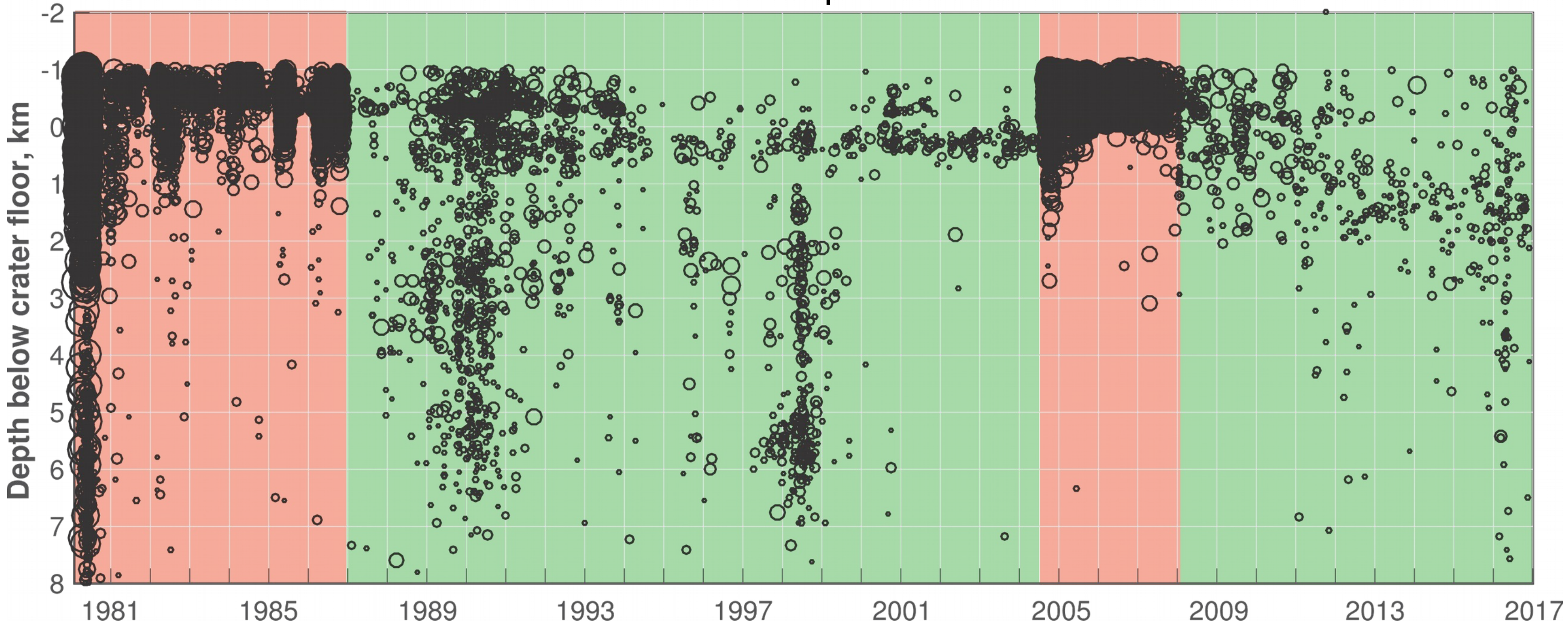

W. Thelen (USGS/CVO), personal comm.

State of the art and future trends

- Laboratory and numerical experiments are elucidating seismo-acoustic source processes in volcanic fluid systems

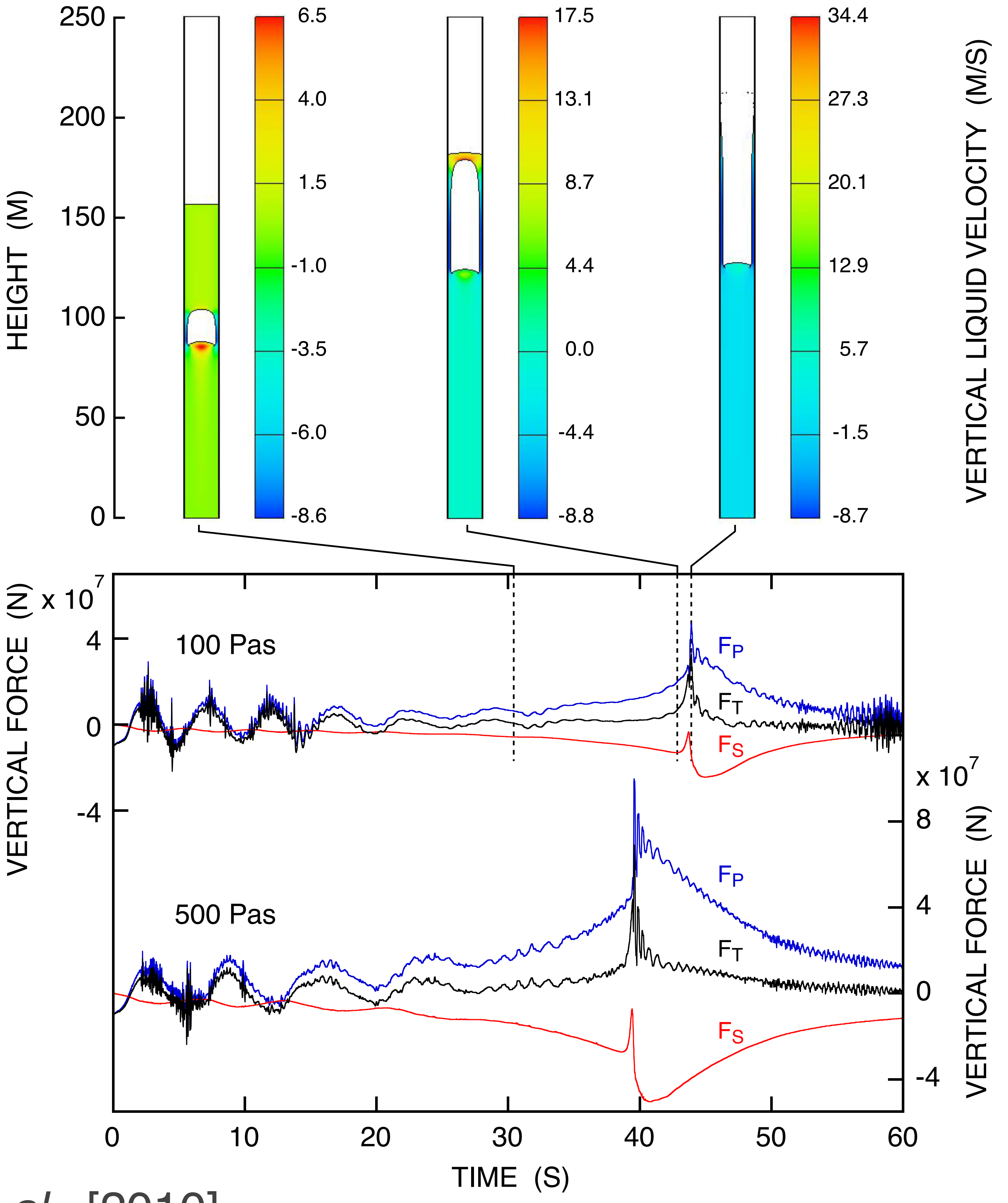

Chouet et al., [2010]

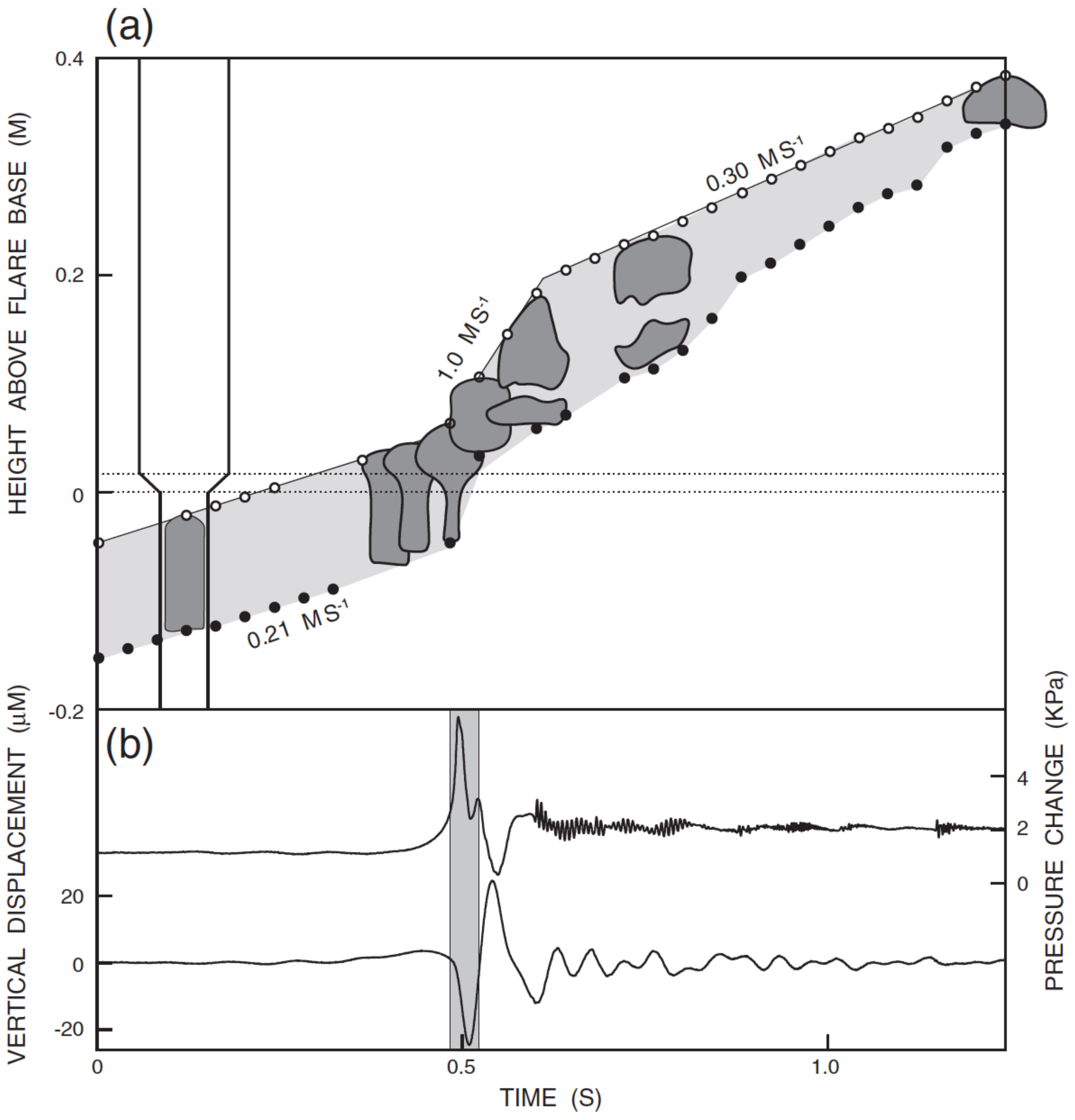

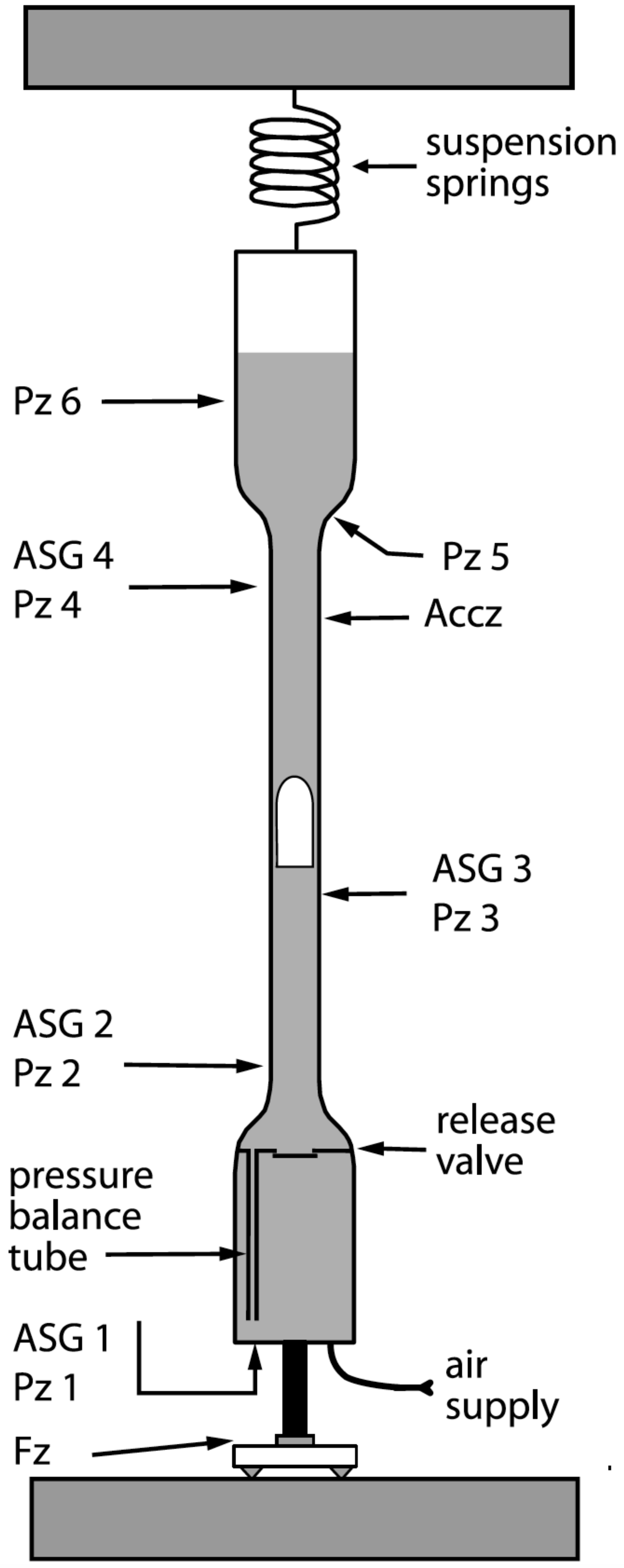

James et al., [2006]

State of the art and future trends

- Observationally constrained by increasingly dense geophysical and multi-parametric field deployments

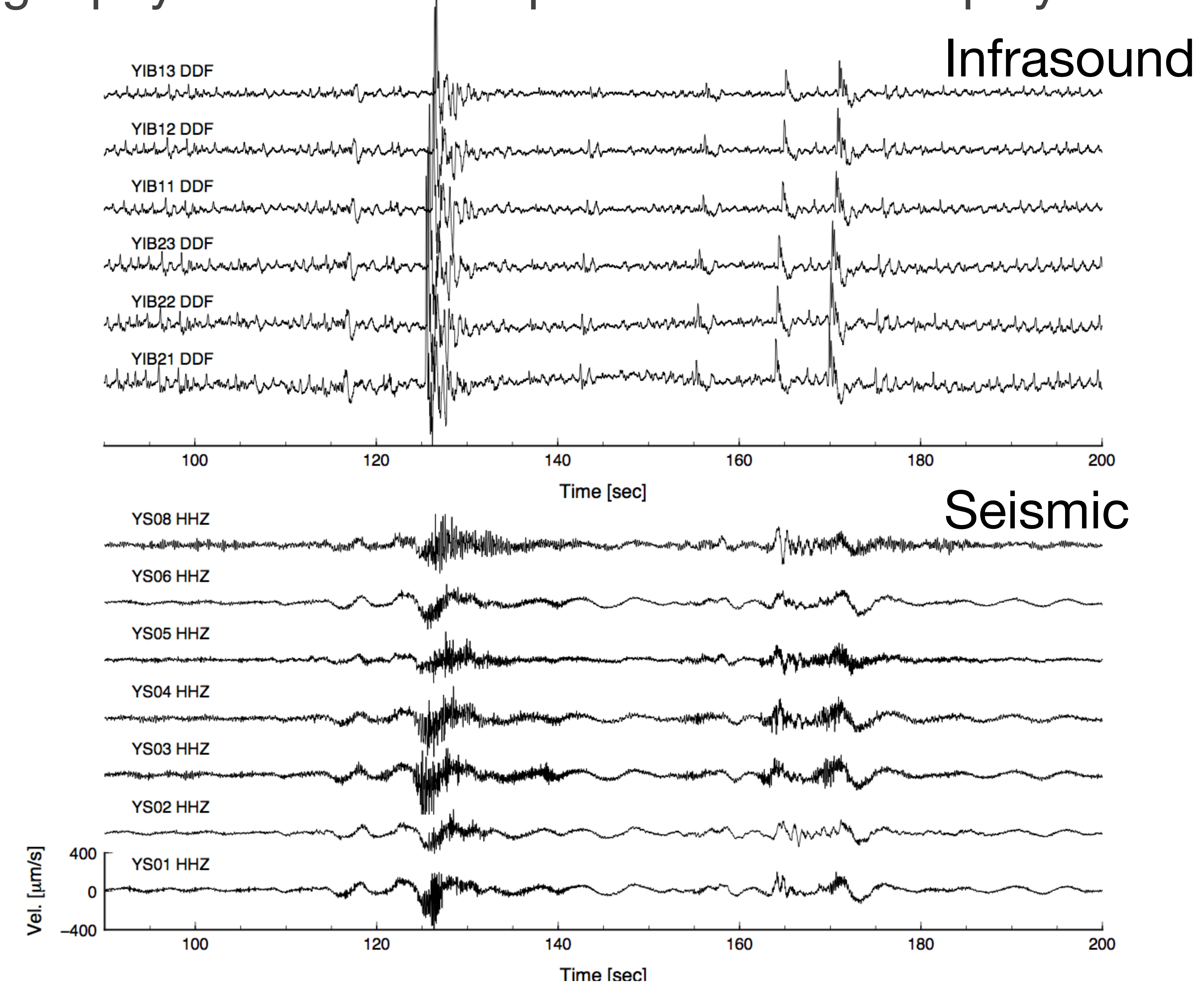

Yasur, Vanuatu 2016

Jolly et al., [2017]; *Matoza et al.* [2018]; *Iezzi et al.* [in press]

State of the art and future trends

- Observationally constrained by increasingly dense geophysical and multi-parametric field deployments

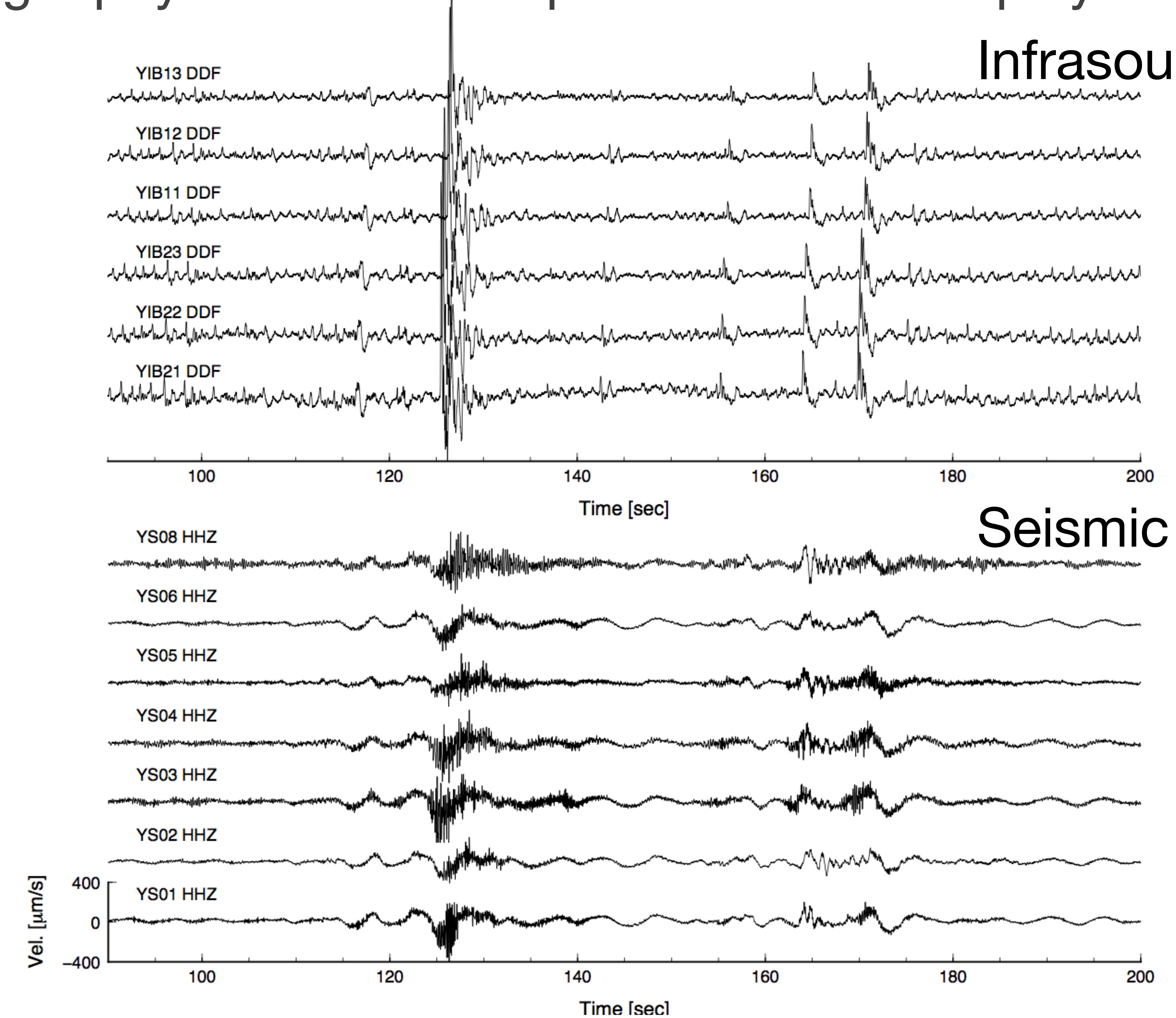

Yasur, Vanuatu 2016

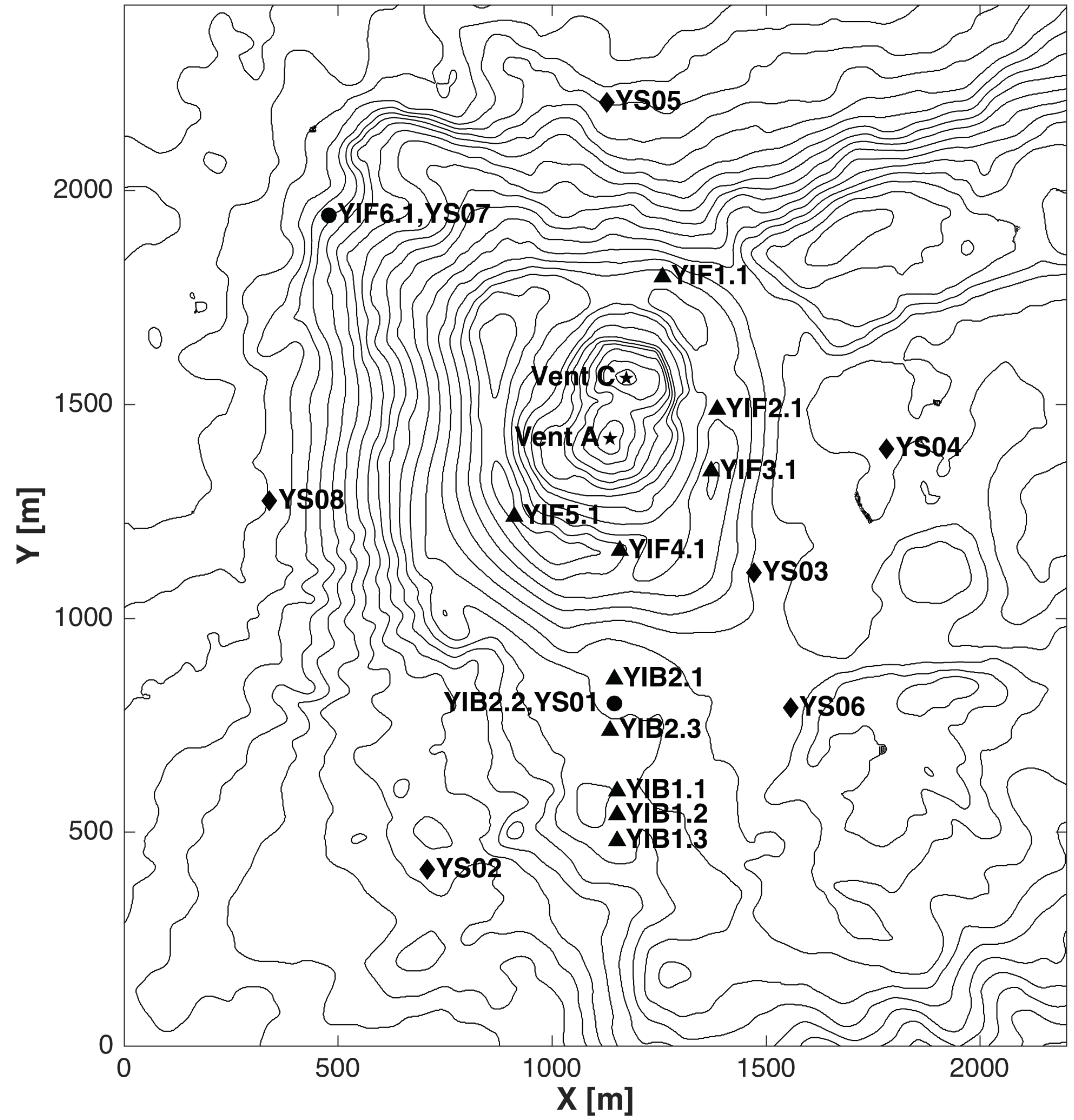

YS: seismic; **YI**: infrasound
Contour interval: 20 m

Jolly et al., [2017]; *Matoza et al.* [2018]; *Iezzi et al.* [in press]

State of the art and future trends

- Observationally constrained by increasingly dense geophysical and multi-parametric field deployments

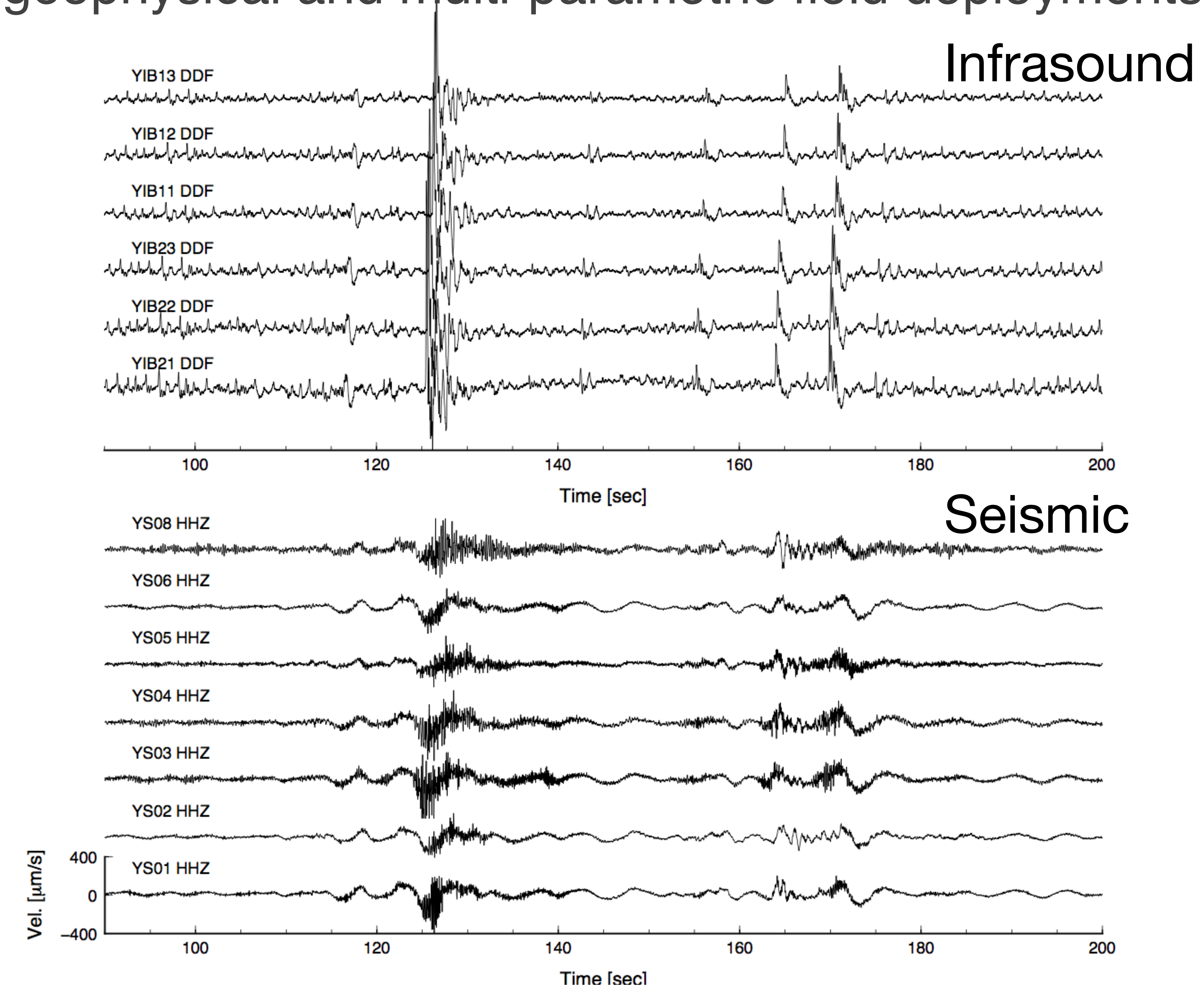

Seismic data

- 11 broadband seismometers (Trillium Compact 120 s; Omnirecs DATA-CUBE digitizer)

Infrasound data

- 6 single infrasound sensors (Chaparral C60V)
- 7 small-aperture 3-element infrasound arrays
- 2 tethered balloon infrasound systems

Gas geochemistry data

- FTIR
- 2 scanning Flyspecs (SO_2)

Imaging data

- High-frame rate DSLR
- UAV DJI Phantom
- Go-Pro cameras
- FLIR (infrared)

Geologic samples

- Scoria and ash samples for petrologic analysis

Jolly et al., [2017]; *Matoza et al.* [2018]; *Iezzi et al.* [in press]

State of the art and future trends

Infrasonic jet noise from volcanic eruptions

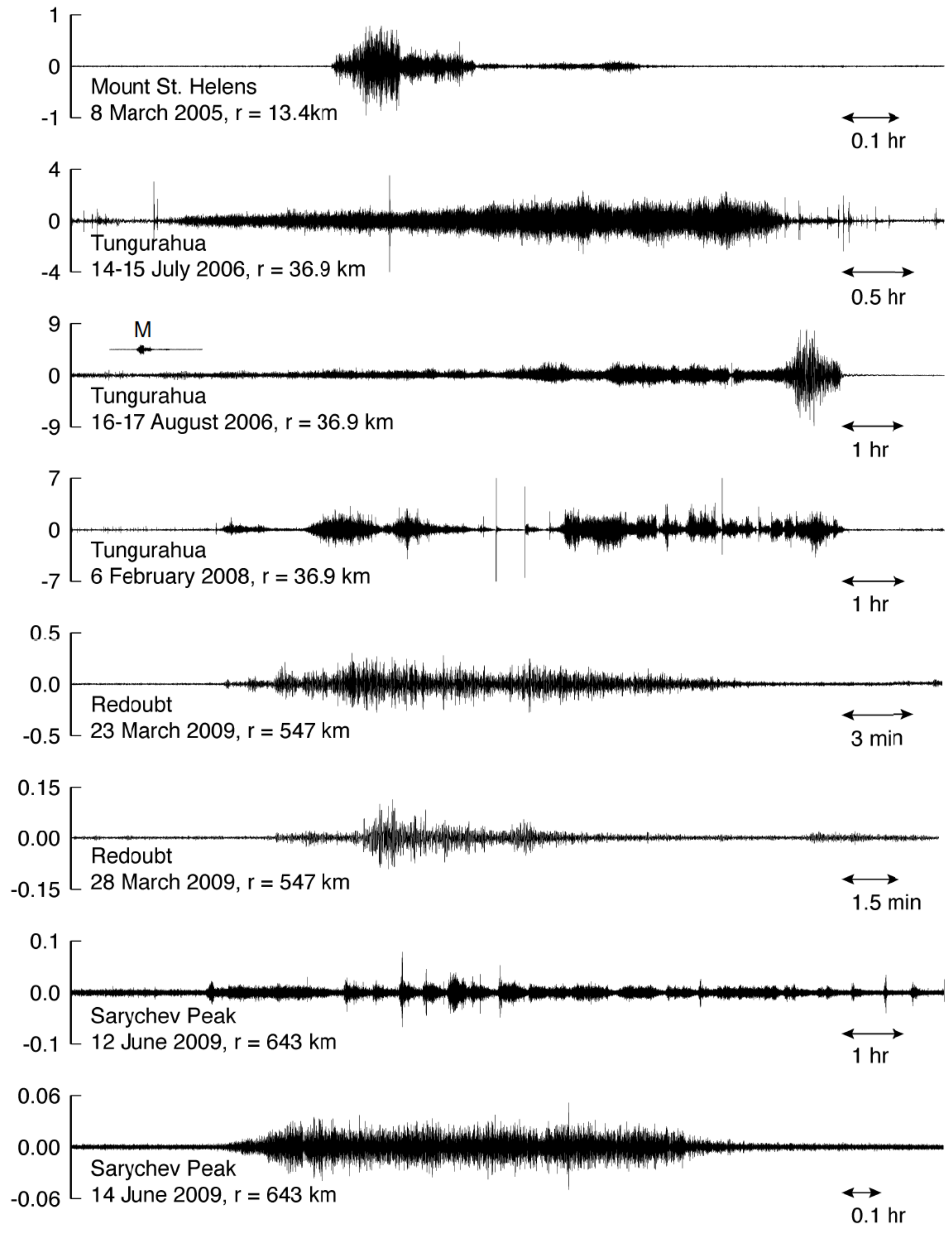

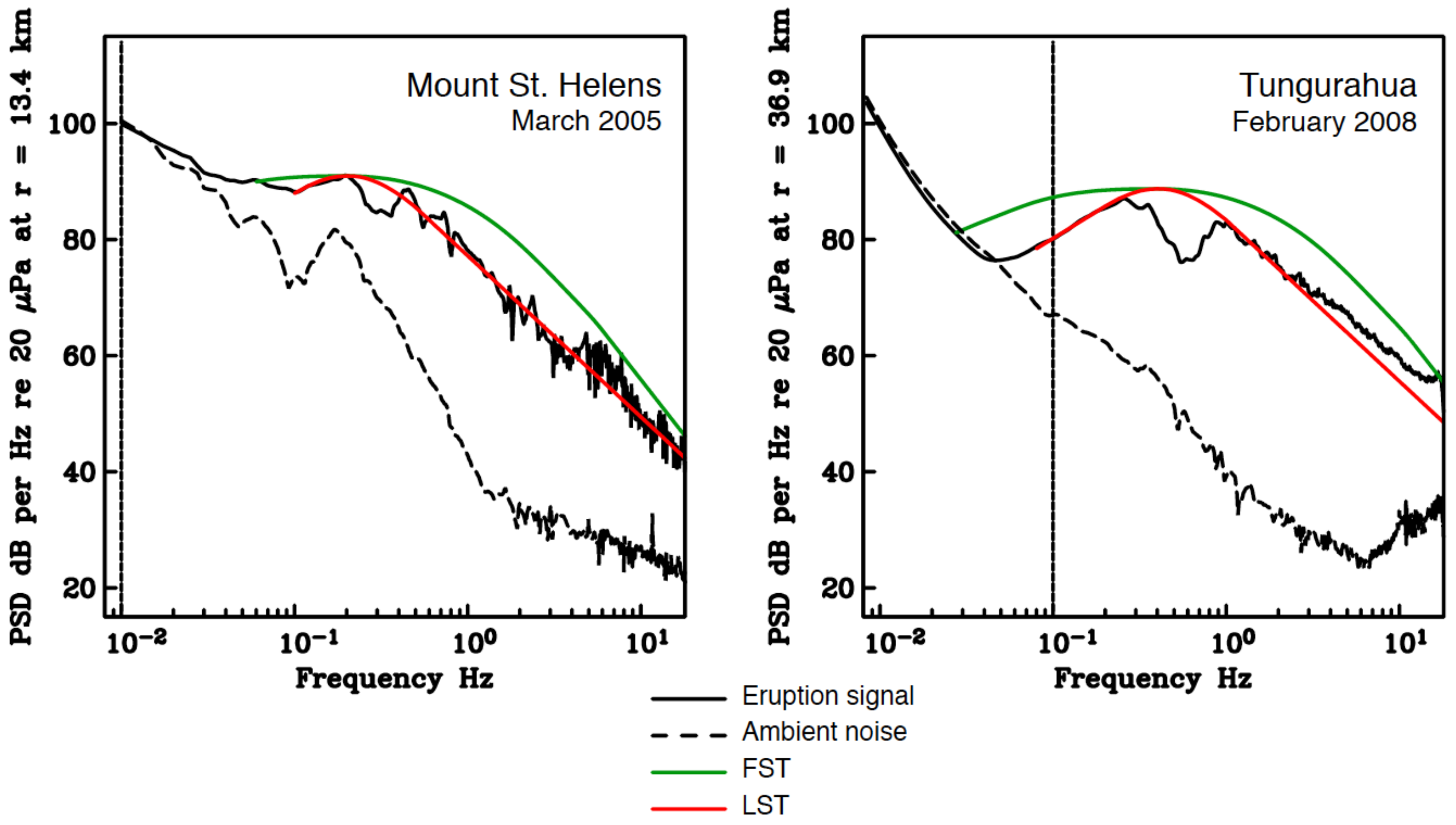

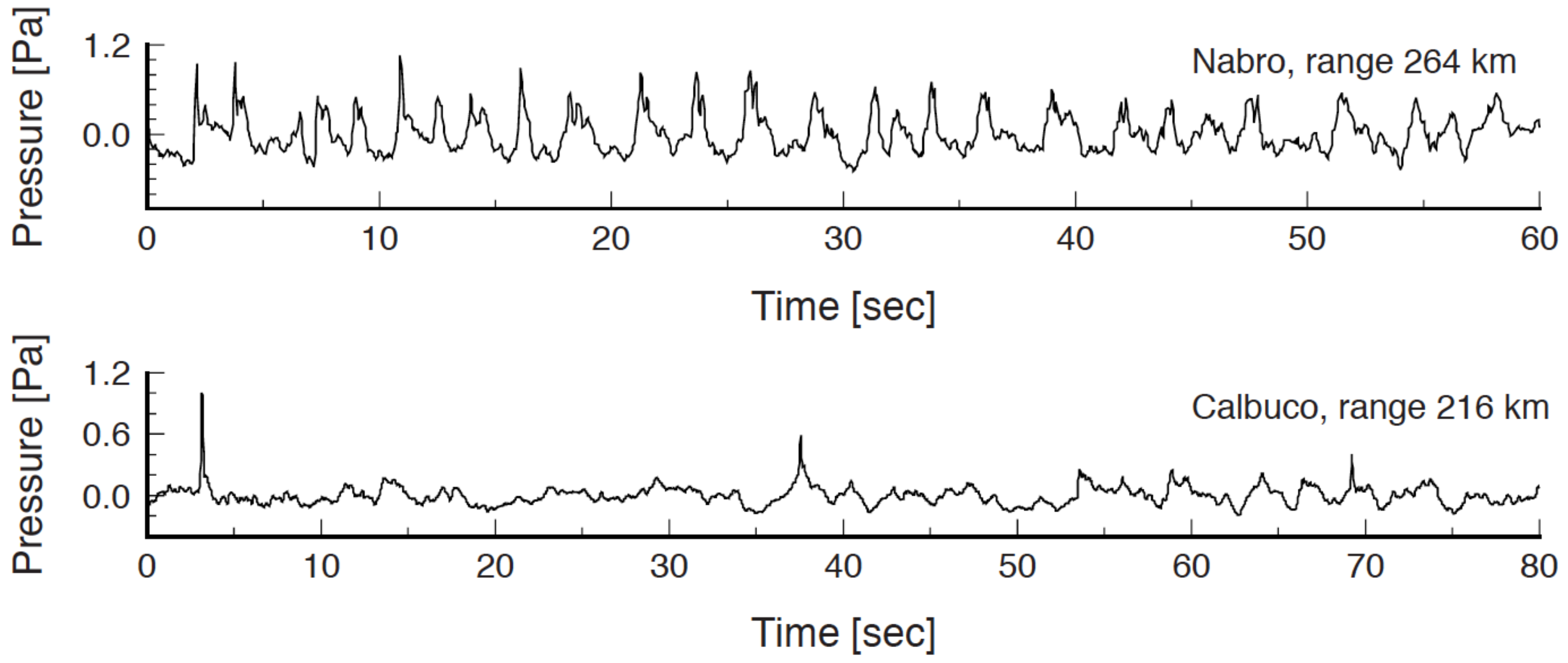

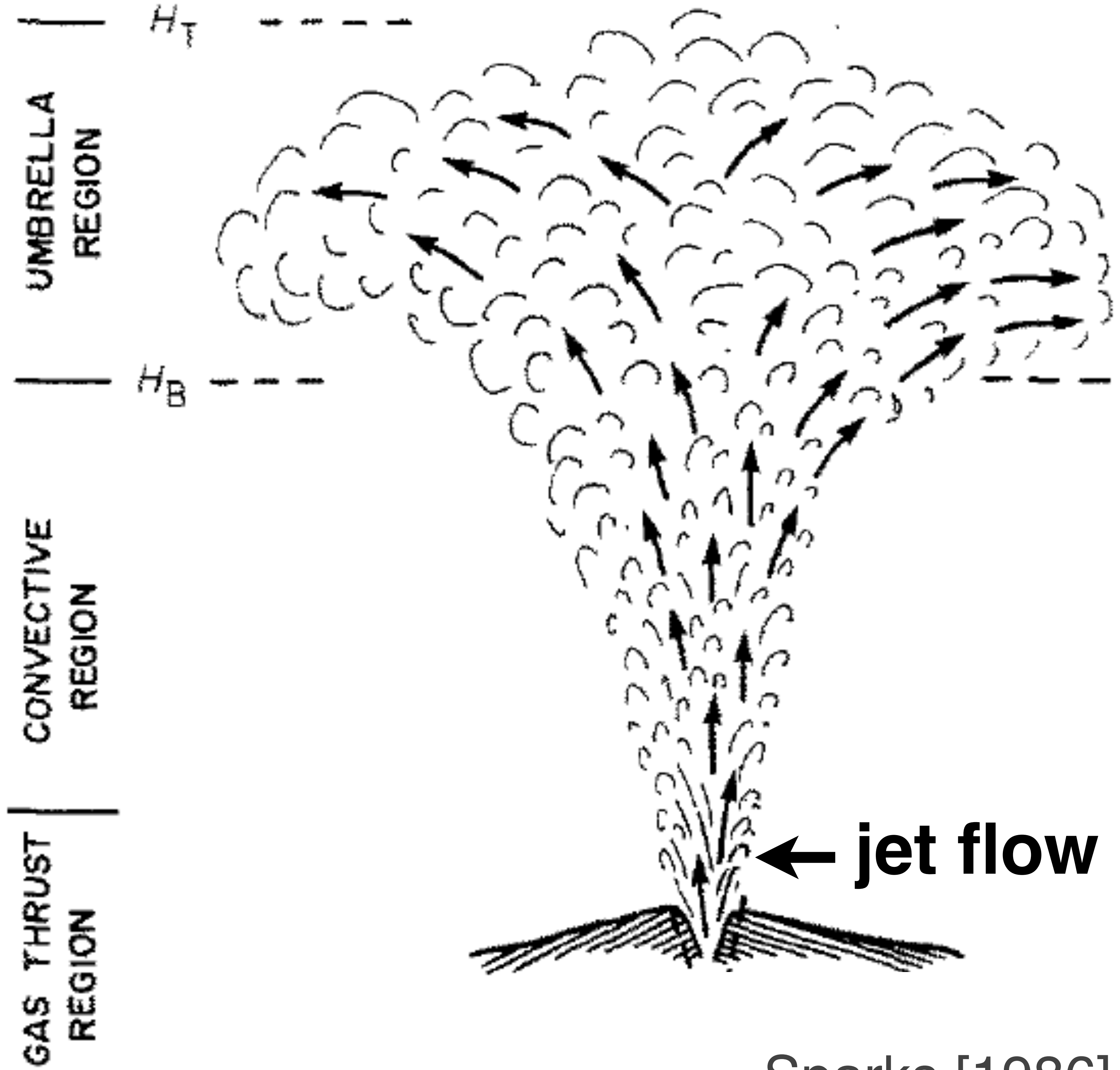

Sparks [1986]

Matoza et al. [2009, 2013]; *Fee et al.* [2013]; *Taddeucci et al.* [2014]; *Matoza and Fee* [2018]

State of the art and future trends

Infrasonic jet noise from volcanic eruptions

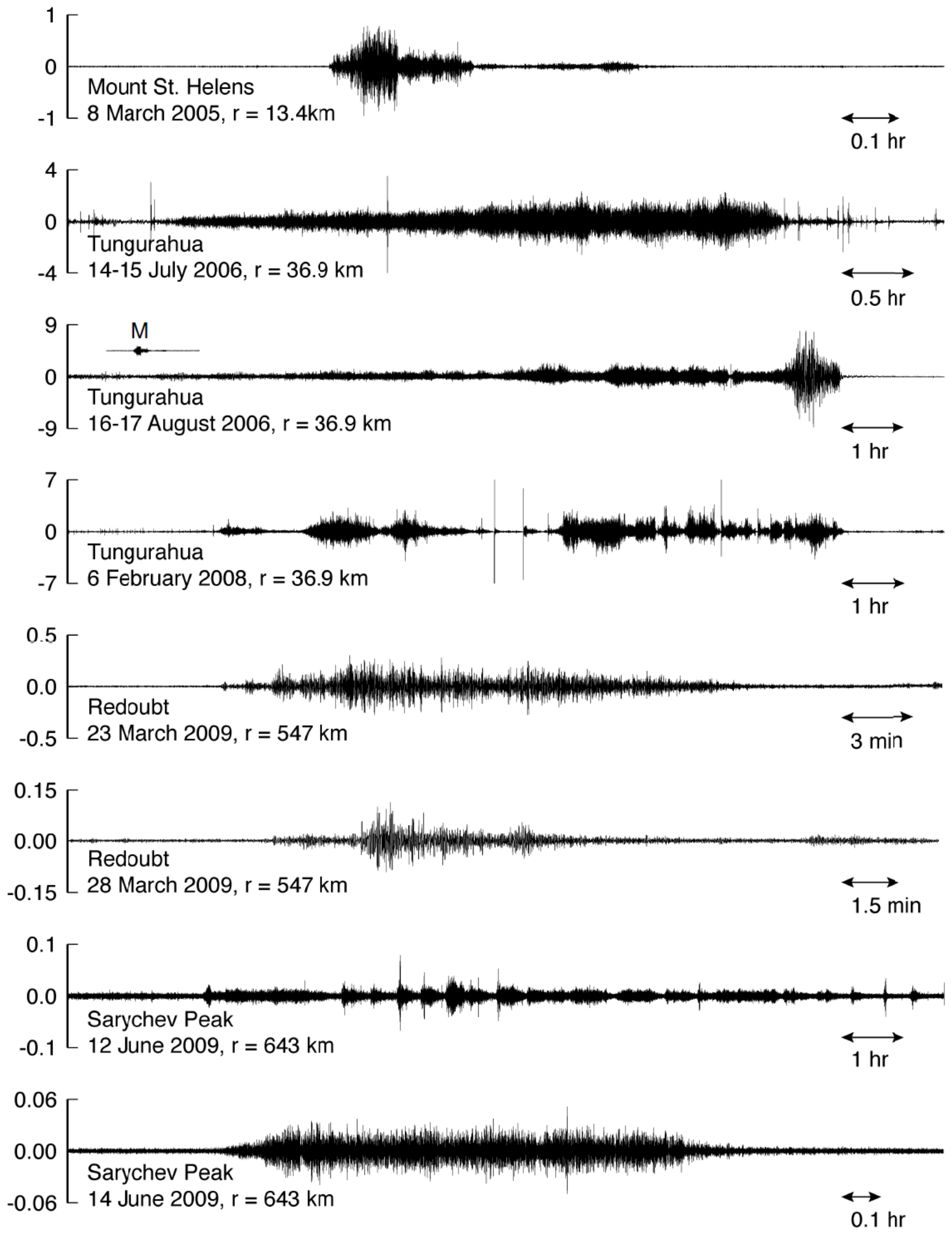

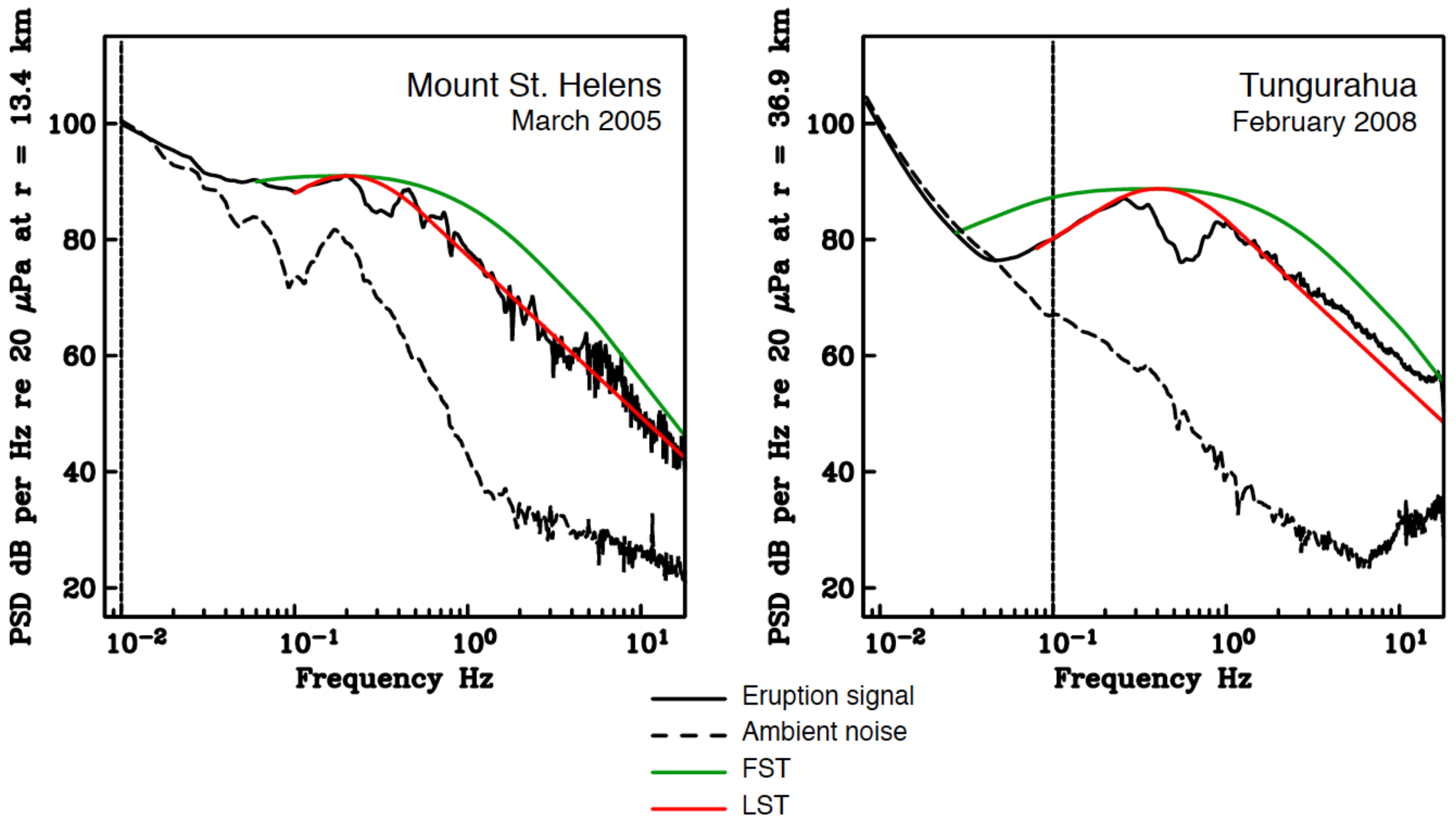

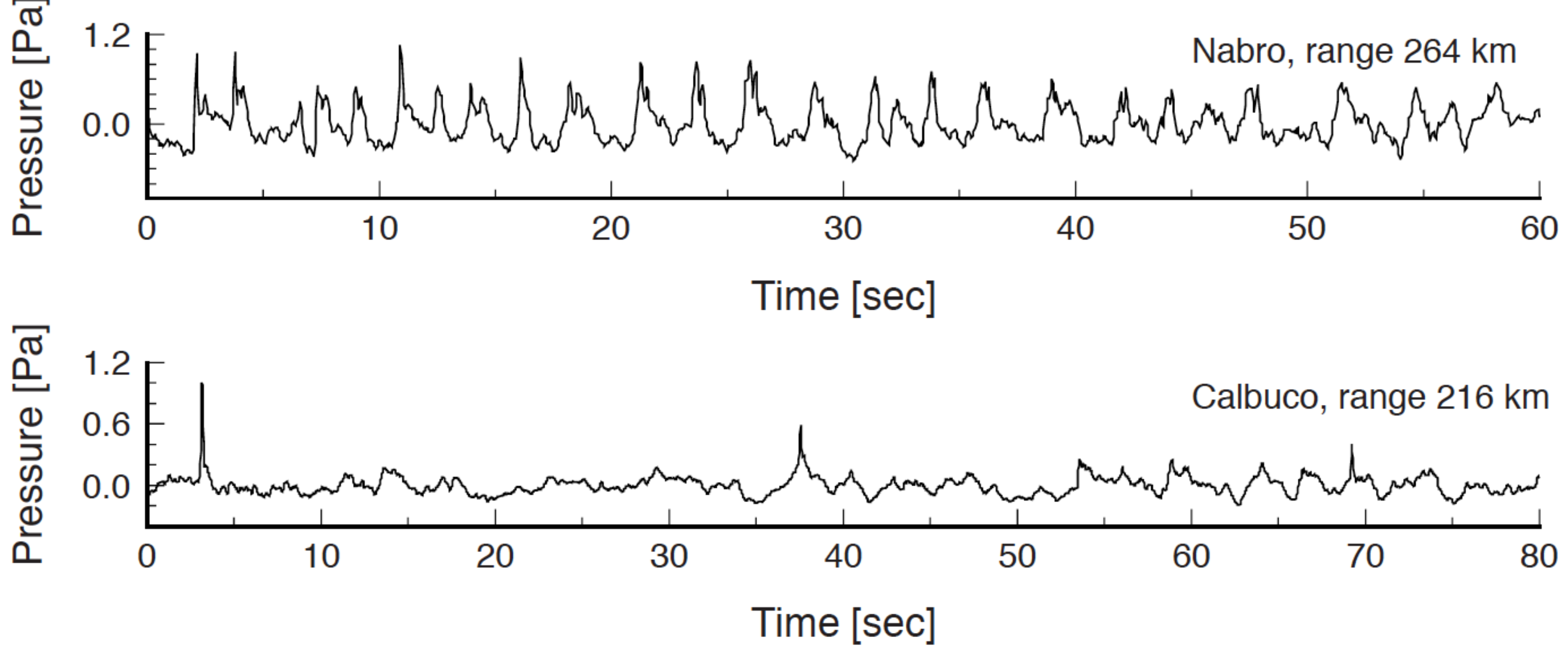

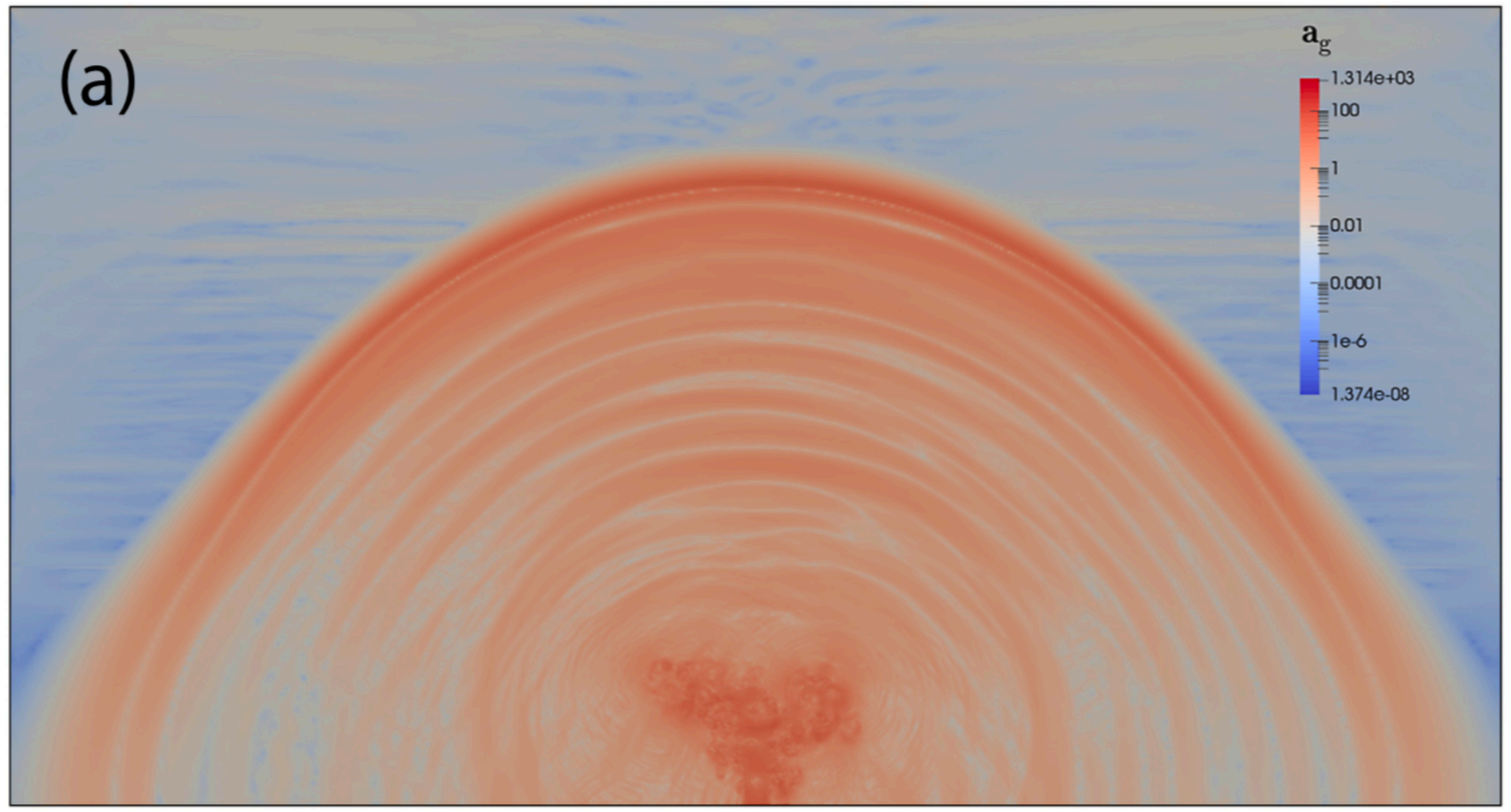

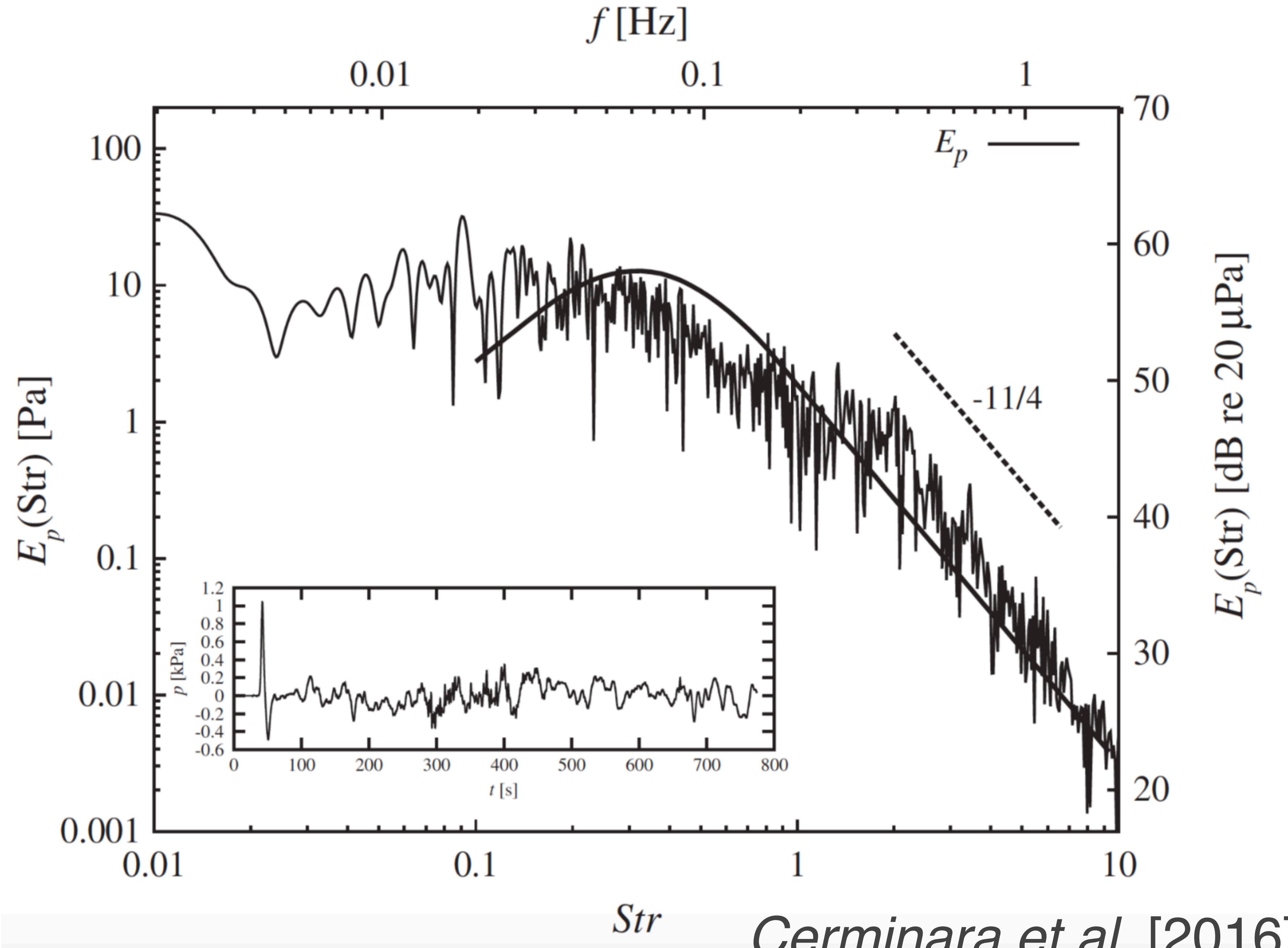

Matoza et al. [2009, 2013]; *Fee et al.* [2013]; *Taddeucci et al.* [2014]; *Matoza and Fee* [2018]

Cerminara et al. [2016]

State of the art and future trends

- Large *N* and nodal deployments
- Improved knowledge of shallow subsurface velocity structure at volcanoes (upper 500 m, within edifice)
- Resolve controversies about source vs. path effects
- Better constrained full-waveform inversion of smaller and higher frequency sources

seismogram: $w(t) = s(t) * l(t) * g(t)$

excitation/trigger (↑ $s(t)$)

crack/conduit resonance (↑ $l(t)$)

path & site effects (← $g(t)$)

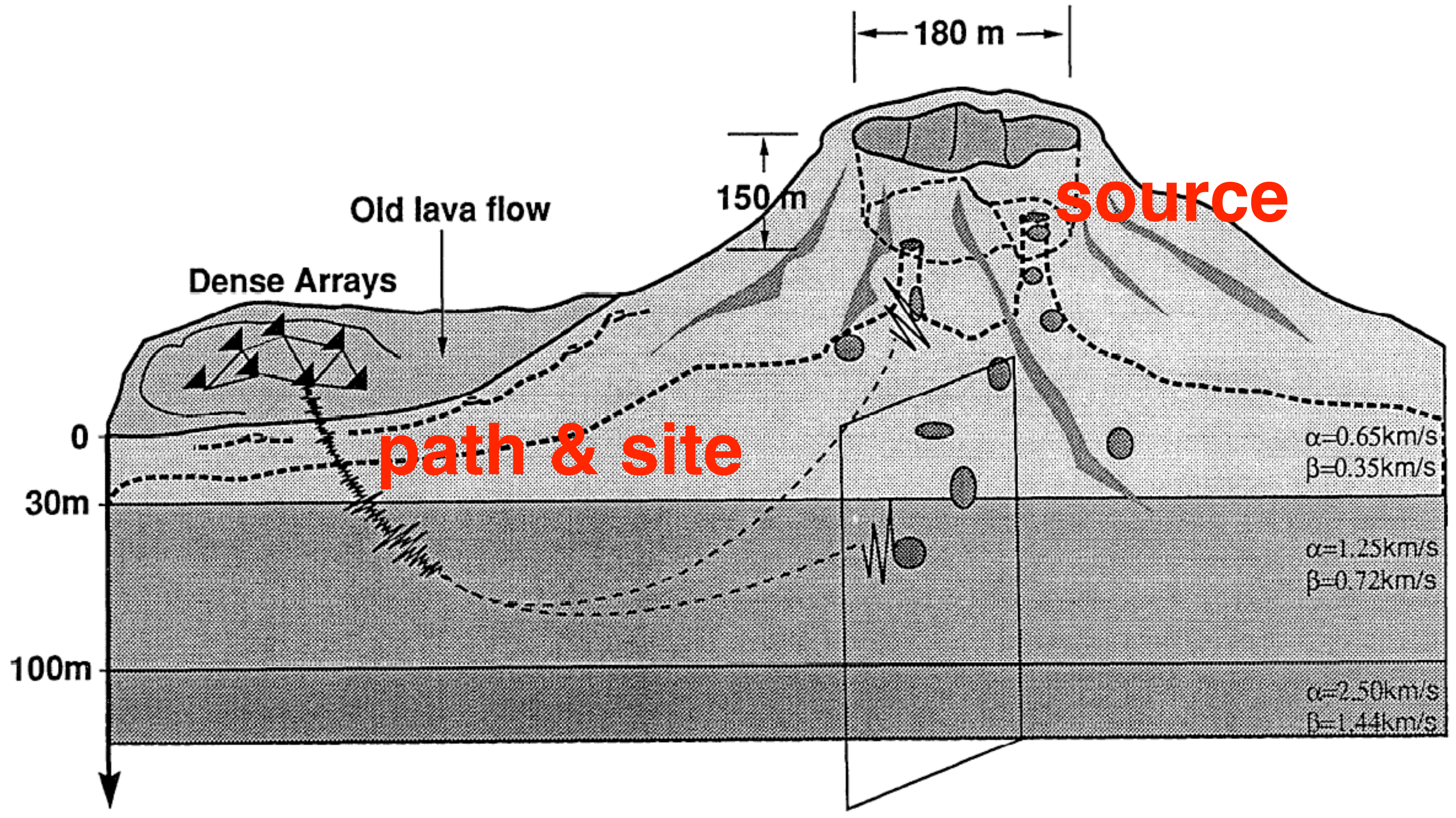

Goldstein and Chouet [1994]

iMUSH active source experiment, Mount St. Helens

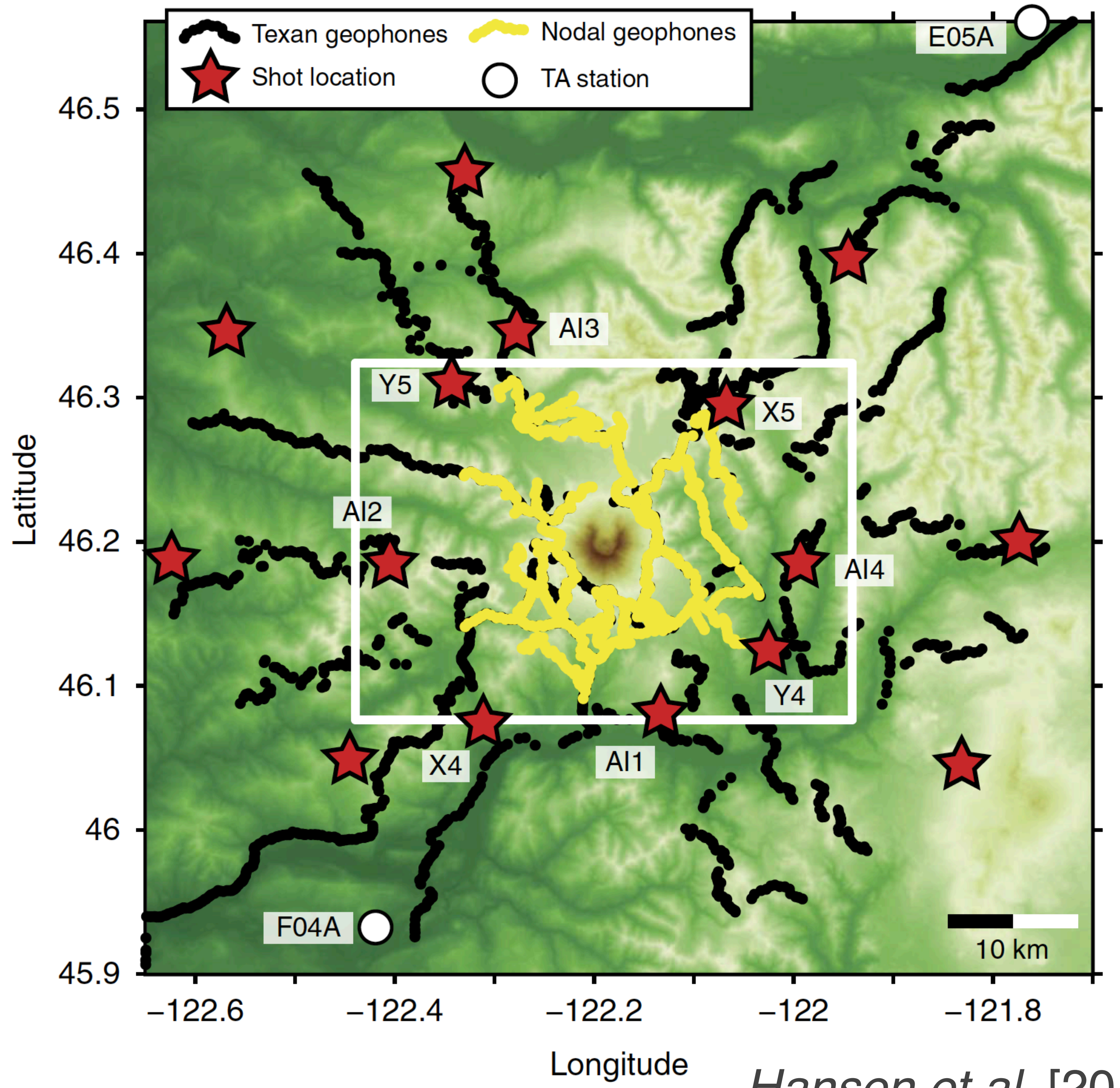

Hansen et al. [2016]

State of the art and future trends

- Laboratory and numerical experiments are elucidating seismo-acoustic source processes in volcanic fluid systems
- Observationally constrained by increasingly dense geophysical and multi-parametric field deployments, which, e.g., enable full seismic and acoustic waveform inversions
- The fields of volcano geodesy, seismology, and acoustics are now merging to track processes on a continuum of spatial and temporal scales in the ground and atmosphere

- Despite vast progress over the past century, major questions remain regarding source processes, patterns of volcano-seismic unrest, internal volcanic structure, and the relationship between seismic unrest and volcanic processes

State of the art and future trends

- More seismic and acoustic sensors on more volcanoes worldwide
- Steady expansion of operational regional and global volcano-acoustic monitoring systems

Seismic stations on the Island of Hawai`i

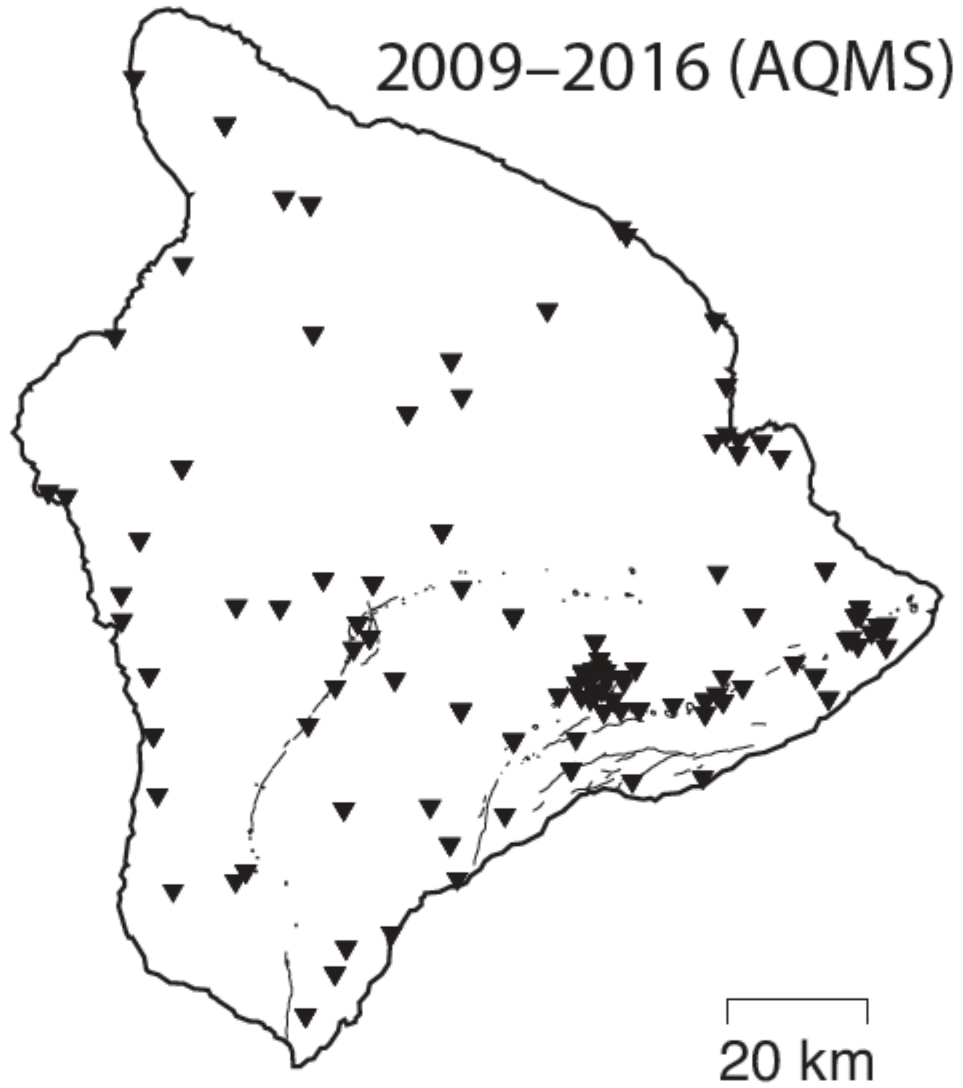

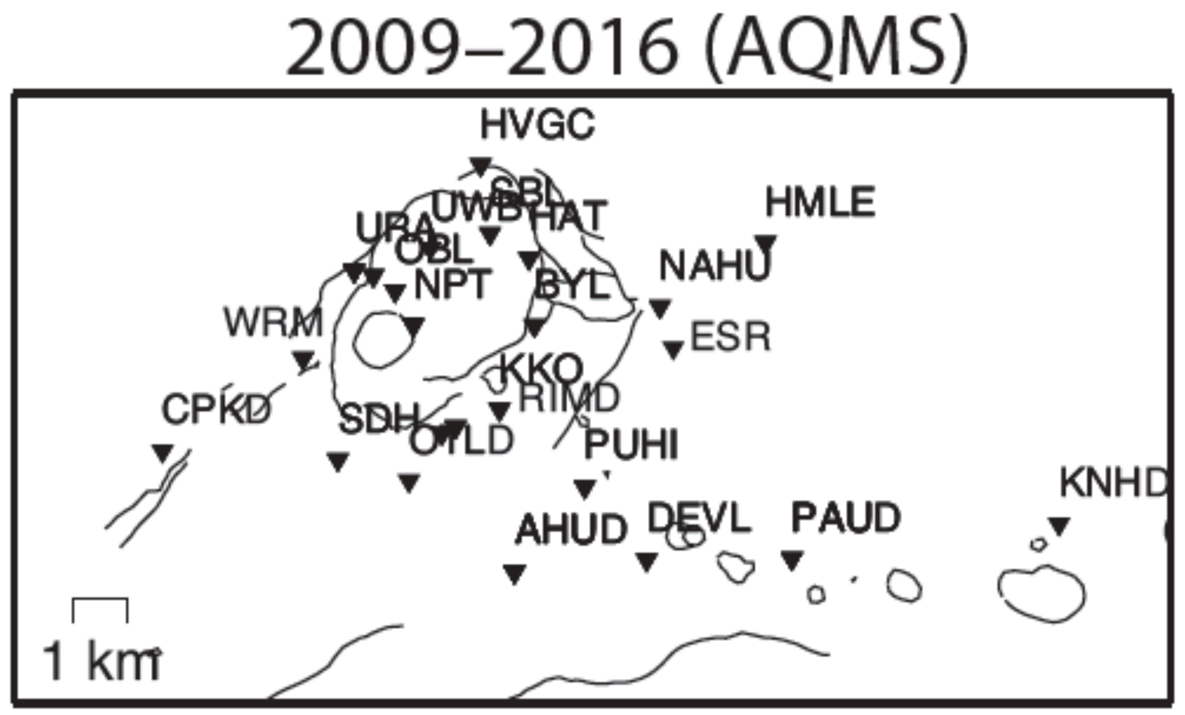

e.g., Thelen et al. [2014]

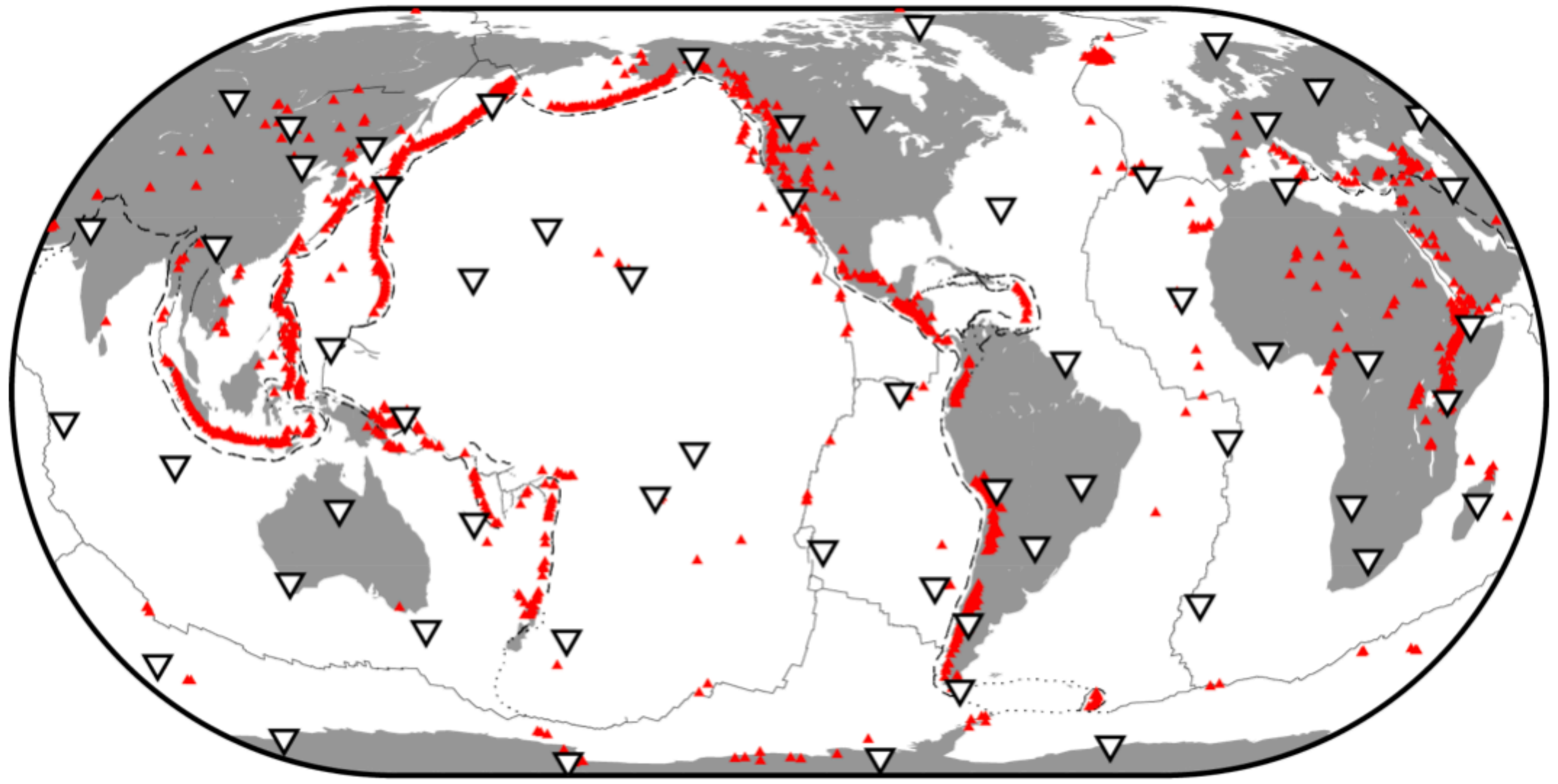

▲ Potentially active volcanoes [*Siebert and Simkin*, 2002-]
▽ IMS infrasound network

Matoza et al. [2017]